

ISSN 1407-5806

**COMPUTER
MODELLING
AND
NEW TECHNOLOGIES**

**Volume 10
No 3**

2006

Transporta un sakaru institūts
(Transport and Telecommunication Institute)

Computer Modelling and New Technologies

Volume 10, No.3 – 2006

ISSN 1407-5806
ISSN 1407-5814
(On-line: www.tsi.lv)

Riga – 2006

EDITORIAL BOARD:

Prof. Igor Kabashkin (Chairman of the Board), *Transport & Telecommunication Institute, Latvia*;
Prof. Yuri Shunin (Editor-in-Chief), *Information Systems Management Institute, Latvia*;
Prof. Adolfas Baublys, *Vilnius Gediminas Technical University, Lithuania*;
Dr. Brent Bowen, *University of Nebraska at Omaha, USA*;
Prof. Olgierd Dumbrajs, *Helsinki University of Technology, Finland*;
Prof. Eugene Kopytov, *Transport & Telecommunication Institute, Latvia*;
Prof. Arnold Kiv, *Ben-Gurion University of the Negev, Israel*;
Prof. Anatoly Kozlov, *Moscow State University of Civil Aviation, Russia*;
Prof. Juris Zakis, *University of Latvia*;
Prof. Edmundas Zavadskas, *Vilnius Gediminas Technical University, Lithuania*.

Editors:

Literary editor Lucija Paegle, *Transport & Telecommunication Institute, Latvia*

Host Organization:

Transport and Telecommunication Institute – Eugene Kopytov, Rector

Co-Sponsor Organization:

PAREX Bank, Latvia – Valery Kargin, President

Supporting Organizations:

Latvian Academy of Sciences – Juris Ekmanis, President

Latvian Transport Development and Education Association – Andris Gutmanis, President

Latvian Operations Research Society – Igor Kabashkin, President

University of Nebraska at Omaha, USA – Brent Bowen, Director of Aviation Institute

The Khaim Kordonsky Charitable Foundation, USA – Inna Kordonsky-Frankel

THE JOURNAL IS DESIGNED FOR PUBLISHING PAPERS CONCERNING THE FOLLOWING FIELDS OF RESEARCH:

- mathematical and computer modelling
- mathematical methods in natural and engineering sciences
- physical and technical sciences
- computer sciences and technologies
- semiconductor electronics and semiconductor technologies
- aviation and aerospace technologies
- electronics and telecommunication
- navigation and radar systems
- telematics and information technologies
- transport and logistics
- economics and management
- social sciences

Articles can be presented in journal in English (preferably), Russian, German and Latvian (at the option of authors). All articles are reviewed.

EDITORIAL CORRESPONDENCE

Transporta un sakaru institūts (Transport and Telecommunication Institute)

Lomonosova iela 1, LV-1019, Riga, Latvia. Phone: (+371)-7100593. Fax: (+371)-7100535.

E-mail: journal@tsi.lv, <http://www.tsi.lv>

COMPUTER MODELLING AND NEW TECHNOLOGIES, 2006, Vol. 10, No.3

ISSN 1407-5806, ISSN 1407-5814 (on-line: www.tsi.lv)

Scientific and research journal of Transport and Telecommunication Institute (Riga, Latvia)

The journal is being published since 1996.

Copyright © Transport and Telecommunication Institute, 2006

CONTENTS

Editors' remarks	5
Applied statistics	7
UPON MULTI-PARAMETRICAL OPTIMIZATION IN RISK MANAGEMENT A. Ben-Yair, D. Golenko-Ginzburg, D. Greenberg, A. Nemenman	7
Solid state physics	14
THE SIMPLEST DEFECT IN SrTiO_3 PEROVSKITE CRYSTALS: ATOMIC AND ELECTRONIC STRUCTURE OF A SINGLE F CENTER Yu.F. Zhukovskii, R.A. Evarestov, E.A. Kotomin, Yu.A. Mastrikov, S.N. Piskunov, Yu.N. Shunin	14
FIRST PRINCIPLES CALCULATIONS OF THE ATOMIC AND ELECTRONIC STRUCTURE OF LaMnO_3 (001) SURFACE E.A. Kotomin, Yu.A. Mastrikov, D.V. Gryaznov, Yu.N. Shunin	29
Information systems	41
INVESTIGATION OF ALGORITHMS FOR GOAL-BASED AGENT CONTROL USING EVOLUTIONARY COMPUTATION <i>/in Russian/</i> V. Chernishev, Yu. Chizhov, G. Kuleshova, A. Borisov	41
DEVELOPMENT OF STANDARD OPERATING ENVIRONMENT (SOE) EXPANDING ON THE BASEMENT OF AUTOMATED AND STANDARDIZED SYSTEM IMAGING V. Gopeyenko, V. Zenin	53
Applied mathematics and mathematical physics	62
SOME MATHEMATICAL MODELS WITH NON-LINEAR BOUNDARY CONDITIONS FOR FOC INTENSIVE COOLING OF STEEL AND ANALYTICAL SOLUTIONS <i>/in Russian/</i> Sh.E. Guseinov, N.I. Kobasko, A.A. Buikis, A.G. Mamedov	62
Information teaching technologies	75
A SURVEY OF DISTANCE ENGLISH TEACHING T. Lobanova	75
Economy and society	82
MULTIFACTOR DYNAMIC LONELINESS MODEL I. Ishmuhametov	82
PSYCHOMETRIC CHARACTERISTICS OF THE UCLA LONELINESS SCALE (VERSION 3) : A RESEARCH OF LONELINESS OF THE HIGHER SCHOOL STUDENTS <i>/in Russian/</i> I. Ishmuhametov	89
Authors' index	96
Personalia	97
Cumulative Index	100
Preparation of publications	106



Editors' Remarks

Mother Nature, Father Technology

Mother Nature, Father Technology,
What lessons of life would you teach to me?
I give you form, my child, that you may walk,
I give you sight, my child, that you may see.

Twin aspects of the greatest unity,
We give to our children this prophecy,
The living will find their ways in this world,
The wise will create their heaven as we.

Light from earth's rainbow, flower, and crystal,
Mix a spectrum of art elemental,
Sound from earth's breathing, water, and thunder,
Blend a song of spirit transcendental.

'Tis not one of nature and one of man,
But one eternal, and one force plan,
All living creatures shall dance with this pair,
Wonders shall be born of this caravan.

Bee buzzes round his hexagonal home,
Spider weaves downy webs of silken chrome,
Bird knits a sturdy nest of leaves and twigs,
Beaver builds great dams around his log dome.

All told, lord man won the ultimate prize,
Creative genius inside of him vies,
Born of nature and seeing the pattern,
He invents and learns with all that he tries.

Mother Nature, Father Technology,
What lessons of life did you teach to me?
I gave you form, my child, that you could walk,
I gave you sight, my child, that you could see.

*Rubaiyat of Omar Khayyam*¹ /Edward Fitzgerald

¹ Abu ol-Fath ebn-Ebrahim Omar ol-Khayyami of Nishapur.

Birth: Date: 1048 CE, Place: Nishapur, Persia (Iran), Khayyam means "tent maker".

Work: Mathematician, Scientist, Astronomer, Philosopher, Poet. **Major Contributions:** Jalali Calendar (more accurate than the Julian and almost as accurate as the Gregorian intercalation system), Contributions to Algebra (geometric solution of cubic equations), Astronomical tables and the Rubaiyat. **Death:** Date: 1123 CE, Place: Nishapur, Persia (Iran)

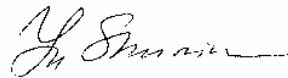
Computer Modelling and New Technologies, 2006, Volume 10, No.3

This 10th volume No.3 points out an attention to solid state physics problems, which are really actual for this day. Some particular tasks in information technologies, applied mathematics and statistics are considered. Models of teaching technologies and distance education for English are also discussed in details.

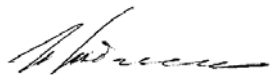
This means that our journal policy is directed on the fundamental and applied sciences researches, which is the basement of a full-scale modelling in practice.

This edition is the continuation of our publishing activities. We hope our journal will be interesting for research community, and we are open for collaboration both in research and publishing.

EDITORS



Yu.N. Shunin



I.V. Kabashkin

UPON MULTI-PARAMETRICAL OPTIMIZATION IN RISK MANAGEMENT

A. BEN-YAIR¹, D. GOLENKO-GINZBURG², D. GREENBERG³,
A. NEMENMAN⁴

¹ Department of Industrial Engineering and Management, Sami Shamoon College of Engineering,
Beer-Sheva, 84100, Israel, E-Mail: avnerb@sce.ac.il

² Department of Industrial Engineering and Management, Academic College of Judea and Samaria,
Ariel, 44837, Israel, E-Mail: dimitri@bgumail.bgu.ac.il, and
Department of Industrial Engineering and Management, Ben-Gurion University of the Negev,
Beer-Sheva, 84105,

³ Department of Industrial Engineering and Management, Academic College of Judea and Samaria,
Ariel, 44837, Israel, E-Mail: dorongre@zahav.net.il

⁴ Department of Industrial Engineering and Management, Academic College of Judea and Samaria,
Ariel, 44837, Israel, E-Mail: nemenman@gmail.com

In order to demonstrate the role and the place of the harmonization modelling theory [12–14], we have to show its utilization in certain management areas. It can be well-recognized that harmonization models are applicable mostly to organization systems under random disturbances. This, in turn, enables analyzing various sources of uncertainty, e.g. reliability values including hazardous failures, various environmental parameters, etc. We will examine henceforth two important cases of project management: large-scale complicated projects and medium-level public service projects.

Keywords: project risk analysis; risk assessment models; public service projects; on-line control models; trade-off project optimization models

1. Using harmonization modelling for managing large projects

It can be well-recognized from [13–14] that the input information for the developed harmonization modelling in Project Management comprises a PERT-COST activity-on-arc network project $G(N, A)$ with budget values c_{ij} assigned to all activities $(i, j) \in A \subset G(N, A)$ with restricted upper and lower bounds $c_{ij \min} \leq c_{ij} \leq c_{ij \max}$. Each activity duration t_{ij} is a random value with a probability density function depending parametrically on the assigned budget c_{ij} . Thus, uncertainty in scheduling results in random time delays of the total project's duration which translates directly into an uncertainty in cost. Those uncertainties may cause certain risks in the course of managing the project.

From the other side the projects to be considered in Harmonization Modelling (HM) do not deal with system's engineering aspects, since all the input information is presented in a formalized shape. Harmonization model is regarded as a generalized cybernetic problem which deals with multi-parametric optimization in order to calculate system's utility estimates. Harmonization models, thus, are not linked with such risk factors as technology, complexity and integration, design changes, supportability, marketing, etc., although they usually comprise probabilistic parameters which may affect those risk factors.

Taking into account [2], a conclusion can be drawn that projects of such type have not to be managed by use of regular risk analysis models, e.g. of SCERT and RAER types [2]. Such projects usually perform the duties of public service projects, e.g., by building new populated areas, schools, hospitals, bridges, factories, etc. In our opinion, those projects also have to be properly managed and controlled.

Since harmonization modelling techniques are based on trade-off optimization models which can be used in planning and controlling stochastic network projects as well [8,9], we suggest to unite in one person the harmonization models' analyzing function as well as the analyst responsible for undertaking on-line control for PERT-COST projects. In our opinion, most of the conclusions drawn from harmonization modelling can be implemented in on-line control procedures including decision-making.

However, even in the case of highly complicated large projects with new changing technologies and with tendencies for the latter to become obsolete, harmonization models may prove to be useful. In certain cases the alternatives and scenarios to be determined in the course of risk analysis, on the stage of optimization and refinements of alternatives [2, 17], may be passed to harmonization analysts in order to obtain basic parameters to optimize the corresponding utilities. Those scenarios may be in the form of PERT-COST network projects which is one of the most general forms in Project Management. Thus, a general conclusion can be drawn as follows:

- I. For projects under random disturbances which:
 - do not deal either with advanced technological uncertainty or with capital investments to be returned from marketing;
 - may involve certain risks caused by overrunning pre-given due dates or project's costs, – harmonization techniques can serve both for evaluating the project's utility and as regulation models in the course of planning and controlling the project.
- II. For highly complicated and large projects which have to be managed by the use of risk analysis, harmonization techniques can be used in risk assessment, by systems analyzing and modelling (usually in the form of possible alternatives and scenarios).

Thus, harmonization models can be regarded as an important auxiliary technique to support and facilitate risk management. If, e.g. the management is faced with two different alternatives (scenarios) to manage an organization system, both alternatives have to be analyzed from the point of risk management. Those alternatives may eventually boil down to different system's models with different basic parameters. To implement a trade-off analysis between the two alternatives, the methodology of harmonization modelling may be applied.

The interconnection between risk management and harmonization techniques may be put as follows: at all critical time points in the life cycle of a project (changing the market requirements, needs for developing a new software package, new contingency plans that cut expenses and development time at the cost of lower performance, etc.), risk management analysts form the updated input information of alternative scenarios for harmonization modelling. The new input information comprises [12–14]:

- the updated and renewed alternative's model (e.g. in the form of PERT-COST sub-networks);
- n basic parameters entering the model;
- new partial utility coefficients α_k as well as values R_{k0} and R_{k00} , $1 \leq k \leq n$.

On the basis of the obtained information in the course of harmonization modelling, proper decision-making has to be undertaken and implemented in monitoring the organization system. This has to be carried out by risk management analysts.

In other words, harmonization modelling, similarly to make tree analysis, fault tree models, contingency evaluation and review techniques, etc., may be regarded as special auxiliary technique to improve the system's monitoring. Thus, harmonization modelling, like any generalized cybernetic modelling, may serve as technique in risk assessment.

2. Harmonization models for managing PERT-COST public service projects

We will consider in greater detail the case when a medium-size PERT-COST activity-on-arc network project serves as a system's model in order to undergo harmonization. The project $G(N, A)$ comprises activities $(i, j) \in A \subset G(N, A)$ of random durations t_{ij} with pre-given p.d.f. depending parametrically on the budget value c_{ij} assigned to each activity (i, j) . It is assumed that for each activity (i, j) its p.d.f. $p(t_{ij}/c_{ij})$ satisfies the beta-distribution

$$p(t_{ij}/c_{ij}) = \frac{12}{(b_{ij} - a_{ij})^4} (t - a_{ij})(b_{ij} - t)^2, \quad (1)$$

where $a_{ij} = \frac{A_{ij}}{c_{ij}}$, $b_{ij} = \frac{B_{ij}}{c_{ij}}$, A_{ij} , B_{ij} – constants, and c_{ij} satisfies restrictions

$$c_{ij \min} \leq c_{ij} \leq c_{ij \max}, \quad (2)$$

with pre-given values of $c_{ij \min}$ and $c_{ij \max}$.

Given the total project's budget $C \geq \sum_{\{(i,j)\}} c_{ij \min}$ and the due date D , the problem is to evaluate the project's optimal utility value given in the linear form

$$U = \underset{C,D,R}{\text{Max}} \{ \alpha_C (C_0 - C) + \alpha_D (D_0 - D) + \alpha_R (R - R_0) \}, \quad (3)$$

where C_0 , D_0 and R_0 are the least permissible budget, due date and reliability values which can be implemented in a PERT-COST project, while values C , D and R are current values for the project under consideration. Linear rates α_C , α_D and α_R , i.e., the partial utilities, are pre-given as well. It has been shown in [12-14] that reliability value R is obtained by means of optimizing the partial harmonization model $PHM\{C, D\} = R$ as follows:

determine $c_{ij}^{(opt)}$ to maximize the objective

$$\underset{\{c_{ij}\}}{\text{Max}} R = \underset{\{c_{ij}\}}{\text{Max}} \left[\Pr \left\{ T \left\{ G/c_{ij} \right\} < D \right\} \right] \quad (4)$$

subject to (2) and

$$C = \sum_{\{(i,j)\}} c_{ij}^{(opt)}, \quad (5)$$

$$C_{00} \leq C \leq C_0, \quad (6)$$

$$D_{00} \leq D \leq D_0, \quad (7)$$

$$R_0 \leq R \leq R_{00}. \quad (8)$$

Undertaking a relatively simple look-over in the two-dimensional area of C and D and determining for each couple (C, D) the corresponding $R = PHM\{C, D\}$ in order to maximize objective (3) enables establishing the project's utility U .

In case when project $G(N, A)$ is represented in a formalized shape and activities $(i, j) \in G(N, A)$ do not bear any engineering definitions and have an abstract meaning, we suggest using harmonization modelling as the project's planning and control technique. Note that undertaking harmonization modelling for the project under consideration results in optimal budget reallocation among the project's activities. This basic assertion will be used later on, by implementing the project's on-line control.

We suggest a step-wise procedure to control the PERT-COST public service network project by means of harmonization as follows:

Step 0. Given the input information:

- PERT-COST project $G(N, A)$;
- Pre-given values $c_{ij \min}$, $c_{ij \max}$, A_{ij} and B_{ij} for each activity $(i, j) \in A \subset G(N, A)$;
- Pre-given partial utilities α_C , α_D and α_R ;
- Pre-given admissible intervals $[C_{00}, C_0]$, $[D_{00}, D_0]$ and $[R_0, R_{00}]$.

Step 1. Undertake harmonization modelling for $G(N, A)$ beforehand, i.e., before the project actually starts to be carried out. Denote the corresponding optimized values which define the maximal project's utility, by C^* , D^* and R^* . Note that restrictions

$$\begin{cases} C_{00} \leq C^* \leq C_0 \\ D_{00} \leq D^* \leq D_0 \\ R_0 \leq R^* \leq R_{00} \end{cases} \quad (9)$$

hold, otherwise harmonization cannot be accomplished.

- Step 2.** If budget value C^* is accepted, reassign C^* among the project's activities according to values $c_{ij}^{(opt)}$ obtained in the course of undertaking harmonization at *Step 1*. Afterwards the project starts to be carried out.
- Step 3.** In [8,9], a control model for PERT-COST projects is outlined. The model determines planned trajectories, observes at each control point the progress of the project and its deviation from the planned trajectory, and establishes the next control point. This control model has to be implemented at *Step 3*, in order to determine the routine control point $t > 0$.
- Step 4.** At each control point t the progress of the project is observed, i.e., network graph $G(N, A)$ has to be updated at point t , as well as the remaining budget C^* . Denote those values by $G_t(N, A)$ and C_t^* , correspondingly.
- Step 5.** At each routine control point $t > 0$ solve harmonization problem in order to reallocate later on the remaining budget C_t^* among remaining activities $(i, j) \subset A_t \subset G_t(N, A)$. Denote the corresponding optimal budget values by $c_{ij}^{(opt)}$.
- Step 6.** Reallocate, if necessary, budget C_t^* among activities $(i, j) \subset A_t$ according to the results of *Step 5*. Note that implementing numerous budget reallocations is actually the only control action in the course of performing on-line control. Go to *Step 3*.
- Step 7.** The algorithm terminates after inspecting the project at the due date D , i.e., at the last control point.

It can be well-recognized that, besides undertaking on-line procedures, the suggested step-wise algorithm comprises both harmonization modelling and risk analysis models. Indeed, the latter are not similar to traditional risk management methods which involve technological risks, uncertainties in products' marketing, etc. However, optimal budget reallocation serves actually as a regulation model under random disturbances and can be regarded as a risk analysis element.

Note that in the course of the project's realization certain parameters entering the input information may undergo changes, e.g. restriction values $C_0, C_{00}, R_0, R_{00}, D_0, D_{00}$, as well as partial utility values α_C, α_D and α_R [12-14]. New values have to be implemented in the harmonization model in order to facilitate optimal budget reallocation among the remaining project's activities at *Step 5* of the algorithm. If the problem (4-8) has no solution, the decision-making to be undertaken at the company level results either in obtaining additional budget value ΔC or in increasing the due date by ΔD . Both values can be determined by means of harmonization.

3. Harmonization models for analyzing alternatives and scenarios

We will consider the case of a large complicated project with a high level of uncertainty both in technology and at the marketing stage of the project's life cycle. To manage such projects risk analysis methods similar to RAER or SCERT [2] have to be implemented. Those methods, which we will use henceforth as benchmarks, deal with analyzing various alternatives or scenarios which may be presented in the form of deterministic network sub-projects of CPM type. On the basis of those sub-projects "time – cost" trade-offs outlined in [17], are usually carried out. We will henceforth call those deterministic trade-offs the CPM-COST projects.

We suggest, if possible, to present those scenarios in the form of stochastic PERT-COST network projects and to substitute the former "time – cost" trade-off by a harmonization model. We will demonstrate that the newly developed trade-off optimization model is more effective than the former CPM-COST ones.

In order to perform a proper comparison we have to use similar input information. Since an overwhelming majority of both researchers and practitioners accept the beta-distribution as a probability law for random activities' durations [see, e.g. 1, 3-7, 10-11, 15-16, 18-20] with the p.d.f. of the activity time t_{ij}

$$f_{ij}(t) = \frac{\Gamma(\alpha + \beta)}{\Gamma(\alpha)\Gamma(\beta)} \frac{(t - a_{ij})^{\alpha-1}(b_{ij} - t)^{\beta-1}}{(b_{ij} - a_{ij})^{\alpha+\beta-1}}, \quad a < t < b, \quad \alpha, \beta > 0, \quad (10)$$

where a_{ij} stands for the optimistic time and b_{ij} is the pessimistic time.

In order to simplify the model the p.d.f. in the PERT statements can be modified [5-7, 9] to

$$f_{ij}(t) = \frac{12}{(b_{ij} - a_{ij})^4} (t - a_{ij})(b_{ij} - t)^2 \quad (11)$$

with the mean

$$\mu_{ij} = 0.2(3a_{ij} + 2b_{ij}). \quad (12)$$

Thus, introducing the assumption about the p.d.f. (10) and taking into account that (10) depends on c_{ij} parametrically, relations (1,2) hold.

The simplified time – cost trade-off model for a CPM network [17] is as follows:

given a CPM graph $G(N, A)$ together with functions $t_{ij} = f_{ij}(c_{ij})$, $(i, j) \in G(N, A)$, and values $c_{ij \min}$ and $c_{ij \max}$, determine:

- the minimal total project direct costs C ,

$$\text{Min } C, \quad \text{and} \quad (13)$$

- the optimal assigned budget values c_{ij}^{opt} , subject to

$$T_{cr} \{t_{ij} = f_{ij}(c_{ij}^{opt})\} \leq D, \quad (14)$$

$$\sum_{\{i,j\}} c_{ij}^{opt} = C, \quad (15)$$

$$c_{ij \min} \leq c_{ij}^{opt} \leq c_{ij \max}, \quad (16)$$

where D stands for a pre-given due date.

Since trade-off models in RAER [2] are based on deterministic time – cost trade-offs for CPM-COST models (13-16), the similarity of input information for both models (harmonization and RAER) can be provided by setting

$$t_{ij} = \frac{0.6 A_{ij} + 0.4 B_{ij}}{c_{ij}} \quad (17)$$

for

$$c_{ij} = \begin{cases} c_{ij \min} \\ 0.5(c_{ij \min} + c_{ij \max}) \\ c_{ij \max} \end{cases}, \quad (18)$$

where values A_{ij} , B_{ij} , $c_{ij \min}$, $c_{ij \max}$ are similar to those outlined in (1), and (17) are obtained by substituting the p.d.f. (11) by its mean value (12).

Let us compare the "time – cost" trade-off CPM-COST model (13-16) and the harmonization model (4-8), taking into account that actually activity durations t_{ij} are random variables. It is widely known [see, e.g. 5, 8, 9, 16, 17 etc.] that substituting all p.d.f. activities by their mean values results in essential statistical bias errors for optimization models' objectives (sometimes up to 40-50%). Those errors underestimate the objective, e.g. the critical path's duration. Underestimating planning budget values of any project results in underestimating local budgets assigned to partial project's activities. Such errors might result in increasing the duration of those activities and, thus, decreasing the project's reliability. This, in turn, would affect the life cycle, the cost and the ultimate success of the entire project. As a matter of fact, substituting deterministic trade-offs by harmonization modelling prevents this shortcoming.

Second, implementing harmonization modelling by means of PERT-COST network projects enables decision-making by using reliability parameter R which is difficult to be analyzed by means of solving

CPM-COST problem (13-16). And, third, by using CPM-COST trade-offs of type (13-16) only several scenarios can be examined (since no risk analyst can take into account numerous alternatives), as distinct from harmonization models when the whole spectrum of possible couples (C, D) is looked through and later on optimized. This, in turn, enables more reasonable and realistic decision-making. Thus, harmonization procedures when considered a risk assessment technique are more effective than the former similar risk assessment by means of CPM-COST network models.

Conclusions

The following conclusions can be drawn from the study:

1. Besides optimizing and calculating the system's utility, harmonization models are used in determining various reliability parameters. Thus, those models can be regarded as newly developed operation research models which can be implemented in risk assessment analysis.
2. Harmonization models can be applied directly to all kinds of PERT-COST network projects with uncertainties associated with activities' durations but without either technological risks or uncertainties on the stage of marketing the project's products. Such projects usually refer to the public service area, like constructing new hospitals, schools, stadiums, theatres, bridges and tunnels, new urban areas, factories, etc. In our opinion, those projects represent an overwhelming majority of existing projects and, thus, require good quality monitoring. For such projects we suggest to use the newly developed harmonization techniques both for estimating the project's utility and for introducing regulating control actions at inspection points to enhance the progress of the project in the desired direction. Thus, harmonization modelling enables certain on-line control procedures for projects under random disturbances.
Being a regulation model, harmonization can be implemented (in a random disturbances environment) as a risk assessment tool as well. Thus, for this class of projects, harmonization, controlling and risk assessment actually meet.
3. A comparative analysis of multi-parametrical trade-off optimization models in harmonization and the existing trade-off optimization techniques in CPM-COST risk assessment leads to the conclusion that the newly developed model is more effective for project risk analysis than former trade-off models. The latter usually cover only time – cost trade-offs for deterministic projects while harmonization techniques can be applied to any number of optimized parameters for projects under random disturbances.
4. For highly complicated projects with technological risks, design changes and risks in future marketing, we suggest to apply harmonization modelling for analyzing alternatives and scenarios on condition that the latter may be presented in the form of PERT-COST network projects. This enables undertaking a more effective risk assessment.

Acknowledgement

This research has been partially supported by the Paul Ivanier Center on Robotics and Production Management, Ben-Gurion University of the Negev.

References

- [1] Berny J. (1989) A new distribution function for risk analysis. *Journal of the Operational Research Society* **40** (12), 1121–1127.
- [2] Cooper D. F., Chapman C. B. (1987) *Risk Analysis for Large Projects*. Wiley, New York.
- [3] Donaldson W. A. (1965) The estimation of the mean and variance of PERT activity time. *Operations Research* **13**, 382–385.
- [4] Elmaghraby S. E. (1977) *Activity Networks: Project Planning and Control by Network Models*. Wiley, New York.
- [5] Golenko D. (1968) *Statistical Methods in Network Planning and Control*. Nauka, Moscow (in Russian).
- [6] Golenko-Ginzburg D. (1988) On the distribution of activity time in PERT. *Journal of the Operational Research Society* **39** (8), 767–771.
- [7] Golenko-Ginzburg D. (1989) PERT assumptions revisited. *Omega*, **17** (4), 393–396.
- [8] Golenko-Ginzburg D., Gonik A. (1996) On-line control model for cost-simulation projects. *Journal of the Operational Research Society* **47**, 266–283.

- [9] Gonik A. (1995) Planning and controlling multilevel stochastic projects. *Ph.D. Thesis*. Ben-Gurion University of the Negev, Beer-Sheva, Israel.
- [10] Littlefield T. K. Jr., Randolph P.H. (1987) Another note on PERT times. *Mgmt. Sci.* **33**, 1357–1359.
- [11] MacCrimmon K. R., Ryavec C. A. (1964) An analytical study of the PERT assumptions. *Operations Research* **12**, 16–37.
- [12] Menipaz E., Ben-Yair A. (2001) Optimal harmonization model in multi-parametrical organization systems. *Communications in Dependability and Quality Management* **4** (2), 12–24.
- [13] Menipaz E., Ben-Yair A. (2001) Harmonization model for stochastic network projects. *Communications in Dependability and Quality Management* **4** (2), 40–55.
- [14] Menipaz E., Ben-Yair A. (2002) Three-parametrical harmonization model in project management by means of simulation. *Mathematics and Computers in Simulation* **59** (5), 431–436.
- [15] Murray J. E. (1962) *Consideration of PERT Assumptions*. Conduction Corporation. Ann. Arbor, Michigan.
- [16] Scully D. (1989) A historical note on PERT times. *Omega* **17** (2), 195–196.
- [17] Shtub A., Bard J., Globerson Sh. (1994) *Project Management: Engineering, Technology and Implementation*, Prentice Hall International, Inc., New York.
- [18] Welsh, D. (1965) Errors introduced by a PERT assumption. *Operations Research* **13**, 141–143.
- [19] Williams T. M. (1992) Practical use of distributions in network analysis. *Journal of the Operational Research Society* **43** (3), 265–270.
- [20] Williams T. M. (1995) What are PERT estimates? *Journal of the Operational Research Society* **46** (12), 1498–1504.

Received on the 1st of August 2006

THE SIMPLEST DEFECT IN SrTiO_3 PEROVSKITE CRYSTALS: ATOMIC AND ELECTRONIC STRUCTURE OF A SINGLE F CENTRE

YU. F. ZHUKOVSKII¹, R. A. EVARESTOV², E. A. KOTOMIN^{1,3},
 YU. A. MASTRIKOV³, S. N. PISKUNOV¹, YU. N. SHUNIN⁴

¹ Institute of Solid State Physics, University of Latvia, 8 Kengaraga Street, LV-1063, Riga, Latvia
 E-mails: quantzh@latnet.lv, kotomin@latnet.lv, piskunov@lanet.lv, fax: +371 7132778,
 phone: +371 7187480;

² St. Petersburg State University, Faculty of Chemistry, Stary Petergof, 198504 St. Petersburg,
 Russian Federation
 E-mail: evarest@hm.csa.ru, fax: +7 812 4286939, phone: +7 812 4286755;

³ Max-Planck-Institut für Festkörperforschung, Heisenbergstraße 1, Stuttgart, D-70569, Germany
 E-mails: e.kotomin@fkf.mpg.de, j.mastrikovs@fkf.mpg.de,
 fax: +49 -711 689 1722, phone: +49 -711 689 1771;

⁴ Information Systems Management Institute, 1 Lomonosov Street, LV-1019, Riga, Latvia
 E-mail: shunin@isma.lv, fax: +371 7241591, phone: +371 7100593

Various properties of a cubic phase of SrTiO_3 perovskite containing single F centres (O vacancies), including energies of their formation and migration, were simulated using different formalisms of Density Functional Theory (DFT) as implemented into CRYSTAL-2003 and VASP computer codes. The lattice relaxation around the F centre was found to be sensitive to both shape and size of used supercells. The larger is supercell, the closer defect energy level in the band gap lies to the conduction band bottom. It approaches the optical ionization energy of 0.49 eV for 270- and 320-atomic supercells, where the distance between neighbouring defects is as large as four lattice constants. The defect bandwidth decreases for these supercells down to 0.02 eV, i.e. the defect-defect interaction becomes negligible. Thus, different first principles periodic approaches being combined provide results, which are converged with respect to the supercell size.

Keywords: DFT calculations, CRYSTAL-2003 and VASP computer codes, cubic phase of SrTiO_3 perovskite, supercell shape and size, the F centre, formation and migration, electronic properties

1. Introduction

Beneficial properties of ABO_3 -type perovskite materials can be obtained by means of a deliberate deviation of oxygen content from the ideal stoichiometry, which is relevant for their numerous high-tech applications as sensors, fuel cells, microelectronic devices, etc. [1,2]. At low partial oxygen pressure an electric conductivity of SrTiO_3 perovskite is controlled by both concentration and mobility of oxygen vacancies, which act as effective donors, therefore this material becomes n -type conductive [3]. Increasing the partial pressure reduces the carrier concentration and at high pressures the conductivity goes through a minimum: the material becomes p -type [4]. Consequent thermal reduction of oxygen in single-crystalline SrTiO_3 results in the insulator-to-metal transition, up to possible superconducting state, accompanied by intensive formation of vacancies and their high density within the skin region [5].

Considerable experimental efforts were made for understanding the nature of defective strontium titanate, including the ionic transport [5,6] and the structural properties [1,7,8]. The oxygen vacancy in SrTiO_3 perovskite was also simulated theoretically [4,9-15], which is very important since modern scanning transmission electron microscopy (STEM) and reflection high-energy electron diffraction (RHEED) combined with atomic-scale electron energy-loss spectroscopy (EELS) are able to detect the presence of even single impurities and vacancies in SrTiO_3 [1]. The annular dark field (ADF) images (Figure 1) are dominated by heavy strontium and titanium cations, whereas light oxygen anions or their vacancies are still not directly visible. However, the low-angle ADF signal (Figure 1b) can detect the strain fields from oxygen vacancies through their distortion of the adjacent cations and subsequent de-channelling of the electron beam from the cation columns [1]. The strain field is expected to decay below the de-channelling detection limit by the next-nearest neighbour sites, so that at least a unit cell resolution

should be expected for the LAADF image of the vacancy distribution. This experimental study also demonstrates that artificial, vacancy-engineered structures can be produced with a nanometre-scale abruptness. Its limiting factor is the observed clustering of vacancies over a few unit cells.

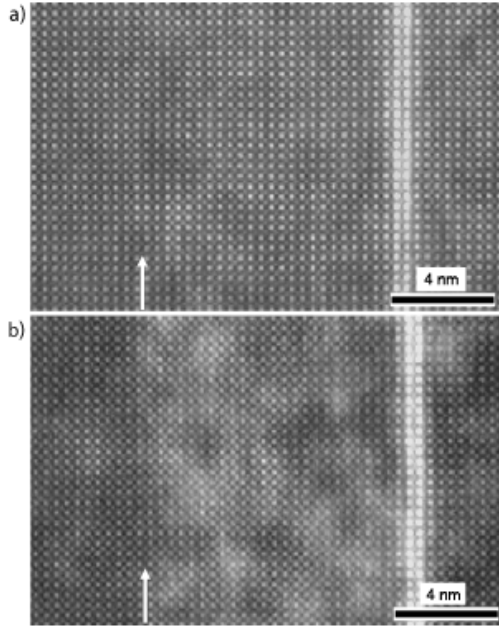


Figure 1. Two STEM images for 25 unit cells of oxygen-deficient $\text{SrTiO}_{3-\delta}$ ($\delta \approx 0.13$) grown on bulk SrTiO_3 (left of white arrow) and capped with a two-layer-thick LaTiO_3 marker (right) and again $\text{SrTiO}_{3-\delta}$ [1]: A) high-angle annular dark field (HAADF) imaging is sensitive mainly to cations and clearly shows the LA marker layer; B) low-angle annular dark field (LAADF) imaging additionally records de-channelling from the strain field surrounding the O vacancies, and the oxygen-deficient layer becomes visible

Oxygen vacancies play a noticeable role in the structural transformations in bulk SrTiO_3 , which possesses two relevant structures: the tetragonal antiferro-distortive (AFD) phase and the cubic phase [9]. The latter (*Figure 2*) is stable above 105 K, whereas AFD (slightly distorted cubic phase) is stable at lower temperatures. When simulating a single point defect, the main problem is to understand changes induced by it in the atomic and electronic structure of a host crystal. Perfect SrTiO_3 crystal has a mixed ionic-covalent nature of the chemical bonding, which is not in complete conformity with the formal charges on Sr^{2+} , Ti^{4+} and O^{2-} ions. The formalism of the Wannier functions applied recently for the determination of charges and bond populations in several perovskite crystals [16] calculated previously using DFT method [17] gives the atomic charge of $+2.55 e$ on titanium and $-1.55 e$ on oxygen, whereas the Ti-O bond order is $0.35 e$; only the charge on Sr is close to the nominal ionic value $+2 e$ confirming that strontium is ionically bounded in SrTiO_3 . Thus, the adequate simulation of the structural defects in strontium titanate is rather complicated, even for a cubic phase. This simplest defect may be described in terms of either *neutral oxygen vacancy* (single O atom removed from the lattice site) or *neutral F centre* (O vacancy with electron density $(2-\delta) e$ remaining in host crystal [16]). Theoretical studies predict mainly equal contributions of the $3d$ orbitals of the two nearest titanium ions (*Figure 2*) into the wave function of the *F* centre [4,10-12]. According to our recent DFT calculations on a cubic phase of SrTiO_3 perovskite [10], the Mulliken electron charge of $1.1-1.3 e$ is localized in the neutral O vacancy (depending on the supercell size) or $0.6-0.8 e$ are equally divided by the two nearest Ti ions if we consider the neutral *F* centre. This result does not confirm formal conclusions made by experimentalists that the neutral *F* centre is supposed to have released both electrons whereas the nearest titanium ions change their valence $\text{Ti}^{4+} \rightarrow \text{Ti}^{3+}$ [1,4,7].

The position of the *F* centre level in the optical band gap of SrTiO_3 is also not completely clear: it is open question, whether it lies well below the conduction band bottom [12] or close to it [4,10,11]. The latter is supported by the indirect experimental study on the conductivity of SrTiO_3 ceramics, suggesting that the *F* centre is a quite shallow defect [18]. Periodic *ab initio* calculations on the SrTiO_3 bulk give the values of the formation energy for O vacancy in the range of $6.5-8.5 eV$ [4,9-11], whereas in cluster models [13], removal of an O atom from the lattice has a higher energy cost ($> 9 eV$). However, this value cannot be directly experimentally measured. Conductivity in SrTiO_3 at low partial oxygen pressures depends on the mobility of O vacancies [3,4,18]. Experiments performed at high temperatures suggest the energy barrier of $0.86 eV$ for the *F* centre diffusion in bulk [6], whereas semi-empirical pair-potential calculations on migration of the empty O vacancy result in the barriers of $0.65 eV$ [14] and $0.76 eV$ [15].

In this paper, we analyze results of both *CRYSTAL* [19] and *VASP* [20] DFT calculations on the *F* centre in a cubic phase of SrTiO_3 perovskite. We have optimized the lattice structural relaxation around

oxygen vacancy for the supercells of different shapes and sizes created by a consequent equidistant extension of crystalline lattice vectors (*Figure 2*) giving from 80- up to 320-atomic cells, in order to eliminate the interaction of periodically repeated point defects. We follow the recent study for the Fe impurities in SrTiO₃ [21]. In such a case we reach the limit of really *single F* defect.

2. Supercell model of a defective crystal

In the first principles band structure calculations, using the primitive unit cell in the direct space, the convergence of the bulk electronic properties (total energy *per* unit cell, band gap and one-electron energies of band edges, the density of states, and electronic charge distribution) can be obtained by an increasing the number of the used \mathbf{k} -points in the primitive Brillouin Zone (BZ) [21]. The one-to-one correspondence was demonstrated [22] between any fixed \mathbf{k} -mesh and the supercell $\{\mathbf{A}_j\}$ in a real space defined by translation vectors \mathbf{a}_i and volume V_a :

$$\mathbf{A}_j = \sum_{i=1}^3 l_{ij} \mathbf{a}_i, \quad (1a)$$

$$V_a = \mathbf{a}_1 \cdot [\mathbf{a}_2 \times \mathbf{a}_3], \quad (1b)$$

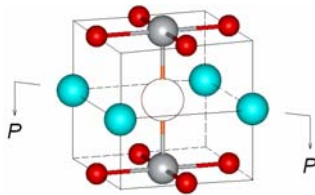
with the index $j = 1, 2, 3$. $L = \det\{l_{ij}\}$ means a number of primitive unit cells in the corresponding supercell. Eq. (1a) can be used to define the corresponding mesh $\{\mathbf{k}_i\}$ of the \mathbf{k} -points in the BZ [23]:

$$\exp(-i \mathbf{k}_t \cdot \mathbf{A}_j) = 1, \quad (2)$$

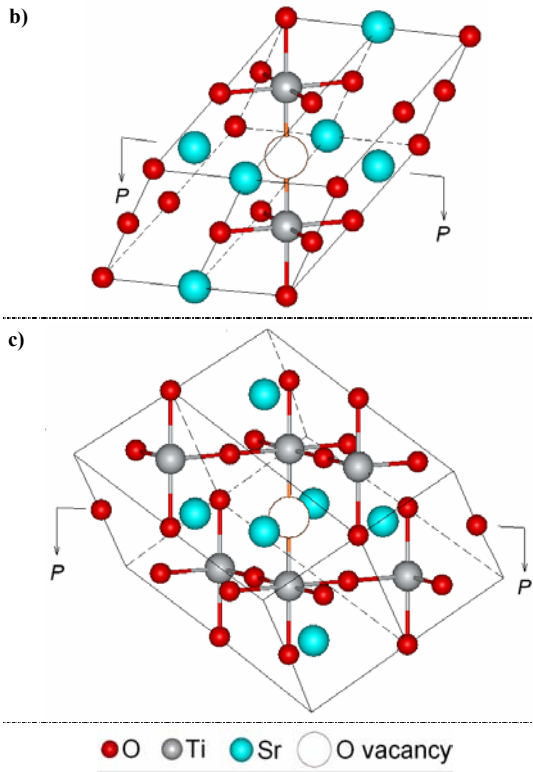
with indexes $j = 1, 2, 3$ and $t = 1, 2, \dots, L$. The absolute value R_M of the smallest \mathbf{A}_j in Eq. (1a) defines the accuracy of the special \mathbf{k} -points set chosen and is called *cutoff length* for a given \mathbf{k} -mesh [21]. Each R_M may be characterized by some number of spheres M of the lattice translation vectors ordered in such a way that the sphere radii are not decreasing [24]. It is possible to choose the matrix $|l_{ij}|$ in Eq. (1a) both diagonal and non-diagonal, but maintaining the point symmetry of the crystalline lattice. By an increasing L , one can ensure increase of the \mathbf{k} -mesh accuracy, and thus the accuracy of the corresponding supercell modelling of the perfect crystal. Thus, one can say that an increase of the \mathbf{k} -mesh accuracy in self-consistent band structure calculations with primitive cell means in fact that the perfect crystal is modelled by a *sequence* of supercells of the increasing size.

Use of supercell model for point defect simulation means, in fact, consideration of a “new crystal” with an artificially introduced periodicity. The point defect period is defined by a choice of supercell, the space group of a defective crystal in superlattice is defined by the local point symmetry of a defect and the chosen lattice of supercells [25]. A new, narrowed BZ is L -fold smaller than the original (primitive) one and may also differ, when the type of lattice is changed by the transformation in Eq. (1a). The calculation is made in the same way as for a perfect crystal using the \mathbf{k} -sampling of the BZ. In practical calculations the \mathbf{k} -sets are used which allow to minimize the defect-defect interaction [26] for a fixed supercell size and shape. Use of the \mathbf{k} -meshes in supercell model allows one to estimate the role of defect-defect interaction through the width of the defect energy bands for each superlattice chosen: the narrower these bands are, the closer the results obtained are to the *single* defect limit. It is possible to find such a \mathbf{k} -mesh, which ensures a compromise between the size of supercell and a reasonable reproduction of the total and one-electron energies, as well as the electron density distribution in the host crystal: the \mathbf{k} -point sets satisfying Eq. (2) is usually used for this purpose [21]. It is reasonable to begin from the smaller supercell containing point defect, *i.e.* corresponding to the converged results of the band calculations. In the particular case of the SrTiO₃ crystal, the supercell of 80 atoms was chosen. When estimating the defect-defect interaction from the calculated defect bandwidth, we make a decision about the necessity of a further increase of the supercell. As shown for Fe impurity in SrTiO₃ [21], the iron bandwidth still changes considerably when supercell is increased from 80 to 160 atoms, which is sufficiently large. The comparison of supercell results for different \mathbf{k} -meshes allows one to decide, if it is necessary to increase a superlattice, in order to surpass artificial defect-defect interaction.

a)



Simple cubic (sc) structure of SrTiO₃ crystal is mainly described using the $Pm\bar{3}m$ space group [19]. However, the origin of crystallographic coordinates in this case is occupied by a strontium ion. To put O vacancy in the centre, we use the $P4/mmm$ space group (*Figure 2*). This model allows us to show both



the nearest neighbours of vacancy and the lattice relaxation around it. *CRYSTAL* and *VASP* calculations on a single *F* centre have been performed for the supercells of different shapes and sizes, created by a consequent equidistant extension of the lattice vectors: 80- and 270- atom face-centred cells, 135- and 320-atom simple cubic cells, as well as 160-atom base-centred cell. The corresponding *sc*-, *fcc*- and *bcc*-extensions of the SrTiO_3 unit cell shown in *Figure 2a* are described by the transformation matrices defined in Eq. (1a):

$$\begin{vmatrix} n & 0 & 0 \\ 0 & n & 0 \\ 0 & 0 & n \end{vmatrix}, \begin{vmatrix} 0 & n & n \\ n & 0 & n \\ n & n & 0 \end{vmatrix} \text{ and } \begin{vmatrix} -n & n & n \\ n & -n & n \\ n & n & -n \end{vmatrix}, \quad (3)$$

respectively, where n is varied between 2 and 4.

Figure 2. Three types of equidistant crystalline cells with a centred O vacancy for the cubic phase of SrTiO_3 perovskite: a) simple cubic (*sc*); b) face centred cubic (*fcc*); c) base centred cubic (*bcc*). Sticks between the oxygen and titanium ions indicate the partly covalent bonds between them. In order to construct the difference electron density plots shown in Figures 3 and 4, each cell is sectioned along the $-\text{Ti}-\text{O}-\text{Ti}-$ axis by the same plane P-P

The length of cube edge in SrTiO_3 unit cell (*Figure 2a*) is equal to the lattice constant (experimental value is 3.905 Å [9]). Strontium titanate supercells with *sc*-extensions of $3 \times 3 \times 3$ (135 atoms) and $4 \times 4 \times 4$ (320 atoms) possess the same cubic symmetry, with 90° angle between the lattice vectors. In its turn, supercells with the *fcc*-extensions $2\sqrt{2} \times 2\sqrt{2} \times 2\sqrt{2}$ (80 atoms) and $3\sqrt{2} \times 3\sqrt{2} \times 3\sqrt{2}$ (270 atoms) are rhombohedral with 60° angle between the lattice vectors (*Figure 2b*). Lastly, for 160-atom rhombohedral *bcc*-supercell (extension $2\sqrt{3} \times 2\sqrt{3} \times 2\sqrt{3}$), the angle is 109.47° . According to Eq. (1b) the ratio of volumes for the supercells extended from the SrTiO_3 unit cell using matrices, Eq. (3), with the same n is:

$$V_{bcc} = 2V_{fcc} = 4V_{sc}. \quad (4)$$

For all three types of equidistant cells shown in *Figure 2*, their shapes correlate with the orientation of $-\text{Ti}-\text{O}-\text{Ti}-$ axis, it may be: (i) the rotation axis joining the centres of opposite faces (*Figure 2a*), (ii) the diagonal joining the opposite apexes of rhombohedron (*Figure 2b*), and (iii) the axis joining the centres of opposite rhombohedron edges (*Figure 2c*).

3. Computational background

3.1. CRYSTAL CALCULATIONS

The computational scheme implemented in *CRYSTAL-03* code [19] includes both Hartree-Fock (HF) and DFT *ab initio* methods achieved via the self-consistent field solution of the one-electron equations:

$$\hat{h}_i \varphi_{\mathbf{k}i}(\mathbf{r}) = \varepsilon_{\mathbf{k}i} \varphi_{\mathbf{k}i}(\mathbf{r}), \quad (5)$$

where crystalline orbitals of the N -electron system are expanded as linear combinations of a set of m Bloch functions built from the local, atom-centred Gaussian-type functions (GTFs):

$$\varphi_{\mathbf{k}i}(\mathbf{r}) = N \sum_{j=1}^m a_{ij}(\mathbf{k}) \left(\sum_{\mathbf{g}} \chi_{\mathbf{g}j}(\mathbf{r}) \exp(i\mathbf{k} \cdot \mathbf{g}) \right), \quad (6a)$$

$$\chi_{\mathbf{g}j}(\mathbf{r} - \mathbf{R}_j) = \sum_{\mu} c_{\mu} G(\alpha_{\mu}; \mathbf{r} - \mathbf{R}_j - \mathbf{g}), \quad (6b)$$

where \mathbf{k} is the wave vector of the irreducible representation of the group of crystal translations $\{\mathbf{g}\}$; \mathbf{R}_j denotes the coordinates of nuclei in the zero cell of which atomic orbital $\chi_{\mathbf{g}}(\mathbf{r})$ is centred; G , c_μ and α_μ are normalized GTF, its coefficients and exponents, respectively.

Crystalline Hamiltonian can be constructed using both HF and DFT (Kohn-Sham) formalisms, in both *direct* and *reciprocal* space:

$$\hat{H}^{HF} = \hat{T}(\mathbf{r}; \mathbf{k}) + \hat{V}(\mathbf{r}; \mathbf{k}) + \hat{J}(\mathbf{r}; \mathbf{k}) + \hat{K}(\mathbf{r}; \mathbf{k}), \quad (7a)$$

$$\hat{H}^{KS} = \hat{T}(\mathbf{r}; \mathbf{k}) + \hat{V}(\mathbf{r}; \mathbf{k}) + \hat{J}[\rho(\mathbf{r}); \mathbf{k}] + \hat{v}_{xc}[\rho(\mathbf{r}); \mathbf{k}], \quad (7b)$$

where \hat{T} , \hat{V} , \hat{J} and \hat{K} are kinetic, electron-nuclei, Coulomb and non-local exchange operators, whereas:

$$\hat{v}_{xc} = \frac{\partial E_{xc}[\rho(\mathbf{r}); \mathbf{k}]}{\partial \rho(\mathbf{r})}, \quad (8a)$$

$$\rho(\mathbf{r}) = \int_{\text{Brillouin zone}} \sum_i^{\text{occupied bands}} |\varphi_{\mathbf{k}i}(\mathbf{r})|^2 \theta\{\varepsilon_F - \varepsilon_i(\mathbf{k})\} d\mathbf{k}, \quad (8b)$$

where E_{xc} is the exchange-correlation energy functional of the electron density $\rho(\mathbf{r})$, θ is a Heaviside zero-temperature occupation function, ε_F is the Fermi energy which determines the occupied manifold in \mathbf{k} -space, and $\varepsilon_i(\mathbf{k})$ are the eigenvalues of the crystalline orbitals.

The choice of exchange-correlation functional \hat{v}_{xc} for *CRYSTAL* calculations using DFT method is an important point necessary to obtain adequate results. When modelling SrTiO₃ perovskite, including bulk [17] and densely packed surfaces [27], the better results were obtained when using non-local Generalized Gradient Approximation (*GGA*), combining Becke exchange functional [28] with a correlation functional constructed by Perdew and Wang [29]. However, even this approach possesses certain shortcomings, especially when estimating band gap $\Delta\varepsilon_{\text{gap}}$: HF calculations markedly overestimate this value, but DFT calculations usually underestimate it. In order to avoid this artefact, *CRYSTAL-03* code [19] realizes a partial incorporation of the exact HF exchange into the DFT exchange functional, with varying mixing ratio. We have chosen hybrid *B3PW* exchange-correlation energy functional [30]:

$$E_{xc} = (1 - a_h)E_x^{LDA} + a_x\Delta E_x^{\text{Becke}} + a_hE_x^{HF} + a_c\Delta E_c^{PWGGA}, \quad (9)$$

where $\Delta E_x^{\text{Becke}}$ is Becke's gradient correction to the exchange energy functional of local density E_x^{LDA} [28], E_x^{HF} the exact HF exchange energy, ΔE_c^{PWGGA} the gradient correction for correlation energy of Perdew-Wang [29], a_h is input parameter of the HF/DFT exchange mixing; a_x and a_c are input parameters of the DFT exchange (x) and correlation (c) non-locality (*GGA/LDA*), respectively.

TABLE 1. All-electron basis set for oxygen

Shell	Exponent (α_μ)	Contraction (c_μ)		
		s	p	d
1s	8020.0	0.00108	-	-
	1338.0	0.00804	-	-
	255.4	0.05324	-	-
	69.22	0.1681	-	-
	23.90	0.3581	-	-
	9.264	0.3855	-	-
	3.851	0.1468	-	-
	1.212	0.0728	-	-
2sp	49.43	0.00883	0.00958	-
	10.47	-0.0915	0.0696	-
	3.235	-0.0402	0.2065	-
	1.217	0.379	0.347	-
3sp	0.4521	1.0	1.0	-
4sp	0.1679	1.0	1.0	-
3d	0.45099	-	-	1.0

A proper choice and further re-optimization of the basis sets (BSs), consisting of the GTFs' coefficients and exponents defined by Eq. (6b), is another crucial point in the *CRYSTAL* calculations. For oxygen, the all-electron 8-411sp-1d BS with re-optimized outermost exponents there was used (*Table 1*). A small core Hay-Wadt pseudopotentials [31] were included in the BSs for both Ti (411sp-311d) and Sr (311sp-1d), their outermost shells were re-optimized more carefully (*Table 2*). Optimization of all BSs was performed using the *ParOptimize* code [32], which implements conjugated gradients optimization technique with a numerical computation of derivatives [33]. Fitting of the optimized BSs has been checked by calculating the lattice constant, bulk modulus and elastic constants of SrTiO₃ bulk as well as its band structure, density of states and other electronic properties [34]. As to the F centres and O vacancies, they were calculated by a removing oxygen ion as shown in *Figure 2* and either retaining in the vacancy the ghost wave function of O or not.

TABLE 2. Basis sets for outermost Ti and Sr orbitals constructed using HayWSC pseudopotential [26]

Shell	Ti				Sr			
	Exponent (α_μ)	Contraction (c_μ)			Exponent (α_μ)	Contraction (c_μ)		
		s	p	d		s	p	d
1s	HAYWSC				HAYWSC			
2sp								
3sp								
	16.6627995	0.0052882765	-0.002472365	-				
	3.82352098	0.348881629	-0.490787025	-				
	3.76734787	0.2	0.5	-				
	1.33437747	1.699	0.875	-				
4sp	0.7725692	1.0	1.0	-	16.7295003	-0.040864984	0.0064288549	-
					2.23218348	1.0	1.0	-
					1.98458795	9.26146754	-0.963768104	-
5sp	0.4369296	1.0	1.0	-	0.6537827	1.0	1.0	-
6sp	-	-	-	-	0.2609586	1.0	1.0	-
3d	21.429541	-	-	0.088078981	HAYWSC			
	6.08722431	-	-	0.417373956				
	2.07945196	-	-	1.0				
4d	0.8310327	-	-	1.0	0.4699451	-	-	1.0
5d	0.3562744	-	-	1.0	-	-	-	-

The reciprocal space integration for models of the F centre in SrTiO_3 (Section 2) has been performed with the suitable integer shrinking factors for the Monkhorst-Pack and Gilat nets [35,36]: $2 \times 2 \times 2$ and $4 \times 4 \times 4$.

3.2. VASP CALCULATIONS

The computational procedure of the *VASP* code [20,37] includes an iterative solution of the Kohn–Sham equations based on residuum-minimization and optimized charge-density mixing routines [38]. This includes the calculations of the Hellmann–Feynman forces acting on the atoms and of the stresses on the unit cell [37]. The total energy is optimized with respect to the positions of the atoms within unit cell or supercell. The Kohn–Sham method employing a plane-wave basis set and the pseudopotential (PP) approximation are currently among the most successful techniques in computational material science [39]. However, its formal simplicity demanded a price: first-row elements, transition metals, and rare-earth elements were found to be computationally consuming to treat with standard norm-conserving PPs [40]. Various attempts were made to generate more soft PPs: one of the most advanced approaches was the concept of *ultra soft* pseudopotentials (US-PP) introduced by Vanderbilt [41], which was briefly described in our previous paper [42]. But its success is partly hampered by the difficult construction of the pseudopotentials, *i.e.*, too many parameters (several cut-off-radii) must be chosen and therefore extensive tests are required to obtain an accurate and highly transferable US-PP. Further development of this concept has been made by Blöchl [43] by combining ideas from pseudopotential and LAPW (Linearized Augmented-Plane-Wave) methods in a framework, called the Projector Augmented-Wave Method (PAW). Recently, formalism of PAW method has been successfully implemented into the *VASP* code [20,44], which allows users to combine it with earlier implemented US-PP approach.

The main idea of PAW method is to transform the physically relevant full all-electron (AE) Kohn–Sham wave functions Ψ_n onto computationally convenient pseudo-wave soft (PS) variation functions $\tilde{\Psi}_n$ [43]. The AE function may be derived from the PS function by means of a linear transformation:

$$|\Psi_n\rangle = |\tilde{\Psi}_n\rangle + \sum_i (|\varphi_i\rangle - |\tilde{\varphi}_i\rangle) \langle \tilde{p}_i | \tilde{\Psi}_n \rangle, \quad (10)$$

where the AE partial waves φ_i are obtained for a reference atom whereas the PS partial waves $\tilde{\varphi}_i$ are equivalent to the AE partial waves outside a core radius r_c^l and match continuously onto $\tilde{\varphi}_i$ inside the core radius (the augmentation region, similar to the linearized muffin-tin LMTO formalism); the index i is a shorthand for the atomic site \mathbf{R}_i , the angular momentum numbers $M = l, m$, and an additional index k referring to the one-electron reference energy ε_{kl} . The core radius is usually chosen approximately around half the nearest-neighbour distance [44]. The projector functions \tilde{p}_i are dual to the PS partial waves:

$$\langle \tilde{p}_i | \tilde{\varphi}_j \rangle = \delta_{ij} . \quad (11)$$

In the PAW method, the all-electron charge density is given by [41]:

$$n(\mathbf{r}) = \tilde{n}(\mathbf{r}) + n^1(\mathbf{r}) - \tilde{n}^1(\mathbf{r}) , \quad (12)$$

where $\tilde{n}(\mathbf{r})$ is the soft pseudo-charge-density calculated directly from the pseudo-wave-functions on a plane-wave grid *via* the occupations f_n of the states n :

$$\tilde{n}(\mathbf{r}) = \sum_n f_n \langle \tilde{\Psi}_n | \mathbf{r} \rangle \langle \mathbf{r} | \tilde{\Psi}_n \rangle . \quad (13a)$$

The onsite charge densities n^1 and \tilde{n}^1 are treated on a radial support grid, that extends up to r_{rad} around each ion. They are defined as:

$$n^1(\mathbf{r}) = \sum_n \rho_{ij} \langle \varphi_i | \mathbf{r} \rangle \langle \mathbf{r} | \varphi_j \rangle , \quad (13b)$$

$$\tilde{n}^1(\mathbf{r}) = \sum_n \rho_{ij} \langle \tilde{\varphi}_i | \mathbf{r} \rangle \langle \mathbf{r} | \tilde{\varphi}_j \rangle , \quad (13c)$$

where ρ_{ij} are the occupancies of each augmentation channel (i, j) and they are calculated from the pseudo-wave-functions applying the projector functions:

$$\rho_{ij} = \sum_n f_n \langle \tilde{\Psi}_n | \tilde{p}_i \rangle \langle \tilde{p}_j | \tilde{\Psi}_n \rangle . \quad (14)$$

The total charge density n_T is also decomposed into three terms [44], analogously to $n(\mathbf{r})$ in Eq. (12):

$$n_T = n + n_{Zc} = \tilde{n}_T + n_T^1 - \tilde{n}_T^1 = (\tilde{n} + \hat{n} + \tilde{n}_{Zc}) + (n^1 + n_{Zc}) - (\tilde{n}^1 + \hat{n} + \tilde{n}_{Zc}) , \quad (15)$$

where n_{Zc} is the point charge density of the nuclei n_Z plus the frozen core AE charge density n_c and \hat{n} is a compensation charge which is added to the soft charge densities $(\tilde{n} + \tilde{n}_{Zc})$ and $(\tilde{n}^1 + \tilde{n}_{Zc})$ in order to reproduce the correct multi-pole moments of the AE charge density $(n^1 + n_{Zc})$ that is located in each augmentation region. Because n_{Zc} and \tilde{n}_{Zc} have exactly the same monopole ($-Z_{\text{ion}}$) and vanishing multi-poles, the compensation charge \hat{n} must be chosen so that $(\tilde{n}^1 + \hat{n})$ has the same moments as the AE valence charge density n^1 within each sphere [44]. For this purpose, compensation functions $g_l(|\mathbf{r}-\mathbf{R}|)$ are constructed for which the moment l is equal 1.

To obtain the Hamilton operator for the modified PAW total energy functional, the total energy must be varied with respect to the pseudo-density operator $\rho = \sum_n f_n |\tilde{\Psi}_n\rangle \langle \tilde{\Psi}_n|$ [44]:

$$H[\rho, \{\mathbf{R}\}] = \frac{dE}{d\rho} = \frac{d\tilde{E}}{d\rho} + \frac{dE^1}{d\rho} - \frac{d\tilde{E}^1}{d\rho} = -\frac{1}{2}\Delta + \tilde{v}_{\text{eff}} + \sum_{(i,j)} |\tilde{p}_i\rangle \left(\frac{\partial \tilde{E}}{\partial \rho_{ij}} + \frac{\partial E^1}{\partial \rho_{ij}} - \frac{\partial \tilde{E}^1}{\partial \rho_{ij}} \right) \langle \tilde{p}_j| , \quad (16)$$

where the first two terms (kinetic-energy operator $-\frac{1}{2}\Delta$ and effective one-electron potential \tilde{v}_{eff}) are presented in any Kohn-Sham Hamiltonian, as written in Eq. (7b). Potential \tilde{v}_{eff} includes both Hartree and exchange-correlation parts:

$$\tilde{v}_{\text{eff}} = v_H[\tilde{n} + \hat{n} + \tilde{n}_{Zc}] + v_{xc}[\tilde{n} + \hat{n} + \tilde{n}_c] . \quad (17)$$

The last terms of Hamiltonian in Eq. (16) are expressed *via* $-\frac{1}{2}\Delta$, \tilde{v}_{eff} and operator $\hat{Q}_{ij}^M(\mathbf{r})$ of the charge density differences between the partial waves $Q_{ij}(\mathbf{r}) = \varphi_i^*(\mathbf{r})\varphi_j(\mathbf{r}) - \tilde{\varphi}_i^*(\mathbf{r})\tilde{\varphi}_j(\mathbf{r})$ and their moments q_{ij}^M :

$$q_{ij}^M = \int_{\Omega_r} Q_{ij}(\mathbf{r}) |\mathbf{r} - \mathbf{R}|^l Y_M^*(\mathbf{r} - \mathbf{R}) d\mathbf{r} , \quad (18a)$$

$$\hat{Q}_{ij}^M(\mathbf{r}) = q_{ij}^M g_l(|\mathbf{r} - \mathbf{R}|) Y_M^*(\overleftarrow{\mathbf{r} - \mathbf{R}}), \quad (18b)$$

where \int_{Ω_r} stands for the integration on the radial support grid, M is a shortland for (l, m) quantum numbers whereas Y_M is an angular part of wave function. Thus, last terms of PAW Hamiltonian are [44]:

$$\frac{\partial \tilde{E}}{\partial \rho_{ij}} = \sum_M \int \tilde{v}_{eff}(\mathbf{r}) \hat{Q}_{ij}^M(\mathbf{r}) d\mathbf{r}, \quad (19a)$$

$$\frac{\partial E^1}{\partial \rho_{ij}} = \left\langle \tilde{\varphi}_i \left| -\frac{1}{2} \Delta + v_H[n^1 + n_{Zc}] + v_{xc}[n^1 + n_c] \right| \tilde{\varphi}_j \right\rangle, \quad (19b)$$

$$\frac{\partial \tilde{E}^1}{\partial \rho_{ij}} = \left\langle \tilde{\varphi}_i \left| -\frac{1}{2} \Delta + \tilde{v}_{eff} \right| \tilde{\varphi}_j \right\rangle + \int_{\Omega_r} \tilde{v}_{eff}(\mathbf{r}) \hat{Q}_{ij}^M(\mathbf{r}) d\mathbf{r}. \quad (19c)$$

To define the PAW data set, the following quantities are required: (i) the AE and PS partial waves φ_i and $\tilde{\varphi}_i$; (ii) the projector functions \tilde{p}_i ; (iii) the core-charge density n_c , the pseudized core-charge density \tilde{n}_{Zc} and the partial electronic core-charge density \tilde{n}_c ; (iv) the compensation functions $g_l(|\mathbf{r} - \mathbf{R}|)$ [20,44].

The *VASP* plane wave calculations of the oxygen vacancy in SrTiO_3 crystal (for supercells described in Section 2) have been performed by us using the PAW pseudopotentials for the inner cores of all atoms [20,44], while the kinetic energy cut-off (determining the whole set of plane waves with smaller energy included in the basis set) has been chosen as $E_{cut} = 415$ eV. The Monkhorst-Pack [35] \mathbf{k} -mesh has been employed for the energy evaluation with a density ranging from 0.04 to 0.51 \AA^{-1} . The GGA-type exchange-correlation functional was chosen in the PW91 formulation [29]. The advantage of *VASP* plane wave calculations [20] is that the complete optimization of lattice relaxation upon vacancy creation, even for large supercells, can be performed much faster than for *CRYSTAL* calculations based on the localized basis sets [19]. Geometry optimizations have been carried out with an accuracy 10^{-3} eV in the total energy. The electronic structure of defective SrTiO_3 perovskite calculated using both *CRYSTAL* and *VASP* codes has been studied for the diamagnetic closed electronic shell (singlet) state since we did not found any lower state employing the spin polarized calculations [10].

4. Atomic and electronic structure of F centres in a cubic SrTiO_3 crystal

Basic properties of a perfect cubic SrTiO_3 crystal calculated using *CRYSTAL* code were analyzed in detail elsewhere [16,17,34]. The lattice constant, a_o , bulk modulus, B , as well as elastic constants, c_{11} , c_{12} , and c_{44} , were obtained rather close to the experimental values (3.90 \AA [45], 179 GPa [46], and 31.72, 10.25, and 12.35 $\times 10^{11}$ dyne/cm² [47], respectively) in almost all the methods employed in the framework of HF and DFT computational schemes. However, the parameters of the electronic structure were found to be quite sensitive to the method chosen. The best agreement with experimental results was obtained for the *hybrid* exchange technique (B3PW [30]) described in Subsection 3.1. Further improvement of the calculated optical gap was achieved by adding the d polarization orbital into the oxygen basis set (Table 1): at the Γ point of the first BZ $\Delta \varepsilon_{\text{gap}}^\Gamma = 3.65$ eV, quite close to the experiment, 3.25 eV for the indirect band gap [8]. The local properties of the electronic structure (charges and bond orders) for perfect SrTiO_3 crystal obtained using formalism of Wannier functions [16] have been considered above (Section 1).

When performing *VASP*-PAW calculations using the PW91 exchange-correlation functional, the structural parameters of cubic SrTiO_3 again were found to be quite reasonable: $a_o = 3.92$ \AA and $B = 182$ GPa [10]. However, the optical band gap of 2.59 eV is the evident underestimate, typical for this method [48]. Nevertheless, the LDA- U treatment of GGA exchange-correlation functional [49] as recently implemented in the *VASP* code [20] can describe the band gap qualitatively properly, analogously to hybrid HF-DFT methods as implemented in *CRYSTAL* code [19].

4.1. OXYGEN VACANCY FORMATION AND MIGRATION

The formation energy of F centre in SrTiO_3 crystal has been estimated as follows [10]:

$$E^{\text{form}}(F) = E(O) + E(F) - E(\text{perfect}), \quad (20)$$

where $E(O)$ is the energy for spin-polarized isolated oxygen atom (3P state), $E(F)$ and $E(\text{perfect})$ the energies of the defective and perfect crystals, respectively. Similar approach for the determination of $E^{\text{form}}(F)$ was used in Ref. [4]. In alternative approach [9,11], the formation energies of O vacancy were expressed *via* chemical potentials of O, Sr and Ti atoms. However, the range of $E^{\text{form}}(F)$ calculated using both approaches for supercells of different shapes and sizes (6.5–8.5 eV, as mentioned in Section 1) is not so large to give a preference to one of them. Table 3 shows dependence of the vacancy formation energy in SrTiO₃ bulk on both supercell shape and size, which is accompanied by the large contribution coming from the lattice relaxation upon vacancy formation. The formation energy is reduced considerably (1.5–2.0 eV) when the positions of all atoms in the supercells are fully optimized. This demonstrates that the relaxation of even 14 nearest ions (neighbouring Ti-, O- and Sr- coordination spheres directly shown in Figure 2a) might rather insufficient, inclusion of next-nearest coordination spheres is necessary (Table 4). Moreover, the lattice relaxation around the defect is also periodically repeated, thus affecting the calculated total energy *per cell*: the larger is supercell, the smaller is this artefact. We consider here only values of $E^{\text{form}}(F)$ estimated in *VASP* calculations since complete optimization of the lattice relaxation in the large supercells is practically impossible for *CRYSTAL* code. The defect formation energies mainly decrease with the increase of the supercell size, but it also depends on the shape of supercell (*cf.* the corresponding values for *fcc* 80-atomic and *sc* 135-atomic cells).

TABLE 3. Dependence of the nearest distance between F centres (d_{F-F}), the formation energy of a single oxygen vacancy $E^{\text{form}}(F)$ and the energy barrier $\Delta E^{\text{diff}}(F)$ of its (011) migration on both shape and size of supercell used for *VASP*-calculations with $2 \times 2 \times 2$ κ -mesh

Supercell	Extension	Type of lattice	d_{F-F} , Å	$E^{\text{form}}(F)$, eV		$\Delta E^{\text{diff}}(F)$, eV
				un-relaxed	relaxed	
80-atom	$2\sqrt{2} \times 2\sqrt{2} \times 2\sqrt{2}$	<i>fcc</i>	11.04	9,00	7,73	0,41
135-atom	$3 \times 3 \times 3$	<i>sc</i>	11.71	9,17	7,89	0,35
160-atom	$2\sqrt{3} \times 2\sqrt{3} \times 2\sqrt{3}$	<i>bcc</i>	13.52	8,98	7,35	0,50
270-atom	$3\sqrt{2} \times 3\sqrt{2} \times 3\sqrt{2}$	<i>fcc</i>	16.56	8,98	7,17	0,38

In order to calculate the energy barrier $\Delta E^{\text{diff}}(F)$ for oxygen vacancy migration using *VASP* code (Table 3), we consider jump of the O atom from the eight possible sites nearest to the F centre (Figure 2a) towards the vacancy. We have estimated the saddle-point energy by fixing a hopping O atom at the middle between the existing and newly formed vacancies, while the rest of the lattice has been allowed to relax. Values of $\Delta E^{\text{diff}}(F)$ (Table 3) are sensitive to both shape and size of SrTiO₃ supercell, moreover, for optimized rhombohedral *fcc* and *bcc* supercells (Figures 2b,c), the migration trajectories are not completely equivalent. Nevertheless, migration energies mainly decrease with the increase of the supercell size. Unfortunately, values of $E^{\text{form}}(F)$ and $\Delta E^{\text{diff}}(F)$ for the $4 \times 4 \times 4$ supercell of 320 atoms could not be calculated due to computational limitation.

TABLE 4. Dependence of lattice relaxation for the nearest atoms around single F centre in a cubic SrTiO₃ crystal on both shape (Figure 2) and size (Table 3) of supercells (SCs) used in *VASP*-calculations with $2 \times 2 \times 2$ κ -mesh

Atoms nearest to F centre	Un-relaxed distance from F centre, a_0	Un-relaxed coordinates			Number of atoms shifted equivalently	Relative shifts δR_i from un-relaxed positions*, %				
		x_i	y_i	z_i		80-atom SC, <i>fcc</i>	135-atom SC, <i>sc</i>	160-atom SC, <i>bcc</i>	270-atom SC, <i>fcc</i>	320-atom SC, <i>sc</i>
Ti	$a_0/2$	0	0	$\pm a_0/2$	2	7.21	7.16	7.08	8.28	7.76
O	$a_0/\sqrt{2}$	$\pm a_0/2$	0	$\pm a_0/2$	8	-7.59	-7.92	-7.98	-7.43	-7.79
		0	$\pm a_0/2$	$\pm a_0/2$						
Sr	$a_0/\sqrt{2}$	$\pm a_0/2$	$\pm a_0/2$	0	4	3.51	3.48	3.45	3.42	3.94
O	a_0	$\pm a_0$	0	0	4	3.16	2.98	2.49	2.87	3.56
		0	$\pm a_0$	0						
O	a_0	0	0	$\pm a_0$	2	-1.72	-1.56	-1.67	-1.05	-1.28

* Positive shift corresponds to expansion of the atomic coordination sphere whereas negative sign means its compression

The sensitivity of lattice relaxation to both supercell shape and size is clearly seen in Table 4. For the same type of superlattice (*sc*, *fcc* or *bcc*), expansion of the first coordination sphere (two Ti ions) is larger whereas compression of the second sphere (eight O ions) is smaller with increasing size of supercell, *etc.* However, the convergence of the lattice relaxation is complex and very low concentration

of single F centres should be used in crystalline models to achieve it. For instance, fcc supercells are stretched along the z axis and compressed in the xy -plane (Figure 2b). This causes the larger z -shifts of Ti ions nearest to O vacancy in 80- and 270-atomic fcc supercells as compared to 135- and 320-atomic cubic supercells (Table 4), whereas xy -shifts of the nearest O and Sr ions are smaller in the first case. Nevertheless, the range of δR_i for equivalently shifted atoms in equidistant supercells of different shapes and sizes is small enough ($\leq 1.0\%$) to conclude about the stabilization of single oxygen vacancy in a cubic SrTiO_3 crystal when using large equidistant supercells (containing ≥ 270 –320 atoms). When trying to use *CRYSTAL* code for the partial optimization of total energy for the same supercells, we obtained markedly smaller expansion of the first coordination sphere involving two nearest titanium ions as compared to *VASP* complete optimization (1.5–2% vs. 7–8%). The same is true for the next-nearest coordination spheres, which is an additional argument in favour the *VASP* optimization. More realistic results were obtained when using *VASP* optimized geometries as external inputs for *CRYSTAL* re-calculations.

4.2. ELECTRONIC CHARGE REDISTRIBUTION AROUND OXYGEN VACANCIES

To get deeper insight to the defective SrTiO_3 bulk from the *CRYSTAL* calculations on superlattices described in Section 2, we have analyzed various parameters of its electronic structure. In this Subsection, we consider the electronic properties of a single F centre in un-relaxed supercells. Redistribution of the electron density after oxygen vacancy formation can be analyzed in Figures 3 and 4 as calculated for the equidistant supercells with different extensions. In both *Figures*, the Mulliken electron charge (1.1–1.3 e) is localized within *neutral* O vacancy, in other words, 0.6–0.8 e is equally divided by the two Ti ions nearest to the *neutral* F centre and mainly localized on their $3d(z^2)$ orbitals, making the largest contribution to the defect bands shown in Figures 5–7.

Figure 3 clearly demonstrates the effect of size of the same fcc -type supercell ($2\sqrt{2} \times 2\sqrt{2} \times 2\sqrt{2}$ and $3\sqrt{2} \times 3\sqrt{2} \times 3\sqrt{2}$ extensions) on localization of the charge redistribution. For 80-atomic SC mutual influence of the neighbouring O vacancies is clearly seen, especially along $-\text{Ti}-\text{O}-\text{Ti}-$ axes, whereas for 270-atomic SC, the more-or-less visible re-distribution of the electron density is limited by ± 1.5 – $2.0 a_0$ in the z -direction. Comparison of charge re-distributions shown in *Figure 4* allows us to draw analogous conclusions. For 160-atomic SC (Figure 4a), mutual influence of the neighbouring O vacancies is not so noticeable as for 80-atomic SC (Figure 3a), however, it is practically absent in 320-atomic SC (Figure 4b) where well-localized charge re-distribution is limited by ± 1.5 – $2.0 a_0$ in the z -direction. Thus, both 270- and 320-atomic supercells of cubic SrTiO_3 crystal may be considered as models of a quasi-isolated F centre.

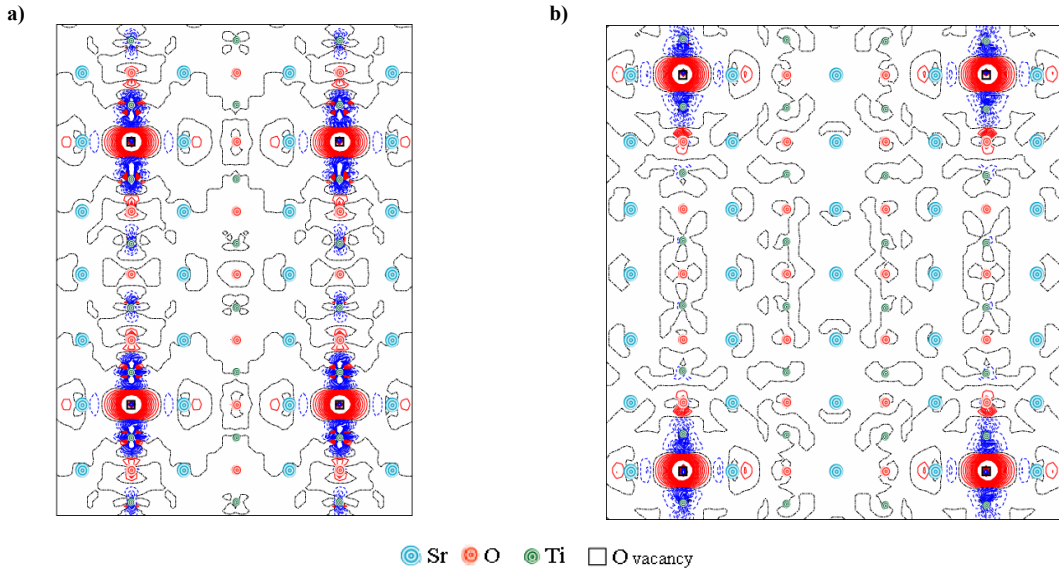


Figure 3. Two-dimensional (2D) difference electron density maps $\Delta\rho(\mathbf{R})$ (the total density in the perfect SrTiO_3 bulk minus the sum of electron densities of both isolated oxygen atoms inside supercells and defective SrTiO_3) projected onto the (110) section plane P - P (Figure 2b) for 80-atomic (A) and 270-atomic (B) FCC supercells containing a single oxygen vacancy. Dash-dot isolines correspond to the zero level. Solid and dash isolines describe positive and negative values of electron density, respectively. Isodensity increment is $0.002 e \text{ \AA}^{-3}$

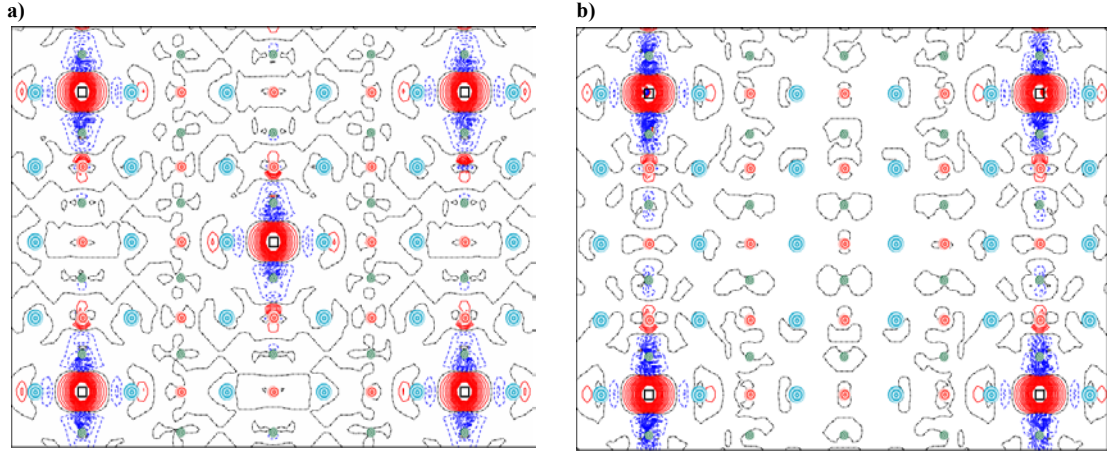


Figure 4. 2D difference electron density maps $\Delta\rho(\mathbf{R})$ projected onto the (110) section plane P - P (Figure 2) for two different supercells containing a single oxygen vacancy: A) 160-atomic BCC cell; B) 320-atomic SC cell. See caption of Figure 3 for explanation

4.3. BAND STRUCTURE OF DEFECTIVE SrTiO_3 WITHOUT AND WITH LATTICE RELAXATION

As mentioned before, the *VASP* code [20] is markedly more efficient for optimization of the lattice relaxation around vacancy than *CRYSTAL* [19]. However, the latter possesses the noticeable advantage when describing the electronic properties of defective crystals. For instance, remaining “ghost” orbitals localized at the position of removed atom allows us to observe the defect band within optical gap (Figures 5-7). The defect-defect coupling is also seen in the *CRYSTAL*-B3PW calculations. This is not possible for the *VASP* code, which can be applied only for the indirect analysis of different O-deficient structures through analysis of the total and projected densities of states (DOS). Moreover, the semi-conducting nature of SrTiO_3 is poorly reproduced within the PW91 exchange-correlation functional [29] used in *VASP* calculations since the optical gap is underestimated as stated before (by 0.8 eV).

According to *CRYSTAL*-B3PW calculations on SrTiO_3 bulk with *un-relaxed* lattice around F centres (Table 5 as well as Figures 5 and 6), the defect energy level in the band gap $\Delta\varepsilon_{db-gap}^{\Gamma}$ approaches the conduction band bottom, beginning with 0.69 eV for 80-atomic supercell (with the bandwidth 0.15 eV), down to 0.57 eV (0.08 eV) for 160-atoms, and reaches the optical ionization energy of 0.49 eV (with almost neglecting dispersion of 0.02-0.03 eV) for 270- and 320-atoms where the distance between the nearest defects is close to four lattice constants. Note that the commonly believed experimental estimate of the F centre ionization energy is much smaller [18]. Achieving the convergence with the supercell increase up to 270-320 atoms, the defect-defect interaction becomes negligible thus approaching a realistic model of *single F* centre, similarly to the study of the Fe impurities in SrTiO_3 [21].

TABLE 5. Dependence of the F centre energy level position with respect to the conduction band bottom of un-relaxed

SrTiO_3 crystal (Figures 5 and 6) with periodically distributed oxygen vacancies ($\Delta\varepsilon_{db-gap}^{\Gamma}$), its dispersion ($\delta\varepsilon_{db-gap}$), and distance between nearest F centres (d_{F-F}) as a function of the supercell size used in *CRYSTAL* B3PW-calculations with $2\times 2\times 2$ k-mesh. The defect level position is calculated at the Γ point of the first Brillouin zone

Atoms in supercell	Extension	Type of lattice	d_{F-F} , Å	$\Delta\varepsilon_{db-gap}^{\Gamma}$, eV	$\delta\varepsilon_{db-gap}$, eV
80	$2\sqrt{2} \times 2\sqrt{2} \times 2\sqrt{2}$	fcc	11.04	0.69	0.15
135	$3 \times 3 \times 3$	sc	11.71	0.72	0.23
160	$2\sqrt{3} \times 2\sqrt{3} \times 2\sqrt{3}$	bcc	13.52	0.57	0.09
270	$3\sqrt{2} \times 3\sqrt{2} \times 3\sqrt{2}$	fcc	16.56	0.49	0.02
320	$4 \times 4 \times 4$	sc	15.61	0.49	0.03

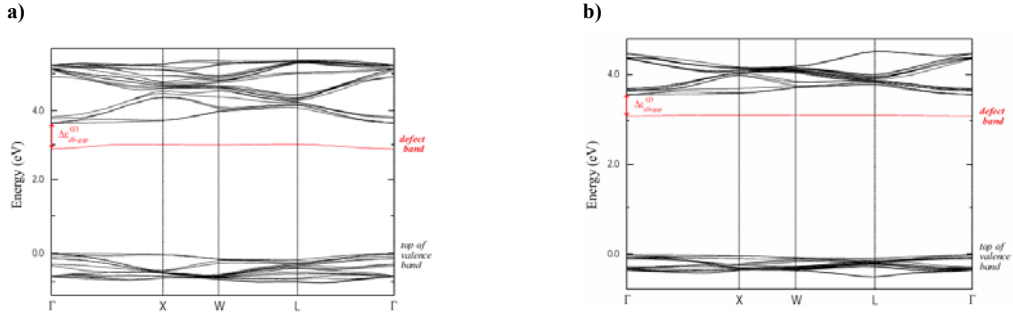


Figure 5. The band structure of un-relaxed SrTiO₃ crystal with a single F centre per fcc supercell containing either 80 atoms (a) or 270 atoms (b). The energy bands corresponding to the F centre are split off the conduction bands. Their depth (gap) relatively to the bottom of the conduction band at the Γ point is $\Delta\epsilon_{db-gap}^{\Gamma}$

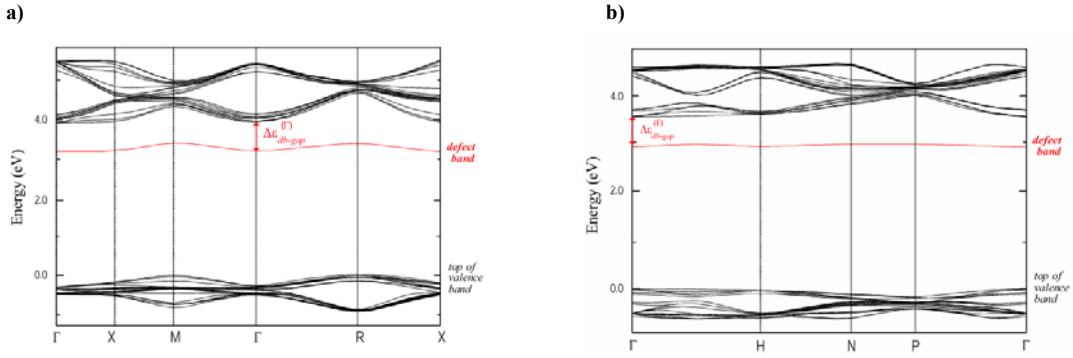


Figure 6. The band structure of un-relaxed SrTiO₃ crystal with a single F centre per supercell containing 135 atoms, $3 \times 3 \times 3$ extension (a) and 160 atoms, $2\sqrt{3} \times 2\sqrt{3} \times 2\sqrt{3}$ extension (b). See caption of Figure 5 for explanation

Figure 6a confirms that 135-atomic SC is small enough to reduce defect-defect interactions; its dispersion ($\delta\epsilon_{db-gap}$) is even larger than for 80-atomic SC with different shape (Table 5), *i.e.* $\delta\epsilon_{db-gap}$ is sensitive to both shape and size of equidistant supercell, similarly to other properties described before. At the same time, the defect band for 270-atomic supercell (Figure 5b) is almost a straight line. And although we could not draw the band structure for the 320-atomic supercell containing single *F* centre (due to limitations of *CRYSTAL* code), Table 5 clearly shows that both 270 and 320 atoms in supercells around the oxygen vacancy practically provide elimination of the interaction between periodically distributed point defects, thus confirming analogous conclusion made when analyzing the electron charge redistributions around oxygen vacancies (Figures 3 and 4).

The band structure and some other electronic properties calculated for each supercell considered before are changed markedly after *VASP*-optimized lattice relaxation around the *F* centre (Figure 7), whereas partial *CRYSTAL* optimization does not result in their noticeable changes. Due to computational limitations in *CRYSTAL* asymmetric recalculations of *VASP*-optimized structures we were able to analyze results for 80-atomic SC only. One of substantially changed parameters is the electronic charge either localized on the *neutral* oxygen vacancy (0.6 *e* vs. 1.2 *e* for un-relaxed supercell) or transferred to the nearest Ti ions from the *neutral F* centre (1.25 *e* vs. 0.7 *e*, respectively). However, the most unexpected result obtained for relaxed supercell was found to be a “hop” of the defect band over the bottom of conduction band (Figure 7b). Obviously, these changes observed when combining *CRYSTAL* and *VASP* simulations on a cubic SrTiO₃ crystal with periodically distributed *F* centres should be studied more carefully in order to understand better the nature of defective perovskites, in particular O-deficient SrTiO₃.

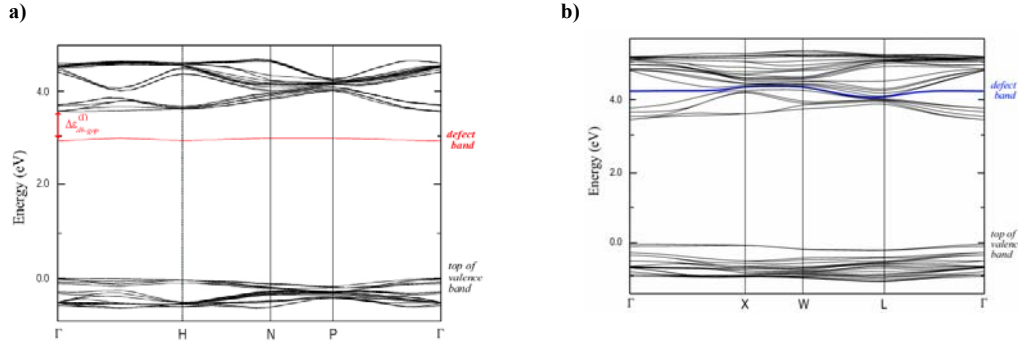


Figure 7. The band structure of a cubic SrTiO₃ crystal with a single F centre per 80-atomic supercell, which is either un-relaxed (a), or relaxed using VASP-optimized coordinates (b). See caption of Figure 5 for explanation

5. Summary

In this paper, we have analyzed the convergence of periodic defect calculations to the limit of the single vacancy. In order to obtain converged values for the atomic structure, formation and migration energies of oxygen vacancy as well as the electronic properties corresponding to a single *F* centre in SrTiO₃ bulk, the large equidistant supercells containing at least 270 atoms ($d_{F-F} \geq 4a_0$) are required when performing DFT calculations on defective perovskites. This study confirms several conclusions based on our recent HF calculations on the Fe impurities in SrTiO₃ bulk [21]. Equidistant supercells with extensions $4 \times 4 \times 4$ (320 atoms) and $3\sqrt{2} \times 3\sqrt{2} \times 3\sqrt{2}$ (270 atoms) necessary for correct description of single oxygen vacancies in strontium titanate markedly surpass supercells containing 40-135 atoms used in most of previous first principles simulations [4,10-13]. Results obtained in those studies should be critically analyzed, in order to avoid wrong conclusions about the nature of *F* centres in perovskites.

Our *VASP* calculations with complete optimization of lattice relaxation around *F* centres give 7.1 eV as a reasonable estimate for the vacancy formation energy $E^{\text{form}}(F)$ and 0.4–0.5 eV for their migration barrier $\Delta E^{\text{diff}}(F)$ at low vacancy concentration. The vacancy formation energy cannot be directly measured experimentally whereas experimental estimate for the barrier of diffusion energy is noticeably larger: 0.86 eV [6]. (The latter energy could correspond to empty vacancy.) *CRYSTAL*-B3PW calculations on the electronic properties of a single *F* centre in the un-relaxed (or partially relaxed) SrTiO₃ lattice show formation of the *defect band* below the conduction band bottom, which is mainly composed of $3d(z^2)$ orbitals of the two nearest Ti ions. Its separation $\Delta \epsilon_{db\text{-gap}}^{\Gamma}$ from the conduction band bottom approaches 0.49 eV with a negligible dispersion $\delta \epsilon_{db\text{-gap}}$ of the bandwidth (0.02–0.03 eV) for both 270- and 320-atomic supercells. Redistribution of the electronic charge around oxygen vacancies remains well localized in large supercells, *i.e.* the interaction between homogeneously distributed point defects is practically eliminated. However, *CRYSTAL* recalculations of *VASP*-optimized SrTiO₃ superlattices containing *F* centres substantially change parameters of the electronic structure. More careful study of these unexpected changes should be done. This paper clearly demonstrates the advantage of combining the *VASP* plane wave calculations [20] with the *CRYSTAL* calculations based on the localized basis sets [19]. The former is necessary for the complete optimization of lattice relaxation upon vacancy creation, even for large supercells, whereas the latter allows us to study details of the electronic structure for both un-relaxed and relaxed lattice.

Acknowledgements

This study was partly supported by the MRSEC program of the National Science Foundation (DMR-0076091) at the Materials Research Centre of North-western University, Evanston, USA (YZ, EK and SP). The authors thank J. Carrasco, R. Dovesi, D.E. Ellis, E. Heifets, F. Illas, N. Lopez, J. Maier, L.D. Marks, and D. Wolf for fruitful discussions.

References

- [1] Muller D. A., Nakagawa N., Ohtomo A., Grazul J. L., and Hwang H.Y. (2004) Atomic-scale imaging of nanoengineered oxygen vacancy profiles in SrTiO₃. *Nature* **430**, 657–661.
- [2] Cox P. A. (1995) *Transition Metal Oxides*. Clarendon Press, Oxford, UK.

- [3] Smyth D. M. (1985) Defects and order in perovskite-related oxides. *Annual Review of Materials Science* **15**, 329–357.
- [4] Astala R. and Bristowe P. D. (2001) *Ab initio* study of the oxygen vacancy in SrTiO₃. *Modelling Simulation in Materials Science & Engineering* **9**, 415–422.
- [5] Szot K., Speier W., Carius R., Zastrow U., and Beyer W. (2002) Localized metallic conductivity and self-healing during thermal reduction of SrTiO₃. *Physical Review Letters* **88**, 075508 (1–4).
- [6] Denk I., Munch W., and Maier J. (1995) Partial conductivities in SrTiO₃: bulk polarization experiments, oxygen concentration cell measurements, and defect-chemical modeling. *Journal of the American Ceramic Society* **78**, 3265–3272.
- [7] Adachi Y., Kohiki S., Wagatsuma K., and Oku M. (1999) Changes in the chemical state of monocrystalline SrTiO₃ surface by argon ion bombardment. *Applied Surface Science* **143**, 272–276.
- [8] Van Benthem K., Elsässer C., and French R. H. (2001) Bulk electronic structure of SrTiO₃: experiment and theory. *Journal of Applied Physics* **90**, 6156–6164.
- [9] Buban J. P., Iddir H., and Ogut S. (2004) Structural and electronic properties of oxygen vacancies in cubic and antiferrodistortive phases of SrTiO₃. *Physical Review B* **69**, 180102(R) (1–4).
- [10] Carrasco J., Illas F., Lopez N., Kotomin E. A., Zhukovskii Yu. F., Piskunov S., Maier J. and Hermansson K. (2005) First principles simulations of *F* centre in SrTiO₃ perovskite. *Physica Status Solidi (c)* **2**, 153–158.
- [11] Tanaka T., Matsunaga K., Ikuhara Y., and Yamamoto T. (2003) First-principles study on structures and energetics of intrinsic vacancies in SrTiO₃. *Physical Review B* **68**, 205213 (1–8).
- [12] Donnenberg H.-J. (1999). *Atomic simulations of Electro-Optical and Magneto-Optical Materials*. Springer Tracts in Modern Physics, Vol. 151, Springer, Berlin.
- [13] Ricci D., Bano G., Pacchioni G., and Illas F. (2003) Electronic structure of a neutral oxygen vacancy in SrTiO₃. *Physical Review B* **68**, 224105 (1–9).
- [14] Akhtar M., Akhtar Z., Jackson R. A., and Catlow C. R. A. (1995) Computer simulation studies of strontium titanate. *Journal of the American Ceramic Society* **78**, 421–428.
- [15] Crawford J. and Jacobs P. W. M. (1999) Point defect energies for strontium titanate: a pair-potentials study. *Journal of Solid State Chemistry* **144**, 423–429.
- [16] Usvyat D. E., Evarestov R. A., and Smirnov V. P. (2004) Wannier functions and chemical bonding in crystals with the perovskite-like structure: SrTiO₃, BaTiO₃, PbTiO₃, and LaMnO₃. *International Journal of Quantum Chemistry* **100**, 352–359.
- [17] Piskunov S., Heifets E., Eglitis R. I., and Borstel G. (2004) Bulk properties and electronic structure of SrTiO₃, BaTiO₃, PbTiO₃ perovskites: an *ab initio* HF/DFT study. *Computational Materials Science* **29**, 165–178.
- [18] Moos R. and Haerdtl K.-H. (1997) Defect chemistry of donor-doped and undoped strontium titanate ceramics between 1000° and 1400°C. *Journal of the American Ceramic Society* **80**, 2549–2562.
- [19] Saunders V. R., Dovesi R., Roetti C., Orlando R., Zicovich-Wilson C. M., Harrison N. M., Doll K., Civalieri B., Bush I. J., D’Arco Ph., and Llunell M. (2003) *CRYSTAL-2003 User Manual*. University of Turin, Italy.
- [20] Kresse G. and Hafner J. (2003) *VASP Guide*. University of Vienna, Austria.
- [21] Evarestov R. A., Piskunov S., Kotomin E. A., and Borstel G. (2003) Single impurities in insulators: *ab initio* study of Fe-doped SrTiO₃. *Physical Review B* **67**, 064101 (1–9).
- [22] Evarestov R. A. and Smirnov V. P. (1997) Symmetrical transformation of basic translation vectors in the supercell model of imperfect crystals and in the theory of special points of the Brillouin zone. *Journal of Physics: Condensed Matter* **9**, 3023–3031.
- [23] Evarestov R. A. (2005) Trends in calculation of point and extended defects in wide-gap solids: periodic models of aperiodic systems. *Physica Status Solidi (a)* **202**, 235–242.
- [24] Pisani C., Dovesi R., Roetti C., Causà M., Orlando R., Casassa S., and Saunders V. R. (2000) *CRYSTAL* and *EMBED*, two computational tools for the *ab initio* study of electronic properties of crystals. *International Journal of Quantum Chemistry* **77**, 1032–1048.
- [25] Bredow T., Evarestov R. A., and Jug K. (2000) Implementation of the cyclic cluster model in Hartree-Fock LCAO calculations of crystalline systems. *Physica Status Solidi (b)* **222**, 495–518.
- [26] Makov G., Shach R., and Payne M. C. (1996) Periodic boundary conditions in *ab initio* calculations. II. Brillouin-zone sampling for aperiodic system. *Physical Review B* **53**, 15513–15517.
- [27] Piskunov S., Heifets E., Kotomin E. A., Maier J., Eglitis R. I., and Borstel G. (2005) Hybrid DFT calculations of the atomic and electronic structure for ABO₃ perovskite (001) surfaces. *Surface Science* **575**, 75–88.

- [28] Becke A. D. (1988) Density-functional exchange-energy approximation with correct asymptotic behavior. *Physical Review A* **38**, 3098–3100.
- [29] Perdew J. P. and Wang Y. (1992) Accurate and simple analytic representation of the electron gas correlation energy. *Physical Review B* **45**, 13244–13249.
- [30] Becke A. D. (1988) Density-functional thermochemistry. III. The role of exact exchange. *Journal of Chemical Physics* **98**, 5648–5652.
- [31] Hay P. J. and Wadt W. R. (1984) *Ab initio* effective core potentials for molecular calculations. I. Potentials for the transition metal atoms Sc to Hg. *Journal of Chemical Physics* **82**, 270–283; Hay P. J. and Wadt W. R. (1984) *Ab initio* effective core potentials for molecular calculations. II. Potentials for main group elements Na to Bi. *Ibid*, 284–298; Hay P. J. and Wadt W. R. (1984) *Ab initio* effective core potentials for molecular calculations. III. Potentials for K to Au including the outermost core orbitals. *Ibid*, 299–310.
- [32] Heifets E., Eglitis R. I., Kotomin E. A., Maier J., and Borstel G. (2001) *Ab initio* modeling of surface structure for SrTiO₃ perovskite crystals. *Physical Review B* **64**, 235417 (1–5).
- [33] Press W. H., Teukolsky S. A., Vetterling W. T., and Flannery B. P. (1997) *Numerical Recipes in Fortran 77*. Cambridge University Press, Cambridge (MA), USA.
- [34] Piskunov S., Heifets E., Kotomin E. A., and Shunin Yu. N. (2003) B3PW and B3LYP exchange-correlation techniques in CRYSTAL computer code: the case of ABO₃ perovskites. *Proceedings of the 1st International Conference "Information Technologies and Management"* (Riga, 2003), 70–81.
- [35] Monkhorst H. J. and Pack J. D. (1976) Special points for Brillouin-zone integrations. *Physical Review B* **13**, 5188–5192.
- [36] Gilat G. (1982) General analytic method of zone integration for joint densities of states in metals. *Physical Review B* **26**, 2243–2246.
- [37] Kresse G. and Hafner J. (1993) *Ab initio* molecular dynamics for open-shell transition metals. *Physical Review B* **48**, 13 115–13118; Kresse G. and Hafner J. (1994) *Ab initio* molecular-dynamics simulation of the liquid-metal-amorphous-semiconductor transition in germanium. *Physical Review B* **49**, 14251–14269.
- [38] Kresse G. and Furthmüller J. (1996) Efficiency of *ab initio* total energy calculations for metals and semiconductors using a plane-wave basis set. *Computational Materials Science* **6**, 15–50; Kresse G. and Furthmüller J. (1996) Efficient iterative schemes for *ab initio* total-energy calculations using a plane-wave basis set. *Physical Review B* **54**, 11169–11186.
- [39] Singh D. J. (1994) *Planewaves, Pseudopotentials and the LAPW Method*. Kluwer Academic, Norwell (MA), USA.
- [40] Hamann D. R., Schlüter M., and Chiang C. (1979) Norm-conserving pseudopotentials. *Physical Review Letters* **43**, 1494–1497; Bachelet G. B., Schlüter M., and Chiang C. (1982) Pseudopotentials that work: from H to Pu. *Physical Review B* **26**, 4199–4228.
- [41] Vanderbilt D. (1990) Soft self-consistent pseudopotentials in a generalized eigenvalue formalism. *Physical Review B* **41**, 7892–7895.
- [42] Mastrikov Yu. A., Zhukovskii Yu. F., Kotomin E. A., Maier J., and Shunin Yu. N. (2004) Diffusion of silver vacancies on AgCl(111)/ α -Al₂O₃(0001) interface: first principles simulations. *Proceedings of the 2nd International Conference "Information Technologies and Management"* (Riga, 2004), 118–125.
- [43] Blöchl P. E. (1994) Projector augmented-wave method. *Physical Review B* **50**, 17953–17979.
- [44] Kresse G. and Joubert D. (1999) From ultrasoft pseudopotentials to the projector augmented-wave method. *Physical Review B* **59**, 1758–1775.
- [45] Abramov Yu. A., Tsirelson V. G., Zavodnik V. E., Ivanov S. A., and Brown I. D. (1995) The chemical bond and atomic displacements in SrTiO₃ from X-ray diffraction analysis. *Acta Crystallographica B* **51**, 942–951.
- [46] Hellwege K. H., and Hellwege A. M. (eds.) (1969) *Ferroelectrics and Related Substances*, Landolt-Börnstein, New Series, Group III, vol. 3, Springer Verlag, Berlin, Germany.
- [47] Bell R. O. and Rupprecht G. (1963) Elastic constants of strontium titanate. *Physical Review* **129**, 90–94.
- [48] Moreira I. P. R., Illas F., and Martin R. L. (2002) Effect of Fock exchange on the electronic structure and magnetic coupling in NiO. *Physical Review B* **65**, 155102 (1–14).
- [49] Fang Z. and Terakura K. (2000) Spin and orbital polarizations around oxygen vacancies on the (001) surfaces of SrTiO₃. *Surface Science* **479**, L65–L70.

Received on the 21st of July 2006

FIRST PRINCIPLES CALCULATIONS OF THE ATOMIC AND ELECTRONIC STRUCTURE OF LaMnO_3 (001) SURFACE

E. A. KOTOMIN^{1,2}, YU. A. MASTRIKOV², D. V. GRYAZNOV^{1,2},
 YU. N. SHUNIN³

¹ Institute of Solid State Physics, University of Latvia, Kengaraga Street 8, LV-1063, Riga, Latvia
 E-mail: kotomin@latnet.lv, fax: +371 7132778, phone: +371 7187480

² Max Planck Institute for Solid State Research, Heisenbergstr., 1, D-70569, Stuttgart, Germany
 E-mail: kotomin@fkf.mpg.de, j.mastrikovs@fkf.mpg.de, fax: +49 711 689 1722;

³ Information Systems Management Institute Department of Natural Sciences
 and Computer Technologies, Lomonosov Street 1, LV-1019, Riga, Latvia
 E-mail: shunin@isma.lv, fax: +371 7241591, phone: +371 7100593

The results of *ab initio* DFT plane-wave periodic structure calculations of the surface of LaMnO_3 (001) are presented and discussed. The effects related to three different kinds of pseudopotentials, the slab thickness, magnetic ordering, and surface relaxation are analysed. The antiferromagnetic surface lowest in energy (that is, spins on Mn ions are parallel in basal plane and anti-parallel from plane to plane) has a considerable atomic relaxation up to forth plane from the surface. The calculated (Bader) effective charges and the electronic density maps demonstrate a considerable reduction of the Mn atom ionicity on the surface accompanied by a covalent contribution to the Mn-O bonding. These results are compared with hybrid LCAO-B3PW calculations.

Keywords: *ab initio* DFT plane-wave periodic structure calculations, LaMnO_3 (001) surface

1. Introduction

Sr-doped LaMnO_3 perovskite crystal (LMO) attracts great attention as a cathode material for solid oxide fuel cells [1] as well because of its bulk magnetic properties [2-5]. Surprisingly, LMO *surface properties* have been studied very little, especially theoretically. To our knowledge, there exist only a few surface structure calculations for manganese perovskites; LSDA study refers to CaMnO_3 and $\text{La}_{1/2}\text{Ca}_{1/2}\text{MnO}_3$ (100) surfaces in their non-cubic modifications [6] whereas our LMO studies of the LMO (110) surfaces involve both classical shell model [7-9] and *ab initio* Hartree-Fock (HF) calculations [10,11]. In the latter papers, the results of first HF calculations for the un-relaxed (001) surface were reported.

Ab initio calculations of the bulk LMO electronic structure were performed earlier in the HF LCAO approximation [2,3] and using the relativistic full-potential-GGA LAPW [4]. In these calculations several different crystalline structures were considered. The ideal perovskite (cubic) structure with five atoms (one formula unit) per a primitive unit cell (Fig. 1 a), is stable above 750 K, with the experimental lattice constant $a_0=3.95$ Å. The UHF LCAO calculations [3] gave the optimised lattice constant very close to this experimental value. In the UHF calculations [2] the tetragonal structure, consisting of $\sqrt{2} \cdot \sqrt{2} \cdot 2 = 4$ primitive unit cells of the undistorted perovskite structure, was assumed. For such a structure, it was found, in both HF and LSDA approximations, that the ground state of LMO is ferromagnetic (FM, spins are parallel of the all 4 Mn atoms in a supercell).

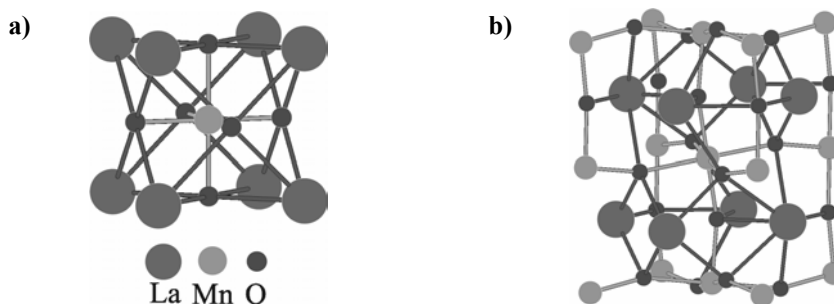


Figure 1. Ideal perovskite cubic (a) and relaxed orthorhombic (b) structure

The low-temperature LMO structure is orthorhombic (comprising four formula units, space group Pbnm, Fig. 1 b). The experimental values of the lattice parameters $a = 5.532 \text{ \AA}$, $b = 5.742 \text{ \AA}$, $c = 7.668 \text{ \AA}$ [12], can be compared with $a = b = 5.582 \text{ \AA}$, $c = 7.894 \text{ \AA}$ for the above mentioned tetragonal structure containing four formula unit cells, and the experimental value of the cubic lattice constant $a_0 = 3.95 \text{ \AA}$. The difference in these two sets of structure parameters arises due to strong Jahn-Teller (JT) distortions of the MnO_6 octahedra and their rotations (this effect is known as MnO_6 octahedra tilting). For the orthorhombic structure, HF, LSDA calculations [2,3], as well as LAPW [4] predict the LMO ground state to be an antiferromagnetic (AFM) insulator, in agreement with the experiment. The calculated energy of this state is lower than for the FM state, by 1.055 eV per Mn in the HF calculation and 0.156 eV per Mn in the LSDA calculation [2]. This demonstrates a strong dependence of the FM-AFM energy difference on the calculation scheme. The orthorhombic lattice parameters optimised in HF calculations [3] are $a = 5.620 \text{ \AA}$, $b = 5.740 \text{ \AA}$, $c = 7.754 \text{ \AA}$. Corresponding to these parameters the “virtual” cubic structure has the lattice constant $a_0 = \frac{1}{2 \cdot 3} (a\sqrt{2} + c + b\sqrt{2}) = 3.97 \text{ \AA}$. (The latter value is obtained by averaging over the orthorhombic lattice parameters.) Along with the lattice parameter optimisation, to our knowledge there exists only a single study on the UHF optimisation of the local atomic coordinates *inside* the orthorhombic unit cell [3]. The UHF method was also successfully used for calculating the magnetic coupling constants in LMO [13]. It was shown that the magnetic coupling constants depend considerably on the hybrid functional used.

In this paper, we present the results of detailed *ab initio* calculations for the LMO (001) polar surface with emphasis on its relaxation for different magnetic configurations. Its MnO_2 termination could be important for fuel cell applications, during which adsorption of O_2 molecule occurs, followed by its ionization, dissociation and ion transfer in the electrolyte. In order to check results obtained by means of the UHF, we performed DFT-GGA plane wave calculations which also permit considerably faster structure optimisation. In Section 2 we discuss basic results for the bulk properties of LMO which serve as a test of the method ability to calculate the atomic and electronic structure of ABO_3 perovskites. The results of surface calculations are presented in Section 3. We analyse how the results depend on the different kinds of pseudopotentials, the slab thickness, and magnetic ordering. Special attention is paid to the surface relaxation.

TABLE 1. Projector-Augmented Wave (PAW), Generalised Gradient Approximation (GGA) Pseudo-Potentials (PP) used in these calculations [14]

Pseudopotential	Cut-off energy, eV	N_0 of valence electrons	Valence electrons shell
La	219.044	11	5s2 5p6 6s2 5d1 (4f)
Mn	269.944	7	4s1 3d6
Mn_pv	269.887	13	3p6 4s1 3d6
O	400	6	2s2 2p4
O_s	250	6	2s2 2p4

TABLE 2. Optimised lattice constants for a cubic unit cell (\AA). Expt value is 3.95 \AA , the k-set is 4 4 4, PP-1, PP-2 and PP-3 correspond to three types of pseudopotentials – La,Mn,O; La, Mn_{pv} , O_s ; and La, Mn_{pv} , O—see explanation of the pseudopotentials and magnetic structures NM, FM and AAF in the text. The relevant unit cells contain 5,5 and 10 atoms, respectively

PP	PP-1		PP-2		PP-3	
$E_{\text{cut}}, \text{eV}$	269.9	600	269.9	600	269.9	600
NM	3.745	3.751	3.821	3.837	3.815	3.827
FM	3.763	3.772	3.887	3.919	3.887	3.917
AAF	3.778	3.791	3.882	3.916	3.880	3.908

TABLE 3. The cohesive energies E_0 (in eV) for cubic structures as in Table 2 for expt lattice constant (3.95 Å) and the relaxation energies, ΔE , due to lattice constant optimisation also are shown. The experimental estimate of the cohesive energy is 30.3 eV

PP-1						
Ecut	269.9			600		
	E_0	E_{rel}	ΔE	E_0	E_{rel}	ΔE
NM	33.99	35.02	1.03	34.55	35.43	0.88
FM	34.85	35.51	0.65	35.41	35.92	0.51
AAF	34.83	35.4	0.57	35.39	35.82	0.43
PP-2						
Ecut	269.9			600		
	E_0	E_{rel}	ΔE	E_0	E_{rel}	ΔE
NM	29.66	30.06	0.4	29.59	29.85	0.26
FM	30.7	30.78	0.09	30.62	30.64	0.02
AAF	30.66	30.76	0.1	30.59	30.61	0.03
PP-3						
Ecut	269.9			600		
	E_0	E_{rel}	ΔE	E_0	E_{rel}	ΔE
NM	29.91	30.31	0.4	30.46	30.74	0.28
FM	30.94	31.03	0.08	31.49	31.51	0.02
AAF	30.91	31.01	0.1	31.45	31.48	0.03

2. Bulk $LaMnO_3$ Calculations

For calculations we employed the *ab initio* DFT plane-wave-based computer code VASP [14,15]. For the exchange-correlation potential, the GGA-Perdew-Wang-91 was used [16]. We checked results for three types of the projector augmented-wave pseudopotentials for the inner electrons (referred hereafter as PP-1,2,3) – La, Mn, O; La, Mn_{pv}, O_s; and La, Mn_{pv}, O, where the lower index *pv* means that Mn *3p* states are treated as valence states, and *s* means soft pseudopotentials with reduced cut-off energy and/or reduced number of electrons (Table 1). The typical plane-wave cut-off energy was $E_{cut} = 600$ eV. We used the Monkhorst-Pack scheme [17] for *k*-point mesh generation, which was typically 4 4 4 (if not otherwise stated).

Depending on the four Mn spin orientations in the orthorhombic unit cells of 20 atoms, there are four possible magnetic orderings: ferromagnetic (FM, all spins are parallel), as well as A-, G-, and C-type antiferromagnetic (AAF, GAF, CAF). In the AAF case the Mn spins are parallel in basal plane and antiparallel from plane to plane; in the GAF each nearest neighbour pair of Mn spins are antiparallel, and in the CAF each nearest neighbour pair of Mn spins are antiparallel in the basal plane and parallel along the *z* axis. (We neglect in this paper the fifth option of the ferromagnetic ordering where the spin of one of the four Mn atoms in the cell is antiparallel to those of the other three.) Neglect of spins on Mn atoms corresponds to the non-magnetic (NM) state. The ground state electronic configuration of a single Mn³⁺ ion is $t_{2g}^3 e_g^1$ (all four electrons have the same spin projection, i.e. a high spin state). The VASP code calculates magnetic moments on atoms which are not necessarily coincide with the initial guess.

Table 2 and Fig. 2 show the optimised cubic (high temperature) lattice constant for three possible magnetic states, three kinds of pseudopotentials, and two cut-off energies. As one can see, an increase of the cut-off energy from 269.9 eV up to 600 eV increases the lattice constant only by 0.01-0.02 Å. In all cases the optimised lattice constant is smaller than the experimental one. The closest agreement is observed for the FM magnetic ordering and PP-2 pseudopotentials. The optimised magnetic moments on Mn atoms are close to expected $\pm 4 \mu_B$. The results for PP-3 potentials are quite similar to those of PP-2, however, the latter are computationally much less costly. This is why we used PP-2 pseudopotentials in the surface calculations. Table 3 gives the cohesive energies E_0 calculated using three types of pseudopotentials. The cohesive energies were calculated as the difference of the VASP unit cell total

energy and the sum of the atomic energies of the constituent atoms. The analysis for relaxed and un-relaxed cubic unit cells shows that the cohesive energies for the PP-1 exceed by 10-20 per cent the experimental value of 30.3 eV, whereas those calculated using the PP-2 and PP-3 are in very good agreement with the experiment.

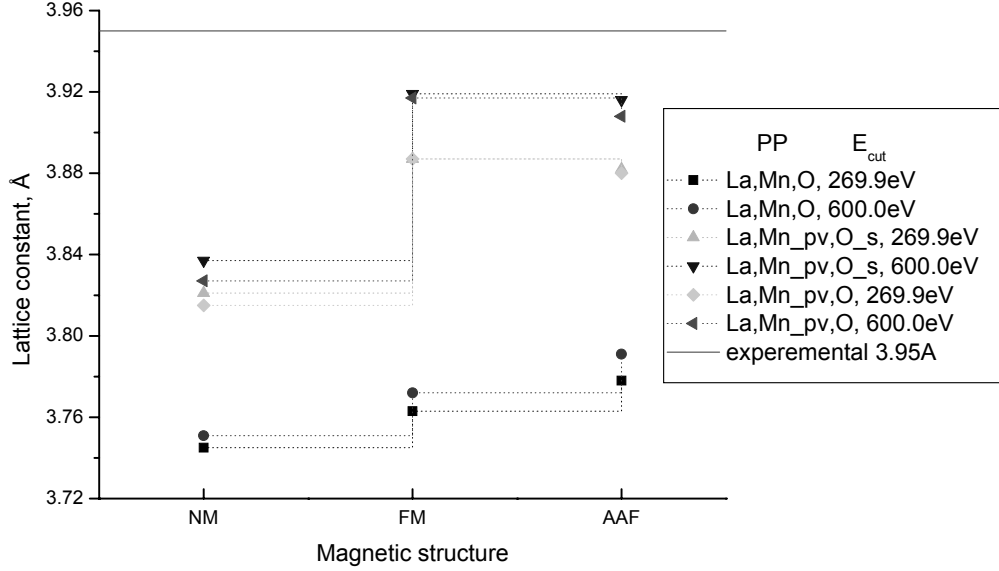


Figure 2. Optimized lattice constant for a cubic five-atom (NM and FM) and ten-atom (AAF) unit cells

Table 4 presents three optimised lattice parameters of the low-temperature orthorhombic phase and the cohesive energies for five different magnetic orderings. The atomic coordinates in the unit cell were fixed according to the experimental data [12]. In agreement with the experiment, the lowest energy corresponds to the AAF structure. The optimised a and b lattice parameters are also close to experimental values; the c parameter differs from the experiment by 0.05 Å. Recent calculations [13] based on UHF and several hybrid functionals also suggest a similar energetic ranging of the magnetic structures: AAF < GAF < CAF. The results of our atomic coordinate optimisation inside the unit cell with fixed lattice parameters are summarized in Table 5. One can see that the calculated AAF structure is very close to the experimental one, while the difference between the AAF and FM structures is small.

Lastly, Table 6 and Fig. 3 present results of *simultaneous* optimisation of the lattice parameters and atomic coordinates in the orthorhombic unit cell using four different magnetic ordering. In contrast to the experimentally observed ground state, the AAF structure in our calculations is higher in energy than FM structure; however the difference (0.06 eV per Mn atom) lies in the limits of the method accuracy. Based on these results, we can conclude that the DFT-GGA plane-wave calculation reliably reproduces the low-temperature experimental structure of the bulk LMO.

TABLE 4. Optimization of lattice constants (Å) with fixed experimental positions of atoms inside the orthorhombic unit cell of 20 atoms (Table 5)

	a	b	c	Cohesive energy, eV/cell
Expt.[12]	5.7473	7.6929	5.5367	30.3
NM	5.5285	7.6434	5.5610	29.77
FM	5.7102	7.8063	5.5891	30.84
AAF	5.7661	7.7077	5.5876	30.86
GAF	5.8071	7.6544	5.5628	30.78
CAF	5.7296	7.7927	5.5472	30.79

TABLE 5. Optimized fractional coordinates of atoms in the orthorhombic unit cell. The lattice parameters a,b,c are taken from expt. data (Table 4) $E_{\text{cut}} = 600$ eV, the k-set is 4 2 4. Mn coordinates are (1/2, 0, 0)

		a	b	c	Cohesive energy, eV/cell
Expt.[12]	La	0.0490	0.25	0.9922	
	O ₁	0.4874	0.25	0.0745	
	O ₂	0.3066	0.0384	0.7256	
FM	La	0.0465	0.25	0.9921	30.91
	O ₁	0.4819	0.25	0.0769	
	O ₂	0.2905	0.0406	0.7106	
AAF	La	0.0507	0.25	0.9920	30.87
	O ₁	0.4856	0.25	0.0775	
	O ₂	0.3030	0.0401	0.7202	

TABLE 6. Simultaneously optimized lattice constants in the orthorhombic LMO phase (a) and positions of ions inside the unit cell (b). $E_{\text{cut}} = 600$ eV, the k-set is 4 2 4

a)

	a	b	c	Cohesive energy, eV/cell
FM	5.6209	7.9023	5.5381	30.93
AAF	5.7531	7.7214	5.5587	30.87
GAF	5.9431	7.6174	5.5511	30.82
CAF	5.5792	7.9557	5.4932	30.83

b)

FM	x	y	z
La	0.0427	0.25	0.9916
O ₁	0.4840	0.25	0.0741
O ₂	0.2897	0.0400	0.7112
AAF			
La	0.0512	0.25	0.9913
O ₁	0.4844	0.25	0.0786
O ₂	0.3019	0.0406	0.7194
GAF			
La	0.0643	0.25	0.9883
O ₁	0.4832	0.25	0.0822
O ₂	0.3193	0.0430	0.7199
CAF			
La	0.0409	0.25	0.9915
O ₁	0.4859	0.25	0.0704
O ₂	0.2921	0.0389	0.7112

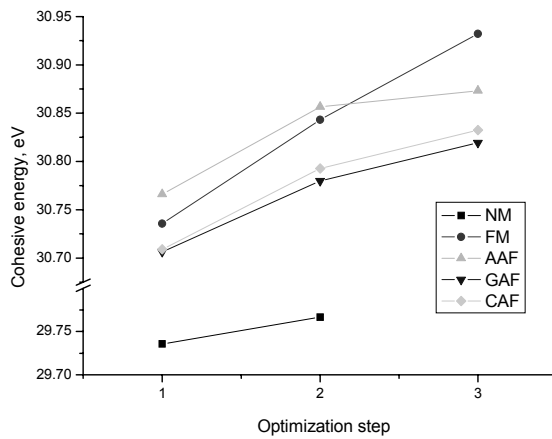


Figure 3. Cohesive energy (per 5-atom cell), calculated for 20-atom orthorhombic cell with optimised lattice constants but fixed internal atomic experimental coordinates (1-st step); optimised atomic coordinates with fixed lattice constants, optimised at the first step (2-nd step); and simultaneous optimisation of the lattice constants

Results of the Unrestricted Hartree-Fock (UHF) method and linear-combination-of-atomic-orbitals (LCAO) basis set for the LMO bulk and un-relaxed LMO surfaces were discussed in Ref. [11]. In this paper we used DFT-HF hybrid method called B3LYP [18] as implemented into the CRYSTAL computer code [19]. This permits to compare results for two DFT-type calculations with very different basis sets (plane-waves vs. LCAO).

3. The (001) Surface Calculations

3.1. PLANE-WAVE CALCULATIONS

Note that in fuel cell applications, the operational temperature is so high ($T > 800$ K) that the LMO unit cell is cubic [4,5], and thus JT lattice deformation around Mn ions and related magnetic and orbital orderings no longer take place. Of primary interest for fuel cell applications are the LMO surface properties, e.g. the optimal positions for oxygen adsorption, its surface transport properties, as well as the charge transfer behaviour. Moreover, the relaxed surface energies for LMO (001), as we show below, are about 1 eV, i.e. larger than the JT energy in LMO [5], and the magnetic exchange energy (10^{-2} eV). Periodic *ab initio* calculations of the crystalline surfaces are usually performed considering the crystal as a stack of planes perpendicular to the surface, and cutting out a 2D slab of the finite thickness but periodic in x,y plane. As the plane-wave calculations require the translational symmetry in all three dimensions, the 2D slab is repeated periodically along the z axis (Fig. 4).

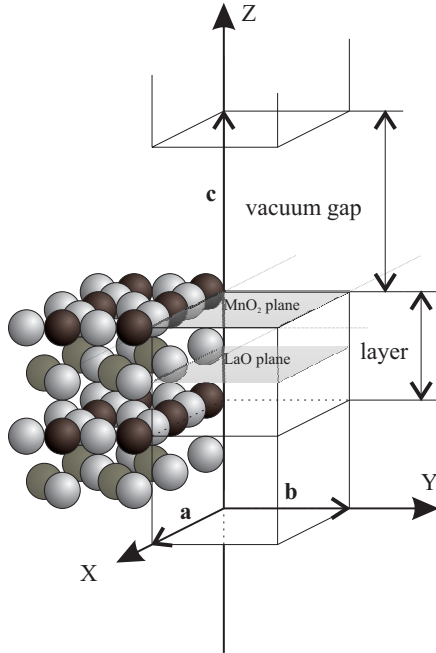


Figure 4. Four-plane slab model with indication of supercell parameters (a , b , c) and vacuum gap

The so-called *vacuum gap* is by definition the difference between the length of z -axis oriented translation vector and the slab thickness. We used for vacuum gap the value of 15.8 \AA . In our calculations, we used stoichiometric $\text{LaO} \dots \text{MnO}_2$ slabs of different thicknesses, varied from 4 to 12 planes. These slabs were built of the cubic unit cells where all atoms were allowed to relax along the z axis to reach the minimum of the total energy. In some calculations we also optimised the lattice parameters a, b of the surface square unit cell. The surface energy was calculated according to ref. [11]:

$$E_s = \frac{1}{2}(E_{\text{slab}} - nE_{\text{bulk}}),$$

where E_{slab} is the total energy of the stoichiometric slabs with MnO_2 and LaO

terminations, E_{bulk} the bulk energy per unit cell, and n the number of formula units in a slab (half the number of planes in a slab). When calculating the surface energy for *relaxed* slabs, we used as the reference the bulk unit cell energies calculated for the relaxed cubic cells (Table 3).

In Table 7 we compare the results for the un-relaxed and relaxed surface energies for the PP-2 pseudopotentials, NM (spins are neglected, closed shell calculations), FM and AAF (half Mn ions in a slab have spins up, another two spins down) magnetic orderings. First of all, the AAF magnetic structure, which mimics the disordered spin orientations at high temperatures, is always lower in energy than the NM structure where spins on Mn ions are neglected. The typical energy difference is as large as ~ 1 eV per Mn atom. In contrast, the FM and AAF configurations are very close in energy. Second, the cleavage (un-relaxed) surface energy is almost constant, independent on the slab thickness. However, surface relaxation reduced this energy down, by a factor about two, similarly for the FM and AAF magnetic structures. The relaxed surface energies show a monotonic but very slight increase with the slab thickness, up to 0.89 eV for 12-plane AAF slab (Fig. 5). This value is close to that found in recent HF calculations [11] and even smaller than the energy for the O-terminated (110) surface [7,11]. This means that the (001) surface is energetically favourable and thus MnO termination could play an important role in fuel cell and other applications. Third, when the on-plane structure relaxation is also allowed, the optimized lattice parameters a, b in both cases are smaller than the experimental value, as it occurs also in the bulk calculations (Table 2). The calculated surface energy for the FM configuration differs from that for the AAF by no more than ~ 0.02 eV/unit cell. In order to compensate the dipole moment of a polar slab, we used dipole moment correction option incorporated into the VASP code.

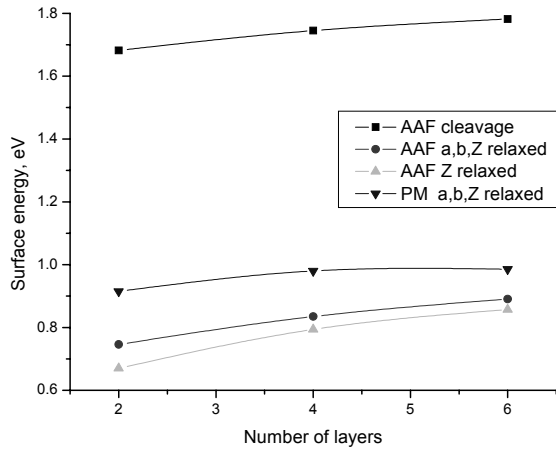


Figure 5. Calculated energies for un-relaxed surface (cleavage energy) and relaxed surface with respect to the Z coordinates, and Z ,a,b translation vectors for LMO slabs of different thickness(eV per surface cell)

The variations of the cut-off energy (from the default value of 269.9 eV up to 400 eV) and the vacuum gap (from 15.8 to 47.7 Å) as well as dipole moment corrections do not affect the main results. In order to reduce computational efforts, we used in most calculations the vacuum gap of 15.8 Å and the cut-off energy of 400 eV. The calculated total magnetic moment is nonzero for the AAF slabs; this is 0.9 μ_B , 0.65 μ_B , and 1.46 μ_B for the 4-, 8-, and 12- plane slabs, respectively.

TABLE 7. Calculated surface energies for the un-relaxed and relaxed (E_{su} , E_s) surface energies (in eV) for LMO slabs of different thickness using PP-2 pseudopotentials; k-points set Monkhorst-Pack 5 5 1; vacuum gap 15.8 Å, $a = b$ is the lattice vector parallel to the slab (in Å), expt bulk value is 3.95 Å, different from this values mean result of the optimisation, $E_{cut} = -400$ eV

N of planes	$a = b$	slab	E_{su}	E_s
4	3.95	NM	1.73	0.94
4	3.75	NM		0.91
4	3.95	AAF	1.68	0.74
4	3.83	AAF		0.67
4	3.95	FM	1.65	0.77
4	3.83	FM		0.70
6	3.95	NM	1.74	0.88
8	3.95	NM	1.74	0.80
8	3.77	NM		0.98
8	3.95	AAF	1.74	0.84
8	3.87	AAF		0.79
8	3.95	FM	1.68	0.84
8	3.86	FM		0.75
10	3.95	NM	1.74	0.72
12	3.95	NM	1.74	0.63
12	3.78	NM		0.99
12	3.95	AAF	1.78	0.89
12	3.88	AAF		0.86
12	3.95	FM	1.69	0.86
12	3.86	FM		0.74
14	3.95	NM	1.74	0.54

This is caused by different magnetic moments of Mn ions occupying different positions in the asymmetrical slab, as illustrated in Fig. 6. The relative atomic displacements and inter-plane distances for 8-plane slabs are shown in Table 8 and Fig 7, respectively. In agreement with bulk and surface energies, atomic displacements for the AAF and the FM configurations are also similar and strongly differ from those for the NM state. All Mn atoms are very moderately displaced from the perfect lattice sites, even on the MnO_2 -terminated surface. Unlike Mn, La ions are strongly displaced towards nearest MnO_2 -planes. Oxygen ions are strongly displaced inwards on the MnO_2 -terminated surface, whereas they show slight displacement outwards on the LaO-terminated surface. Both terminations demonstrated considerable rumpling (i.e. relative displacement of Me, O atoms from the crystallographic MeO plane). Unlike the AAF and FM, in NM slabs most of atoms are displaced inwards which corresponds to a strong

compression of the slab. This results from the fact that the optimised NM bulk lattice constant is considerably smaller than the experimental value of 3.95 Å.

TABLE 8. The atomic relaxation for the NM, FM and AAF configurations of stoichiometric LMO 8-plane slab (displacements are along the z axis, in per cent of the bulk lattice constant of 3.95 Å.). Positive and negative signs mean outward displacements from the slab centre, whereas negative sign – displacement towards the slab centre

plane	atom	relaxation		
		AAF	FM	NM
1	Mn	0.49	0.64	-12.02
	O2	-4.23	-3.95	-11.16
2	La	8.00	8.12	1.24
	O	-3.69	-2.57	-7.91
3	Mn	-0.61	0.19	-4.45
	O2	-4.32	-3.49	-6.19
4	La	5.34	5.69	3.18
	O	-0.93	-0.15	-1.31
5	Mn	-0.37	-0.33	-2.29
	O2	2.08	2.18	-0.63
6	La	-6.41	-6.11	-9.06
	O	-0.01	1.05	-4.27
7	Mn	-0.02	0.81	-6.11
	O2	1.32	1.91	-5.25
8	La	-9.83	-9.05	-16.68
	O	1.33	2.50	-5.80

To characterise the electronic density distribution, we calculated topological (Bader) charges [20] given in Table 9. In the bulk these are considerably smaller than the formal ionic charges (La^{3+} , Mn^{3+} , O^{2-}) what is caused by a covalent contribution to the chemical bonding between the Mn and O ions. MnO_2 - and LaO -terminated surfaces demonstrate a quite different behaviour: the effective charges of the LaO termination remain very close to those in the bulk, whereas the effective charges of the MnO_2 plane are considerably reduced. Very likely this is the result of increased covalent contribution to MnO chemical bonding on the surface. This is in line with our conclusion for the TiO_2 -termination for the SrTiO_3 (001) surface [18]. The effective charges of the rest of the atoms inside the slab are close to the bulk values.

TABLE 9. The effective Bader charges in 8-plane slab (in e), and their difference with those in the bulk (La - +1.94, Mn - +1.9, O - -1.28)

plane	atom	charge	difference
1	Mn	1.63	-0.27
	O2	-1.21	0.07
2	La	2.06	0.12
	O	-1.15	0.12
3	Mn	1.77	-0.13
	O2	-1.23	0.05
4	La	2.05	0.11
	O	-1.26	0.01
5	Mn	1.73	-0.17
	O2	-1.26	0.02
6	La	2.00	0.06
	O	-1.20	0.07
7	Mn	1.79	-0.11
	O2	-1.34	-0.06
8	La	1.99	0.05
	O	-1.33	-0.06

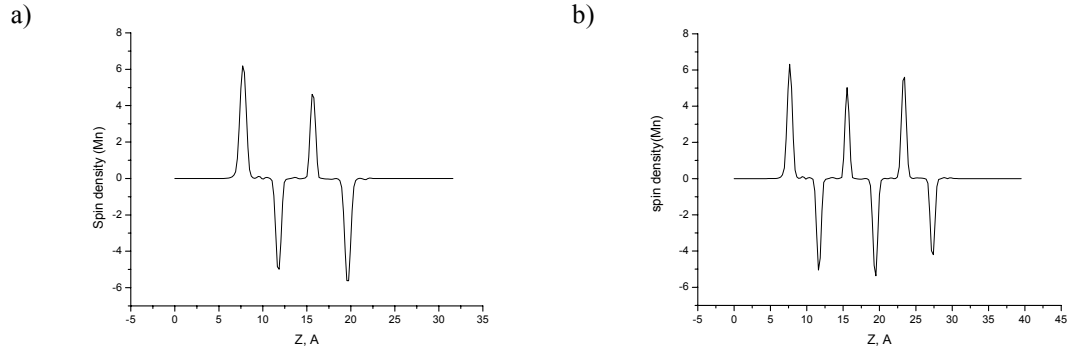


Figure 6. Spin density for four- (a) and six- (b) layer AAF-type slabs along the [001] direction

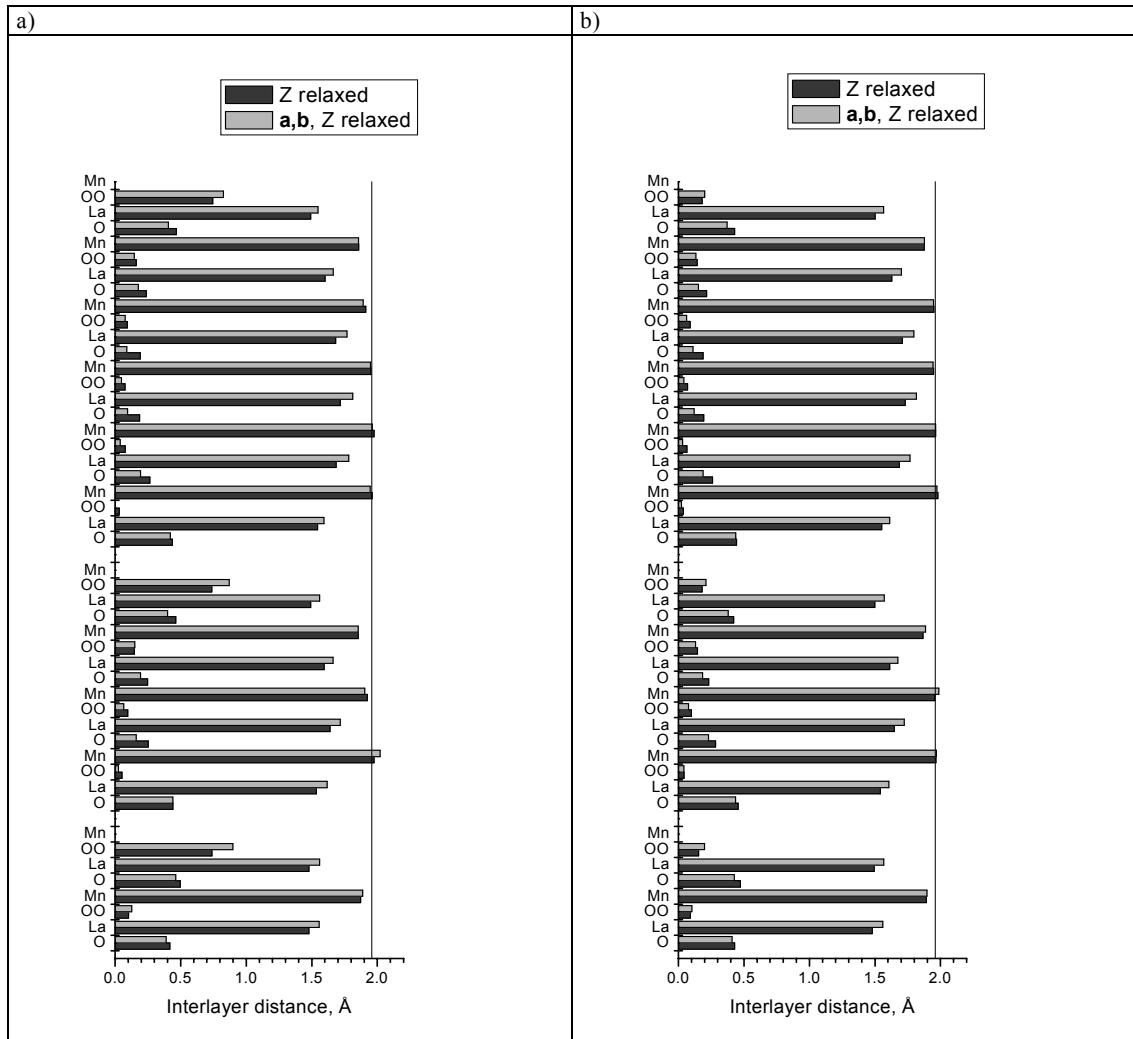


Figure 7. Inter-plane distances in relaxed AAF-(a) and FM-type (b) slabs. The distance between the planes in the bulk is shown by the solid black line

Lastly, Fig. 8 and 9 present the *difference electronic density maps* for the top un-relaxed MnO_2 and LaO planes, calculated with respect to the superposition of atomic densities and the self-consistent density for similar atoms in the bulk plane. From these maps the following conclusions could be drawn: (a) the considerable covalent contribution in the Mn-O bonding takes place, (b) the effective charges on the MnO_2 surface are reduced as compared with those in the bulk.

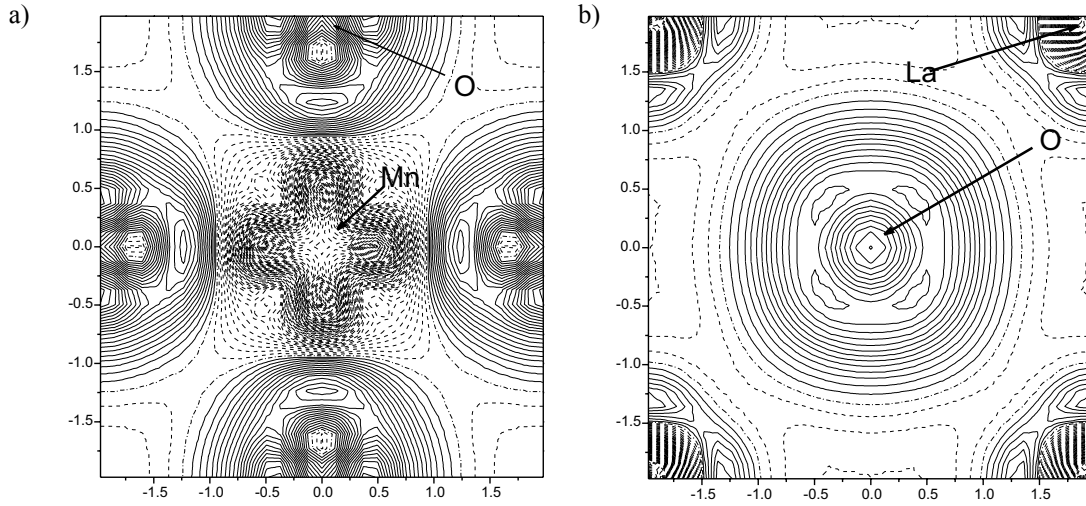


Figure 8. The difference electron density maps for the top un-relaxed MnO (a) and LaO (b) planes calculated with respect to the superposition of atomic densities. Isodensity increment is $0.01 \text{ e}/\text{\AA}^3$, full and dashed lines mean positive and negative electron densities, whereas dot-dash line is a zero level

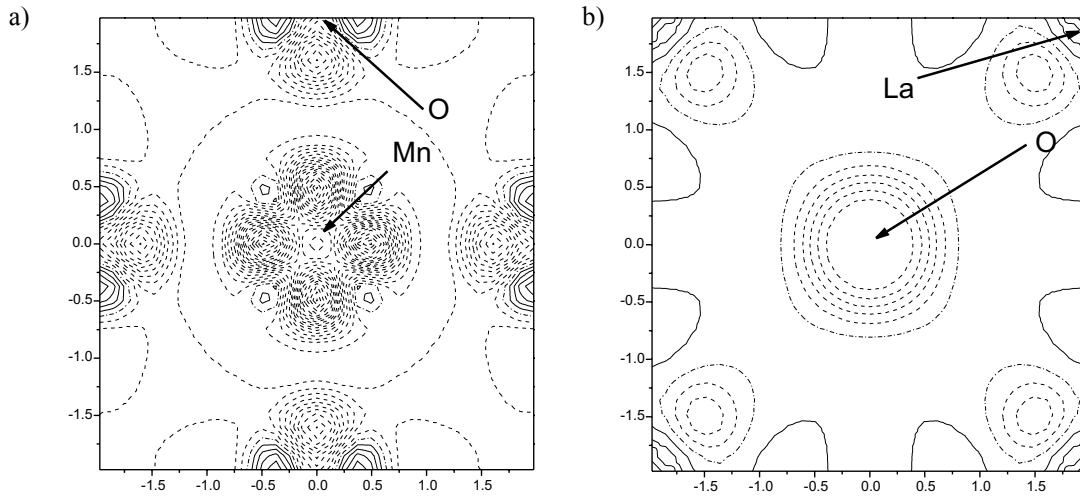


Figure 9. The difference electron density maps for the top un-relaxed MnO (a) and LaO (b) planes calculated with respect to the superposition of self-consistent density for similar atoms in the bulk. Isodensity increment is $0.01 \text{ e}/\text{\AA}^3$

3.2. LCAO CALCULATIONS

In B3LYP LCAO calculations we used four-plane stoichiometric (001) slabs. The slabs contain two Mn atoms per unit cell and thus could have several magnetic states: NM, FM and AAF. Table 10 presents calculated surface energies for un-relaxed and relaxed (001) surface.

TABLE 10. LCAO-calculated energies for un-relaxed (cleavage energy) and relaxed surface for four-plane slabs in different magnetic state (eV/surface cell)

slab	E_{su}	E_s
NM	1.78	0.49
AAF	2.00	1.98
FM	1.81	0.47

As one can see from a comparison of Table 5 and 10, the cleavage energies calculated by two methods are close, whereas the relaxed surface energy is lower in the LCAO calculations. Table 11 presents the calculated effective charges of atoms for the three magnetic configurations.

TABLE 11. The effective (Mulliken) atomic charges calculated for the NM, FM and AAF cases in the LMO bulk (a) and in the four-plane un-relaxed slabs (b), respectively

a)

BULK, effective charges	NM	AAF	UHF
La	2.61	2.62	2.79
Mn	1.87	2.04	2.16
O3	-1.49	-1.55	-1.65

b)

Plane		NM		FM		AAF	
		charge	difference	charge	difference	charge	difference
1	La	2.43	-0.18	2.44	-0.18	2.45	-0.16
	O	-1.74	-0.25	-1.76	-0.21	-1.79	-0.23
2	Mn	1.79	-0.08	2.00	-0.05	1.99	-0.05
	O ₂	-1.49	0.01	-1.56	-0.01	-1.50	0.05
3	La	2.58	-0.03	2.57	-0.05	2.55	-0.07
	O	-1.49	0.00	-1.47	0.08	-1.57	-0.02
4	Mn	1.91	0.04	2.04	0.00	2.03	-0.01
	O ₂	-1.26	0.24	-1.34	0.21	-1.33	0.22

The conclusion could be drawn that the effective charges in the LMO bulk calculated using the B3LYP for the NM and FM configurations are quite close, whereas UHF used in previous studies [13] gives more ionic charges.

Analysis of charges for the FM and AAF cases shows that on the Mn-terminated surface these are nearly the same as in the bulk, whereas O becomes less negatively charged. On the other hand, the O on the La-terminated surface is more negative than in the bulk, as well as La atom. In the NM configuration all surface atoms, except Mn, become more negative, in contrast to the two other cases discussed.

Analysis of the atomic displacements (Table 2) shows that the surface La atoms are strongly relaxed inwards, whereas O in the same plane are displaced much less and outwards. Similarly results hold for all three magnetic configurations.

In contrast, Mn atoms on the opposite surface are displaced inwards, to the slab center, so do O atoms. Unlike the VASP calculations, in CRYSTAL calculations NM and two other magnetic configurations reveal quite similar atomic displacements. In both methods, La atoms show the largest compressive displacement, while O atoms in the same plane move in the opposite direction (in AAF an FM cases).

TABLE 12. Atomic displacements along the z axis perpendicular to the surface, in percent of the bulk lattice constant. Positive sign means displacement outward the slab center, negative sign-inwards

Plane		NM	FM	AAF
1	La	-11.29	-9.82	-11.31
	O	0.05	1.26	-0.26
2	Mn	-0.31	0.51	0.07
	O ₂	0.78	1.86	1.15
3	La	6.02	5.58	6.67
	O	-2.52	-2.55	-2.13
4	Mn	-2.95	-0.35	-3.92
	O ₂	-5.27	-3.50	-4.91

Conclusions

Our first principles calculations show that the surface energy of polar LMO (001) surface is smaller than that calculated earlier for the (110) surface. This indicates the (001) this surface could play an important role in the oxygen-related processes in fuel cells and other high-tech applications. For the first time we calculated the (001) surface relaxation which reduces the surface energy by a factor about two. In

the modelling of this surface, even at high temperatures when Mn spins are randomly distributed and no magnetic effects take place, one should not neglect the atomic spins but treat the slab in the AAF configuration where the total spin is close to zero. Our calculations give a good starting point for the modelling of molecular adsorption and diffusion on manganite surfaces.

The two different implementations of the DFT method – *plane waves* and LCAO – show reasonable agreement on atomic relaxation, effective charges and surface energies.

Acknowledgements

Authors are greatly indebted to Yu.Zhukovskii, D. Fuks, R.Evarestov, E.Heifets and J. Fleig for many stimulating discussions. This study was partly supported by the German-Israeli Foundation (GIF project G-703.41.10/2001) and the collaboration project 05-0005.

References

- [1] Fleig J., Kreuer K. D., Maier J. (2003) In: *Handbook of Advanced Ceramics*, Singapore, Elsevier, 2003, p. 57.
- [2] Su Y.-S., Kaplan T. A., Mahanti S. D., Harrison J. F. (2000) *Phys. Rev. B* **61**, 1324.
- [3] Nicastrò M., Patterson C.H. (2002) *Phys. Rev. B* **65**, 205111.
- [4] Pavindra P., Kjekshus A., Fjellvag H., Delin A., Eriksson O. (2002) *Phys. Rev. B* **65**, 064445.
- [5] Kovaleva N. N., Gavartin J. L., Shluger A. L., Boris A. V., Stoneham A.M. (2002) *J. Expt and Theor. Phys.* **94**, 178.
- [6] Filipetti A., Pickett W.E. (1999) *Phys. Rev. Lett.* **83**, 4184; (2000) *Phys. Rev. B* **62**, 11571.
- [7] Kotomin E. A., Heifets E., Maier J., Goddard III W. A. (2003) *PCCP* **5**, 4180
- [8] Heifets E., Evarestov R.A., Kotomin E.A., Dorfman S., Maier J. (2004) *Sensors and Actuators B* **100**, 81.
- [9] Kotomin E. A., Heifets E., Dorfman S., Fuks D., Gordon A., Maier J. (2004) *Surf. Sci.* **566**, 231.
- [10] Evarestov R. A., Kotomin E. A., Heifets E., Maier J., Borstel G. (2003) *Solid State Comm.* **127**, 367.
- [11] Evarestov R.A., Kotomin E.A., Fuks D., Felsteiner J., Maier J. (2004) *Appl. Surf. Sci.* **238**, 457.
- [12] Rodríguez-Carvajal J., Hennion M., Moussa F., Moudén A. H. (1998) *Phys. Rev. B* **57**, 3190.
- [13] Muñoz D., Harrison N.M., Illas F. (2004) *Phys. Rev. B* **69**, 085115.
- [14] Kresse G., Furthmüller J. (2003) *VASP Guide*. University of Vienna, Austria.
- [15] Kresse G., Hafner J. (1993) *Phys. Rev. B* **48** 13 115; (1994) *Phys. Rev. B* **49**, 14521.
- [16] Burke K., Perdew J. P., Wang Y. (1998) In: *Electronic Density Functional Theory: Recent Progress and New Directions*, Ed. J. F. Dobson, G. Vignale, and M. P. Das, Plenum.
- [17] Monkhorst H. J., Pack J. D. (1976) *Phys. Rev. B* **13**, 5188.
- [18] Piskunov S., Kotomin E. A., Heifets E., Maier J., Eglitis R. I. Borstel G. (2005) *Surf. Sci.* **575**, 75
- [19] Saunders V. R., Dovesi R., Roetti C., Causa M., et al. (1988) *Crystal-98 User Manual*. University of Torino.
- [20] Henkelman G., Arnaldsson A., Jónsson H. (2006) A fast and robust algorithm for Bader decomposition of charge density. *Comp.Mat.Sci.* (in press)

Received on the 10th of May 2006

ИССЛЕДОВАНИЕ АЛГОРИТМОВ УПРАВЛЕНИЯ АГЕНТОМ, ОСНОВАННЫМ НА ЦЕЛИ, С ИСПОЛЬЗОВАНИЕМ ЭВОЛЮЦИОННЫХ ВЫЧИСЛЕНИЙ

В. ЧЕРНЫШЕВ¹, Ю. ЧИЖОВ¹, Г. КУЛЕШОВА², А. БОРИСОВ²

¹ Институт транспорта и связи
 ул. Ломоносова, 1, Рига, LV-1019, Латвия
 E-mail: neznaju@inbox.lv

² Рижский технический университет
 ул. Калькю 1, Рига LV – 1658, Латвия
 E-mail: Arkadijs.Borisovs@cs.rtu.lv

Целью работы является исследование свойств алгоритма генетического программирования, а также выполнение сравнительного анализа с нейронной сетью Элмана для задачи управления агентом в клеточном мире. Для решения задачи разработаны два программных продукта: первый реализует алгоритм генетического программирования, второй – нейронную сеть Элмана. Все программные продукты реализованы на языке Object-Pascal в среде Borland Delphi.

В данной работе каждый метод исследован отдельно, затем произведен их сравнительный анализ.

Ключевые слова: генетический алгоритм, генетическое программирование, нейронная сеть Элмана, клеточный мир, навигация агента

1. Введение

Клеточный мир. Клеточный мир представляет собой двумерное прямоугольное поле (рис. 1), поделённое на клетки [3]. Клетка может быть свободна или занята препятствием. Задача агента – обойти заданное препятствие по периметру. Агент имеет восемь сенсоров: N-«север», S-«юг», E-«восток», W-«запад», NW-«северо-запад», NE-«северо-восток», SW-«юго-запад», SE-«юго-восток». Сенсоры позволяют агенту «видеть» препятствия вокруг себя на расстоянии одной клетки. Агент может перемещаться в четырёх направлениях: GN-«на север», GS-«на юг», GW-«на запад», GE-«на восток». Агент не может перемещаться по клеткам с препятствиями (на рисунке агент обозначен буквой «А»).

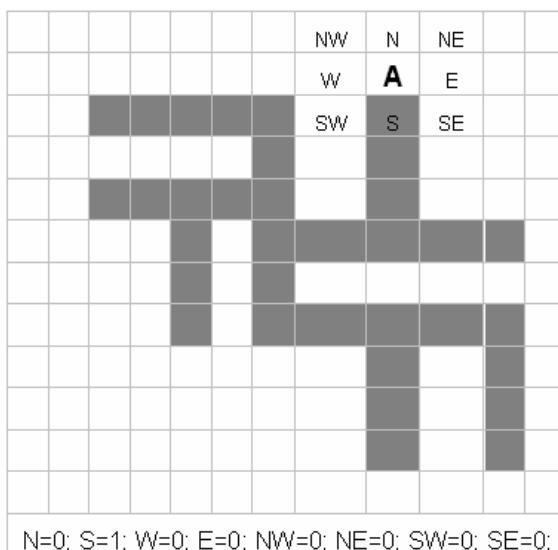


Рис. 1. Пример клеточного мира агента

Идею генетического программирования (ГП) впервые предложил Джон Кожа в 1992 году, опираясь на концепцию генетических алгоритмов (ГА). Эта идея заключается в том, что, в отличие от ГА, в ГП все операции производятся не над строками, а над деревьями. При этом используются такие же операторы, как и в ГА: селекция, скрещивание и мутация. Поэтому, чтобы лучше понять алгоритм генетического программирования, необходимо описать генетические алгоритмы.

2. Генетические алгоритмы

ГА работают с совокупностью "особей" – популяцией, каждая из которых представляет возможное решение данной проблемы [1,2]. Каждая особь оценивается мерой ее "приспособленности" согласно тому, насколько "хорошо" соответствующее ей решение задачи. В природе это эквивалентно оценке того, насколько эффективен организм в выживании и конкурентной борьбе за ресурсы. Наиболее приспособленные особи получают возможность "воспроизводить" потомство при помощи механизмов скрещивания с другими особями популяции. Это приводит к появлению новых особей, которые сочетают в себе некоторые характеристики, наследуемые ими от родителей. Наименее приспособленные особи с меньшей вероятностью смогут воспроизвести потомков, так что те свойства, которыми они обладали, будут постепенно исчезать из популяции в процессе эволюции. Иногда происходят мутации, или спонтанные изменения в генах.

Преимущество ГА состоит в том, что он находит приблизительные оптимальные решения за относительно короткое время.

В общем случае для работы ГА необходимо сформировать следующие компоненты:

- хромосома (решение рассматриваемой проблемы), состоящая из генов;
- начальная популяция хромосом;
- набор операций селекции, скрещивания и мутации для генерации новых решений из предыдущей популяции;
- целевая функция для оценки приспособленности (fitness) решений;
- критерий (признак) останова.

Таким образом, чтобы применить ГА к задаче, сначала следует выбрать метод кодирования решений в виде строки. Пример хромосомы в ГА: 000110110.

3. Особенности генетического программирования

В ГП хромосомами являются программы. Программы представлены в виде деревьев с функциональными (промежуточными) и терминальными (конечными) элементами. Терминальными элементами являются константы, действия и функции без аргументов, функциональными – функции, использующие аргументы.

В качестве примера рассмотрим программу, представленную на рис. 2 в виде дерева:

IF (IF (OR (Wall South; NOT (Wall East)); Go West; Go North); Go East; Go North).

Терминальные элементы:

T = {Wall South, Wall East, Go West, Go North, Go East}.

Функциональные элементы:

F = {IF, OR, NOT}.

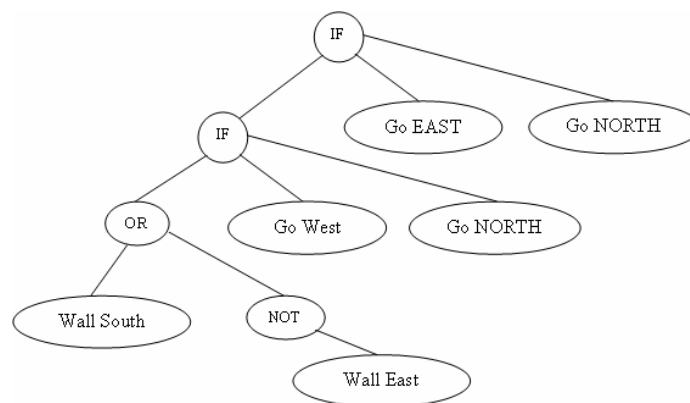


Рис. 2. Древоподобное представление программы

Для того чтобы применить ГП к какой-либо проблеме, помимо компонент ГА, необходимо определить следующие, специфические для ГП компоненты:

- множество терминальных элементов;
- множество функциональных элементов.

Алгоритм работы ГП такой же, как и в ГА: селекция, скрещивание и мутация.

4. Нейронная сеть Элмана

Рекуррентная нейронная сеть Элмана [4] представляет собой синхронную, бинарную двухслойную сеть с обратной связью от выхода к входу скрытого слоя (рис. 3).

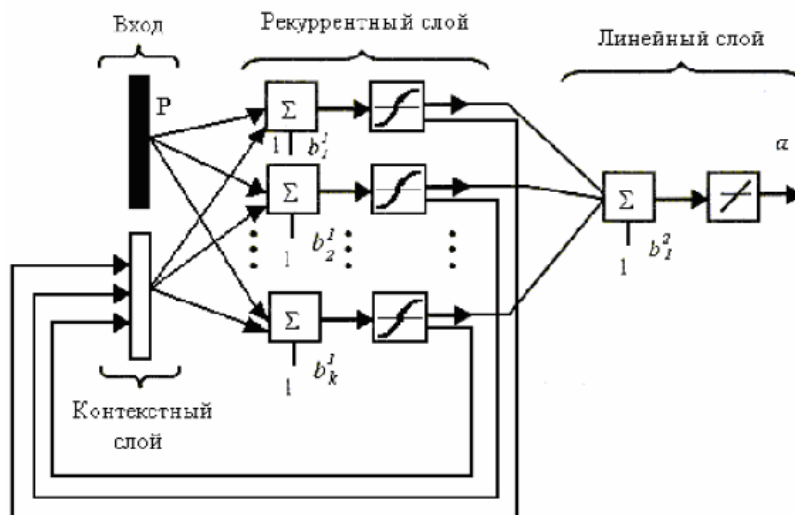


Рис. 3. Структурная схема рекуррентной нейронной сети Элмана

Каждый скрытый нейрон имеет свой аналог в контекстном слое, образующем совместно с внешними входами сети входной слой. В качестве функции активации нейронов скрытого слоя обычно используются сигмоидальные функции. Выходной слой состоит из линейных нейронов, односторонне связанных только с нейронами скрытого слоя. Рекуррентная структура сети Элмана позволяет учитывать непосредственное влияние сигналов в момент $(n - 1)$ на поведение сети в момент n .

5. Цель исследования

Основной целью работы является исследование свойств алгоритма генетического программирования, а также сравнительный анализ с нейронной сетью (НС) Элмана для задачи управления агентом в клеточном мире [3, 5]. Для достижения цели необходимо выполнить ряд подзадач, а именно:

- программную реализацию алгоритма ГП;
- программную реализацию нейронной сети Элмана;
- исследование влияния на скорость обучения параметров ГП таких, как размер начальной популяции, глубина деревьев в начальной популяции, вероятность мутации, вероятность скрещивания.

Для исследования применяются оригинальные программные продукты:

- программный продукт, реализующий эволюционный алгоритм ГП, задача которого – изучить влияние количества нейронов в скрытом слое на скорость обучения нейронной сети Элмана;
- программный продукт, реализующий нейронную сеть Элмана.

Основываясь на полученных результатах, проведён сравнительный анализ методов по их скорости решения задачи. В случае ГП – это поиск решения эволюционным методом, в случае нейронной сети Элмана – обучение с целью распознавания пар «состояние – действие».

6. Программная реализация

Программный продукт, реализующий работу алгоритма ГП, позволяет задавать основные параметры алгоритма ГП. Программа также позволяет получать различные данные по каждой итерации как в цифровом, так и в графическом виде (см. рис. 4 и 5).

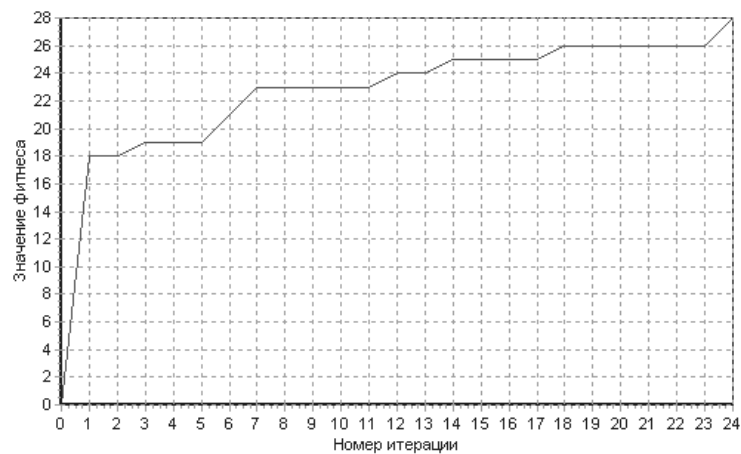


Рис. 4. Размер фитнеса в зависимости от номера итерации (методом ГП)

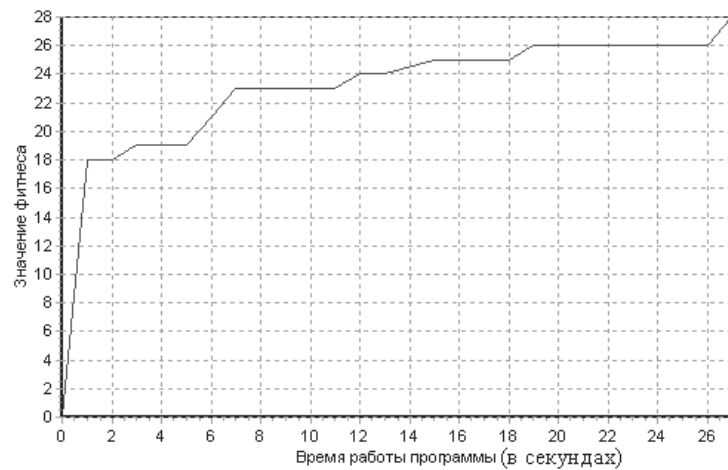


Рис. 5. Размер фитнеса в зависимости от времени работы программы (методом ГП)

Программный продукт, реализующий нейронную сеть, позволяет задавать основные параметры нейронной сети Элмана, а также получать различные данные по каждой итерации как в цифровом, так и в графическом виде (рис. 6 и 7).

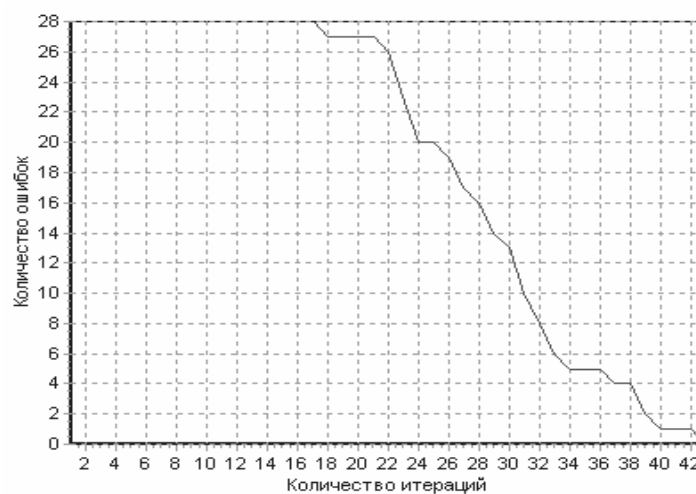


Рис. 6. Количество ошибок в зависимости от количества итераций (методом НС)

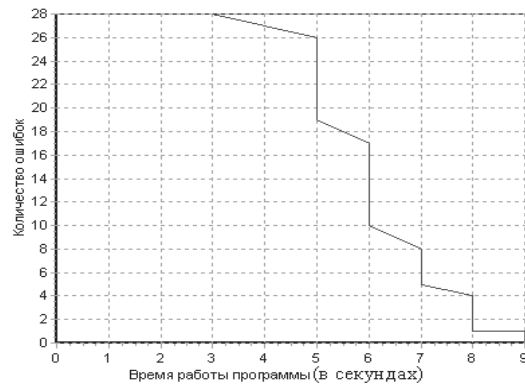


Рис. 7. Количество ошибок в зависимости от времени работы программы (методом НС)

7. Полученные результаты

Клеточные миры. На рисунках 8, 9, 10 и 11 приведены клеточные миры, в которых производились эксперименты с различными параметрами обоих методов. Первые три мира являются марковскими, а четвёртый мир является немарковским. В последнем присутствуют элементы, образующие такие состояния агента, которые однозначно не определяют дальнейшего направления его движения, другими словами, требуется по-разному реагировать на одни и те же состояния. Примером немарковости может служить элемент «коридора», в котором агенту, согласно решению, необходимо пройти вначале в одном направлении, а затем – в обратном. Так как эксперименты показали, что алгоритм ГП не может обучаться в немарковских средах, то из экспериментов с ГП четвёртый мир был исключён. Время работы программ измеряется в секундах.

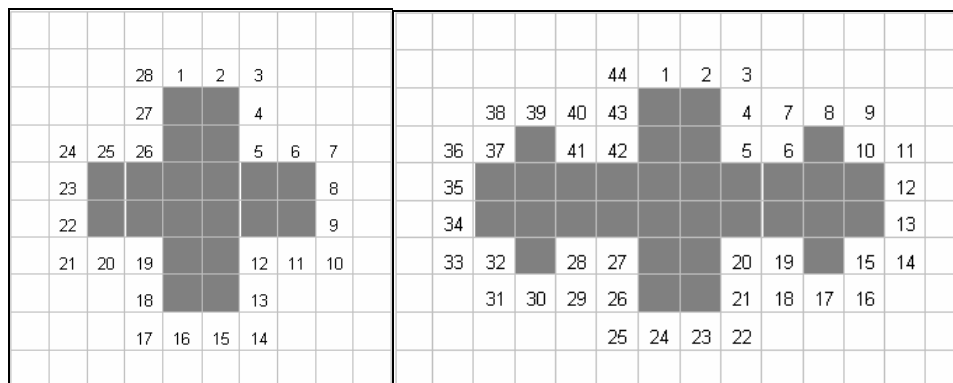


Рис. 8. Первый и второй клеточный мир

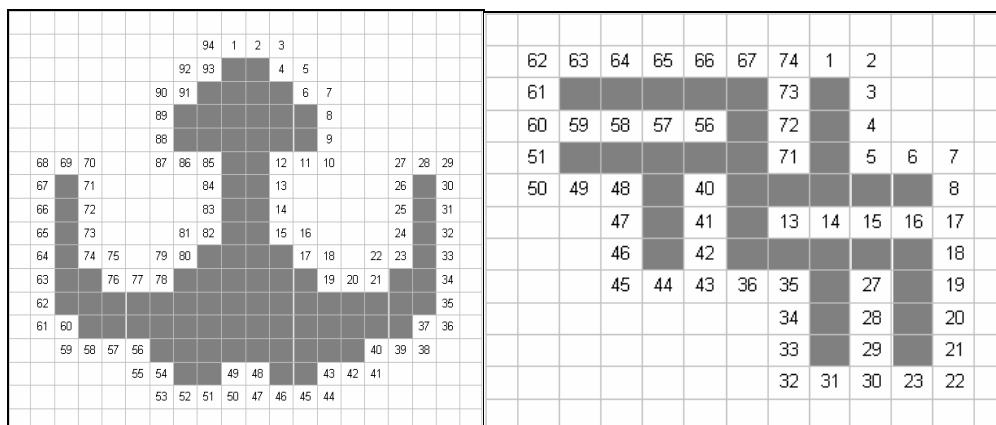


Рис. 9. Третий и четвёртый клеточные миры

Влияние размера популяции на скорость обучения алгоритма ГП. На рис. 10 и 11 приведены графики, объединяющие в себе результаты экспериментов с размером популяции для трёх клеточных миров.

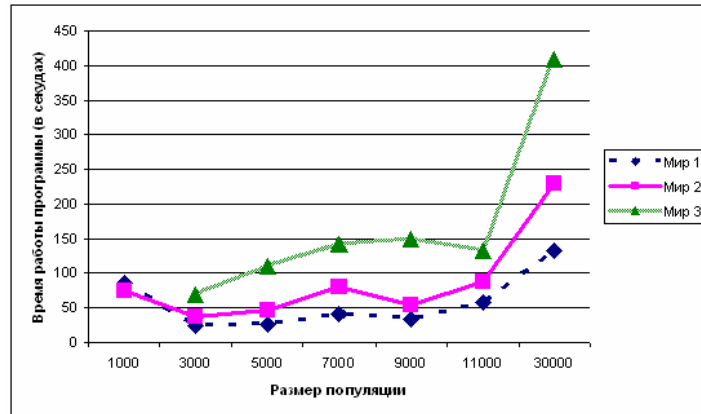


Рис. 10. Время работы программы ГП в зависимости от размера популяции

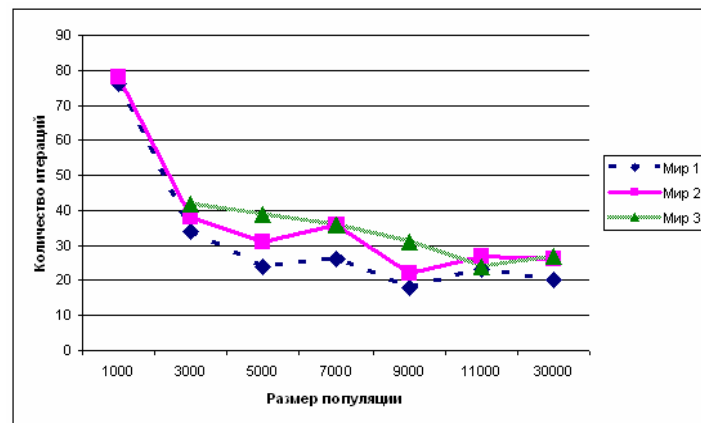


Рис. 11. Количество итераций ГП в зависимости от размера популяции

Из графиков видно, что слишком маленький размер популяции увеличивает время работы алгоритма ГП. Увеличивать размер популяции имеет смысл только в двух случаях, когда не удастся найти оптимальное решение или когда необходимо снизить количество итераций.

Влияние начальной глубины деревьев на скорость обучения алгоритма ГП. На рисунках 12 и 13 приведены графики, объединяющие в себе результаты экспериментов с начальной глубиной деревьев для трёх клеточных миров.

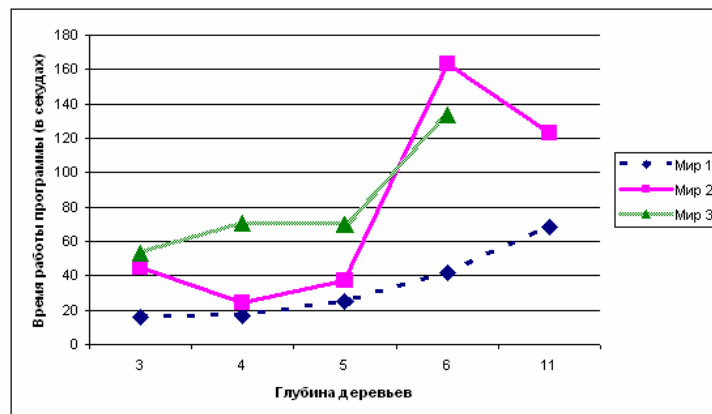


Рис. 12. Время работы программы ГП в зависимости от начальной глубины деревьев

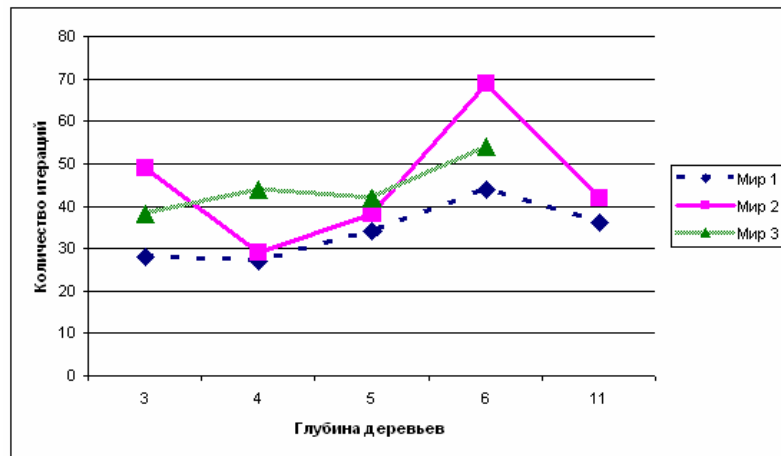


Рис. 13. Количество итераций ГП в зависимости от начальной глубины деревьев

Из графиков видно, что лучше всего использовать минимально допустимую глубину дерева.
 Влияние вероятности мутации на скорость обучения алгоритма ГП. На рис. 14 и 15 приведены графики, объединяющие в себе результаты экспериментов с вероятностью мутации для трёх клеточных миров.

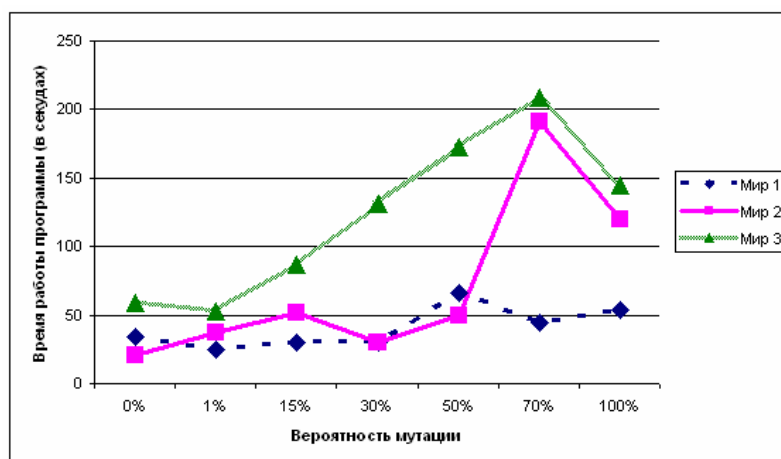


Рис. 14. Время работы программы ГП в зависимости от вероятности мутации

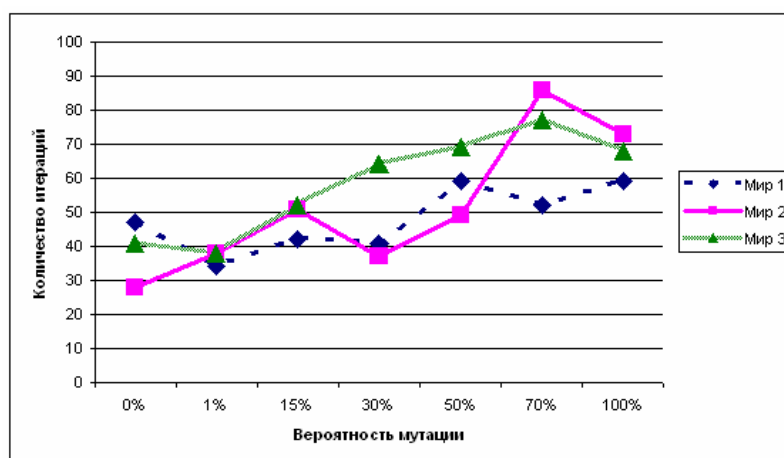


Рис. 15. Количество итераций в зависимости от вероятности мутации

Из графиков видно, что оптимально использовать значение вероятности мутации 0–15%, дальнейшее повышение вероятности мутации ведёт к увеличению времени работы алгоритма ГП.

Влияние вероятности скрещивания на скорость обучения алгоритма ГП. На рис. 16 и 17 приведены графики, объединяющие в себе результаты экспериментов с вероятностью скрещивания для трёх клеточных миров.

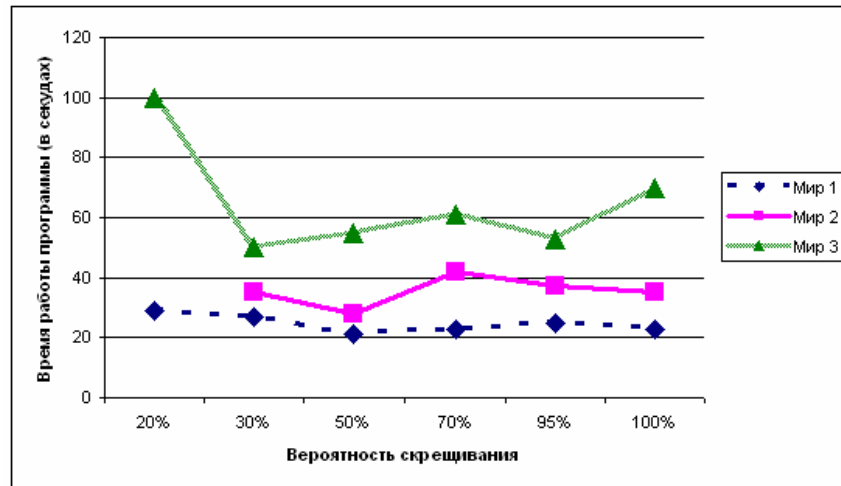


Рис. 16. Время работы программы ГП в зависимости от вероятности скрещивания

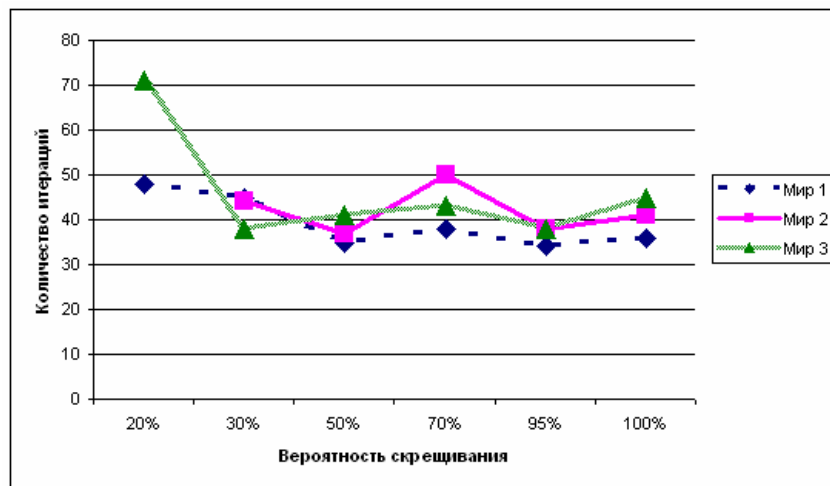


Рис. 17. Количество итераций ГП в зависимости от вероятности скрещивания

Из графиков видно, что время работы программы и количество итераций не очень зависят от вероятности скрещивания. Такие закономерности выявить не удалось: программа одинаково быстро обучалась и с низкой и с высокой вероятностью скрещивания.

Влияние количества нейронов в скрытом слое на скорость обучения нейронной сети Элмана. Так как нейронная сеть Элмана имеет «память предыдущих состояний», то она смогла обучаться и в немарковских средах, поэтому в экспериментах участвовал четвёртый клеточный мир. Также были проведены дополнительные эксперименты с пятым клеточным миром, чтобы выяснить, насколько эффективно нейронная сеть Элмана действует в более сложном мире. На рис. 18 приведён пятый клеточный мир. Пятый клеточный мир является немарковским.

На рис. 19 и 20 приведены графики, объединяющие в себе результаты экспериментов с нейронной сетью Элмана для пяти клеточных миров.

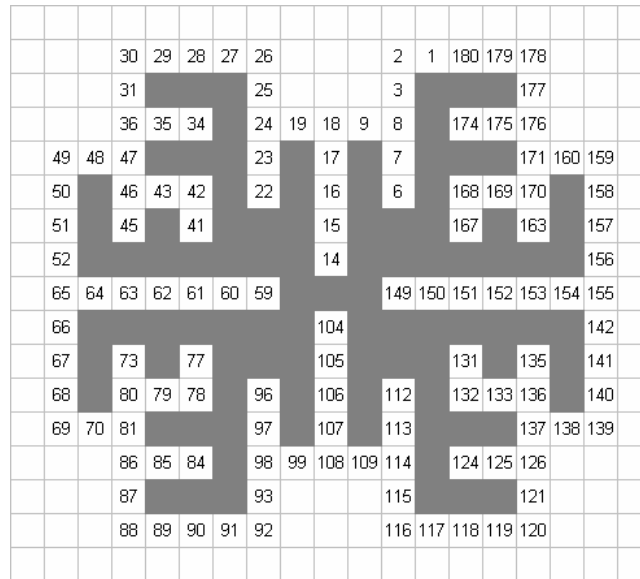


Рис. 18. Пятый клеточный мир

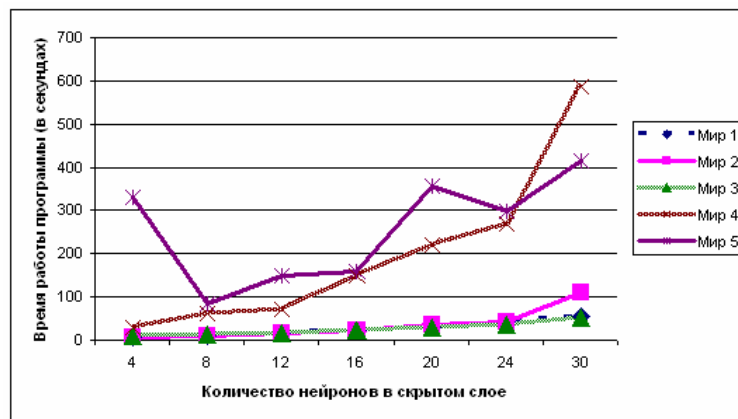


Рис. 19. Время работы программы НС в зависимости от количества нейронов в скрытом слое

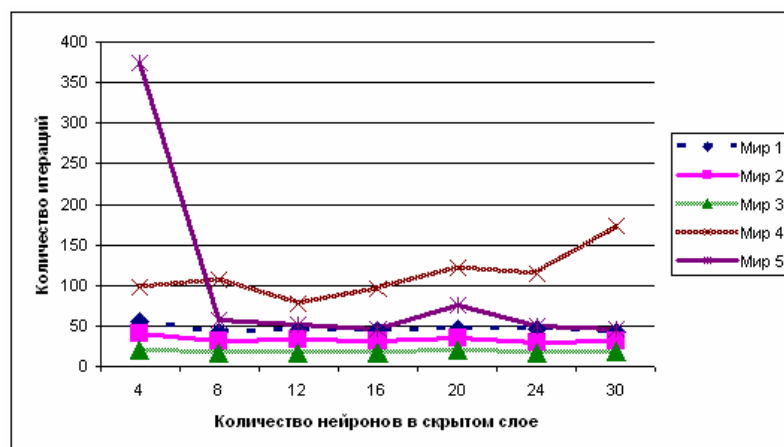


Рис. 20. Количество итераций НС в зависимости от количества нейронов в скрытом слое

Из графиков видно, что для первых трёх миров результаты примерно одинаковы. Все эти миры обладают свойством марковости. Результаты четвёртого мира отличаются, так как данный мир обладает свойством немарковости. Из графиков видно, что время обучения в пятом клеточном мире сравнимо со временем обучения в четвёртом клеточном мире, при этом количество итераций меньше и сравнимо с марковскими средами. Это говорит о том, что сеть Элмана успешно справляется с обучением в более сложных мирах.

Сравнительный анализ алгоритма ГП и нейронной сети Элмана. На рис. 21 и 22 изображены результаты сравнительного анализа методов.

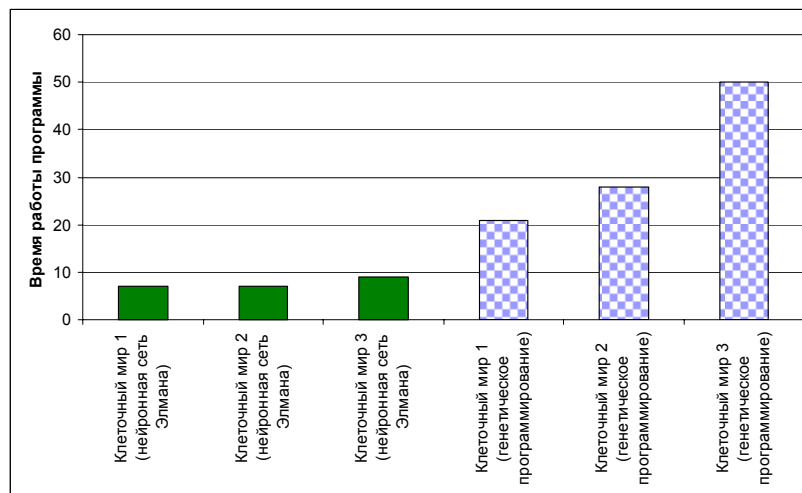


Рис. 21. Время работы программы в зависимости от клеточного мира

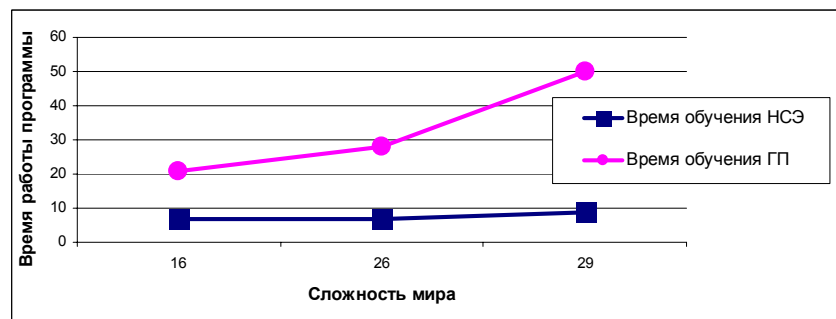


Рис. 22. Время работы программ в зависимости от сложности мира

Из графиков видно, что алгоритм ГП проигрывает нейронной сети Элмана по времени обучения в клеточных мирах, обладающих свойством марковости. Сеть Элмана показала значительно лучшие результаты и затрачивает значительно меньше времени для нахождения решения.

8. Анализ результатов

В процессе экспериментирования были решены следующие задачи:

- исследовано влияние параметров алгоритма генетического программирования на скорость обучения алгоритма;
- исследовано влияние количества нейронов в скрытом слое на скорость обучения нейронной сети Элмана;
- проведены дополнительные эксперименты с нейронной сетью Элмана;
- проведён сравнительный анализ алгоритма генетического программирования и нейронной сети Элмана.

Исследование различных параметров алгоритма генетического программирования позволило сделать следующие выводы.

1. **Исследование размера популяции.** Было выявлено, что слишком маленький размер популяции увеличивает время работы алгоритма ГП. Для клеточных миров, используемых при экспериментах, оптимальный размер популяции составил 3000–5000 особей. Увеличивать размер популяции имеет смысл только в двух случаях: если не удаётся обучить алгоритм клеточному миру и если есть необходимость снизить количество итераций.
 2. **Исследование максимальной глубины деревьев в начальной популяции.** Проведённые эксперименты показали, что лучше всего использовать минимально возможную глубину дерева, при которой возможно обучить алгоритм ГП. Для алгоритма, использованного в данной работе с применением правил построения деревьев, минимальная и оптимальная максимальная начальная глубина деревьев в популяции составила 3–5 узлов. Дальнейшее увеличение начальной глубины деревьев способствует увеличению времени обучения программы. При глубине дерева в 11 узлов уже не удалось обучить алгоритм ГП второму клеточному миру, а при количестве узлов свыше 11 – и остальным мирам. Это происходит из-за того, что в результате скрещивания и мутации глубина деревьев очень сильно возрастает, что способствует быстрому истощению ресурсов компьютера и остановке программы.
 3. **Исследование вероятности мутации.** В ходе экспериментов было выявлено, что оптимальное значение вероятности мутации составляет 0–15%. Дальнейшее повышение вероятности мутации ведёт к увеличению времени работы алгоритма ГП. Для клеточных миров из обучающей выборки оптимальное значение вероятности мутации составило 1%.
 4. **Исследование вероятности скрещивания.** Было выявлено, что при вероятности скрещивания ниже 30% не удаётся обучить алгоритм ГП всем мирам. Поэтому использовать вероятность скрещивания ниже 30% не рекомендуется. Для клеточных миров из обучающей выборки оптимальное значение вероятности скрещивания составило 50%.
- Также был выявлен недостаток алгоритма ГП: он не может быть применён в немарковских средах.

В первых трёх мирах (из обучающей выборки) увеличение нейронов в скрытом слое практически не влияет на скорость обучения нейронной сети Элмана. Это обусловлено тем, что эти среды являются марковскими. Результат в четвёртом клеточном мире отличается, так как эта среда немарковская.

При увеличении количества нейронов в скрытом слое время работы программы возрастает. Время работы достигает минимума при количестве нейронов в скрытом слое, равном 4; свыше этого количество итераций начинает возрастать. Это подтвердили и дополнительные эксперименты с более сложным миром при количестве нейронов в скрытом слое выше 8. Различное количество нейронов в скрытом слое, при котором было достигнуто минимальное время, в четвёртом и пятом мирах отличается, так как сложность пятого мира более чем в два раза выше. Дополнительные эксперименты с пятым клеточным миром показали также, что время обучения в этом мире сравнимо со временем обучения в четвёртом клеточном мире, при этом затрачивалось меньше итераций. Это свидетельствует о том, что нейронная сеть Элмана хорошо справляется даже со сложными клеточными мирами, а то, что время обучения достигло минимума при использовании восьми нейронов в скрытом слое, говорит о том, что повышать количество нейронов в скрытом слое необходимо только при усложнении препятствия.

Сравнительный анализ алгоритма генетического программирования и нейронной сети показал, что алгоритм ГП проигрывает нейронной сети Элмана в скорости, а также не может быть применён в немарковских средах. В свою очередь, нейронная сеть Элмана способна обучаться в таких мирах, а с учётом превосходства во времени обучения такая сеть становится более предпочтительной для решения задачи обхода агентом препятствия по периметру в клеточном мире.

Литература

- [1] Goldberg D. E. (1989) *Genetic Algorithms in Search, Optimization and Machine Learning*. Addison – Wesley Pub. Company. 412 p.

- [2] *Handbook of Genetic Algorithms* (1991) Ed. by L. Davis. Van Nostrand Reinhold, New York, 332–349.
- [3] Nilson N. J. (1998) *Artificial Intelligence: A New Synthesis.*: Morgan Kaufmann Publishers, Inc., San Mateo, California 513 p.
- [4] Оссовский С. (2002) *Нейронные сети для обработки информации*. Пер. с польского И. Д. Рудинского. М.: Финансы и статистика, Москва. 344 с.
- [5] Ziemke T. (1999) Remembering how to behave: recurrent neural networks for adaptive robot behavior. In: L. Medsker & L. Jain (eds.) *Recurrent Neural Networks: Design and applications*. Boca Raton: CRC Press, 355–389.

Received on the 12th of August 2006

DEVELOPMENT OF STANDARD OPERATING ENVIRONMENT (SOE) EXPANDING ON THE BASEMENT OF AUTOMATED AND STANDARDIZED SYSTEM IMAGING

V. GOPEYENKO, V. ZENIN

*Information Systems Management Institute
Department of Natural Sciences and Computer Technologies
Lomonosov 1, Riga, LV-1019, Latvia
E-mail: via@latnet.lv, vadzen@apollo.lv*

It would perhaps be no exaggeration to say that using computers in business increases the productivity and the effectiveness of management. However, with the increasing of the quantity of workstations in the long run, grows the heterogeneity of computer systems on workstations. Non-homogeneous systems make the installation of additional applications and users' support more difficult, increase help desk calls and time for new application compatibility testing, as well as time of system restoring on desktops; create the unstable platform for business applications and decrease uptime. It should be noted as well that increasing the time of updating operation systems and patch distribution decreases the security on the whole. As a result, the costs for supporting workstations extend.

The method of deployment of computer workplaces in education institutes, middle and large corporations, the principals of the creation of different types of clones of Standard Operating Environment, the design, creation and deployment of the real system of Standard Operating Environment based on Microsoft Windows 2000 Professional and Microsoft Windows 2000 Server for the classrooms of Information Systems Management Institute are discussed.

Keywords: *Operating system imaging, Standard Operating Environment*

1. Standard Operating Environment (SOE)

For solving the above-mentioned problems we must standardize operation systems and applications on all desktops and notebooks. The method of standard environment is called **Standard Operating Environment (SOE)**.

The **Standard Operating Environment (SOE)** is a specification for standards for computer hardware, operating system, security and applications software, arrived at through extensive consultation, development and testing undertaken by * company's project.

The major advantage of having an **SOE** within a large scale environment is that the time taken to deploy and configure a new computer is greatly reduced. In a scenario where departments might be buying different computer configurations, it is not possible to have a streamlined install and setup process due to variations such as disk sizes, hardware, and other factors. The **SOE** concept also includes a life cycle component and the **SOE** will be reviewed annually. Hardware will have a life-span of four years. The concept of the **SOE** is currently limited to standard Windows-based PCs, but could be extended to cover other platforms.

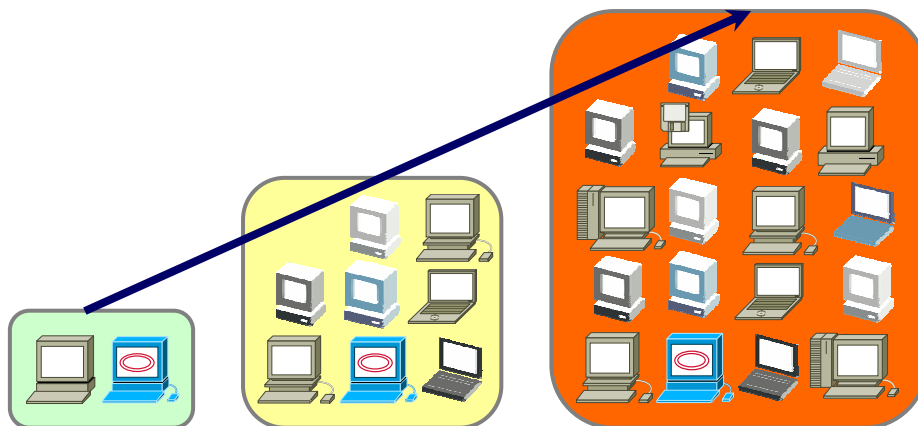


Figure 1. With the increasing of the quantity of workstations in the long run, grows the heterogeneity of computer systems on workstations

Standard Operating Environment (SOE) image includes the following:

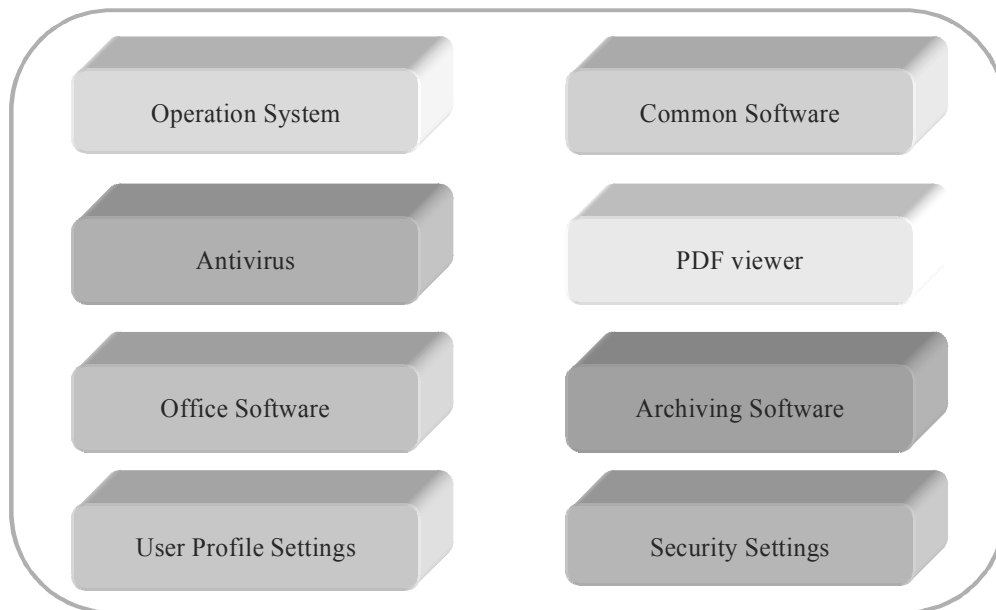


Figure 2. Standard Operating Environment (SOE) image

2. SOE image's best practices

2.1. SEPARATE USERS PROFILES, PROGRAM AND FILES FROM SYSTEM FILES

Best practice is if SOE image has 3 different partitions with:

- Hidden Partition for TOOLS (ZENWORKS, Symantec Ghost system partition etc.);
- Operation System Files;
- Users' Data Files.

If workstation has software problems with operation system or common software, the best solution is to clone only System partition from SOE image. This solution decreases workstation down time and saves User Data Files and User Profile settings (Favourite, Files from Desktop, etc.).

For example, we have workstation with 80 GB HDD. We separate HDD as 10 GB for System partition and 70 GB for User Data Files partition. If we have crash of Windows system, the only clone System partition is needed and there is no need to copy 70 GB of Users' Files from HDD and copy back 70 GB of Users Files to HDD after imaging.

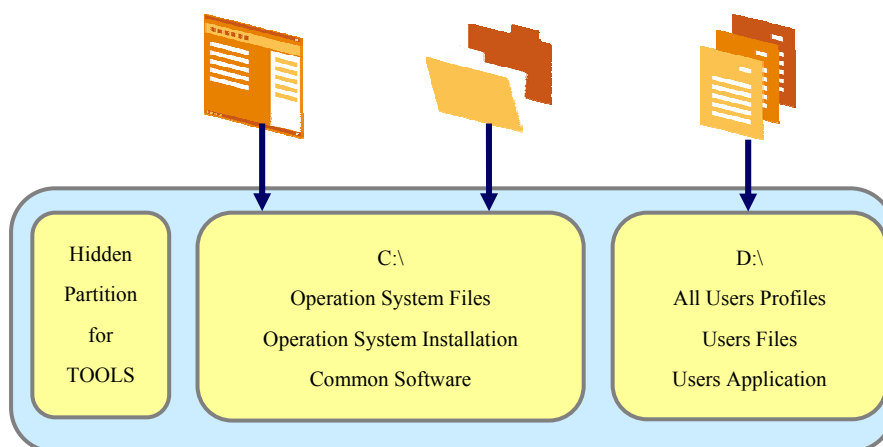


Figure 3. Separate Users' Profiles, Program and Files from System Files

2.2. MOVE A USER'S DOCUMENTS AND SETTINGS FOLDER TO D:\ PARTITION

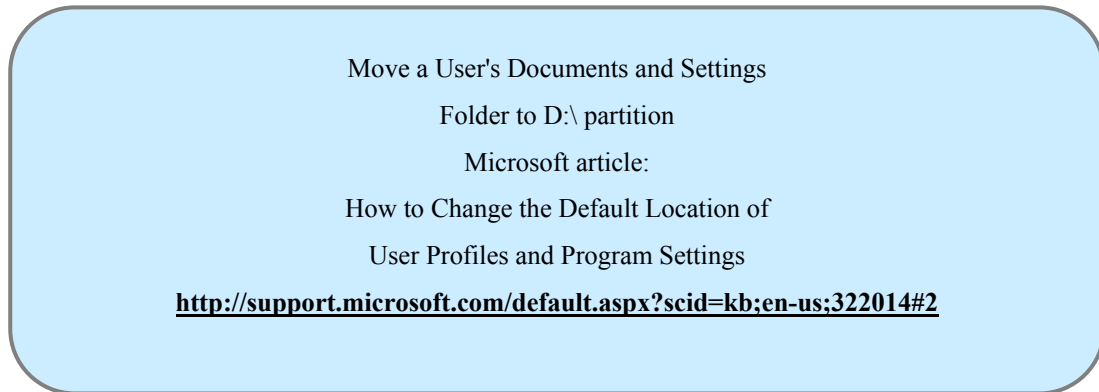


Figure 4. Move a User's Documents and Settings Folder to D:\ partition

2.3. CUSTOMIZE DEFAULT USER PROFILE



Figure 5. Customize Default User Profile

2.4. SECURITY TEMPLATES PREPARING AND USING

With Group Policy, you can ensure that the machines on your network remain in a secure configuration after you deploy them. When you create or modify a Group Policy Object (GPO), you can configure several security settings located under Group Policy Editor (GPE) Computer Configuration, Windows Settings, Security Settings. As you can see, Group Policy makes it easy to configure security settings on the machines in your Win2K domain. In addition, two tools, Security Templates and Security Configuration and Analysis, are extremely useful for applying network security policy and evaluating whether individual machines comply with the policy, as Image shows. With these tools, you can build templates with particular security settings, apply the settings to the machines, and then periodically evaluate the machines to verify that they remain properly configured.

Security Templates. You can use the Microsoft Management Console's (MMC's) Security Templates snap-in to build different templates that you can import into Group Policies. You can either create a new policy from scratch or modify one of the built-in policies. After you decide which template to use, you can import the template settings into your GPO using Group Policy Editor (GPE) by right-clicking Computer Configuration, Windows Settings, and Security Settings and choosing Import Policy. This process applies all the settings you configured in the template to all the computers in the container (e.g., site, domain, OU) that you link the Group Policy to.

Security Configuration and Analysis. You can use the MMC's Security Configuration and Analysis snap-in to verify that the security settings you apply with Group Policy are in use. Before you perform an analysis, create a database to store the results. After you create and open the database and choose the template containing the settings that you want to apply to a specific machine, right-click the snap-in and choose Analyze Computer Now to check the actual security settings against the desired settings. You can also use Security Configuration and Analysis to apply the security template to the machine, but it's better

to use Group Policy. If you use Security Configuration and Analysis to apply the settings, a user can come behind you and change the settings. With Group Policy, if a user changes a security setting, it changes back to its original value the next time Win2K applies the policy.

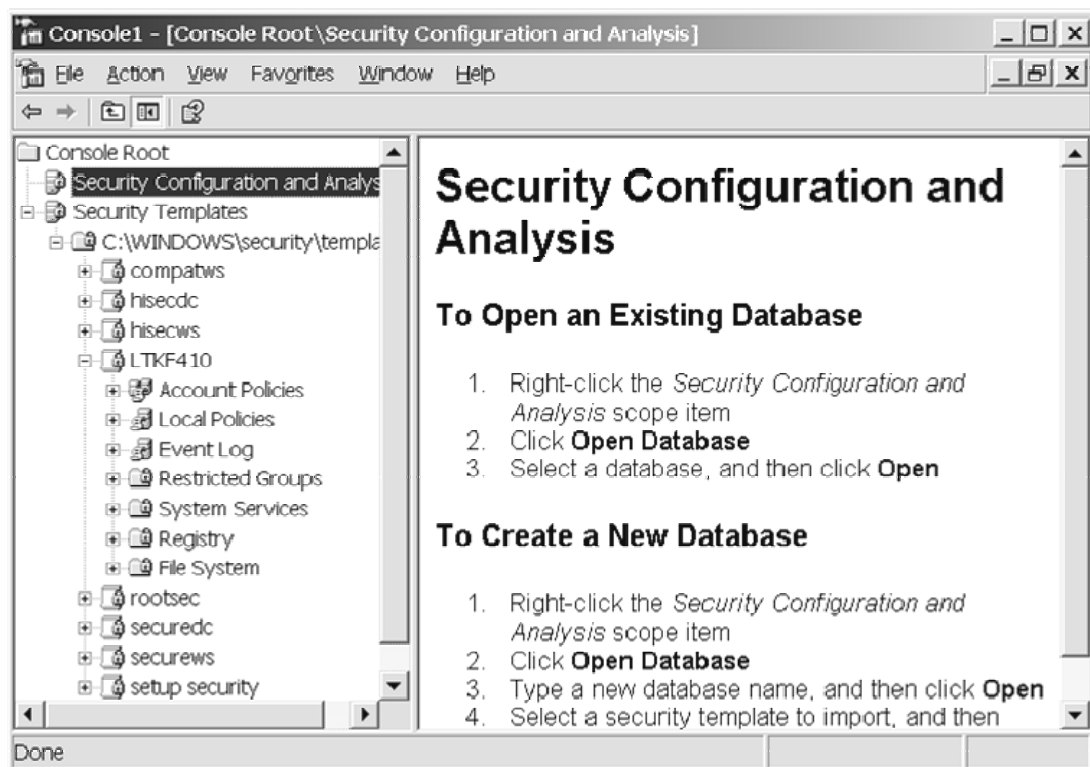


Figure 6. Snap-ins for MMC console: Security Configuration and Analysis, Security Templates

3. Three main methods of deploying a base operating system

3.1. PURE OS IMAGE

This method is used when hardware is near identical Enterprise wide (Classes, Operation Centre, etc.). Extremely rapid development of SOE. Fast installation (5-10 minutes). Really examples: SOE PURE image with higher compression (~ 2:1) 2.6 GB – deploy in 7 minutes; SOE PURE image for Information Systems Management Institute with higher compression (~ 2:1) 6.7 GB or 11 CD – deploy in 15 minutes.

3.2. SYSPREP IMAGE

SOE SYSPREP image allows for more varied hardware. SOE can be developed and customized quickly for middle and large corporation. Fast installation (15–30 minutes). Real example: SOE SYSPREP image with higher compression (~ 2:1) 2.6 GB – deploy in 20 min.

3.3. UNATTENDED OR SCRIPTED INSTALLATION

Install anywhere – almost hardware agnostic. Installation is extremely slow (35–90 minutes).

Scripted installation doesn't guarantee homogeneous Standard Operating Environment; therefore we don't discuss this method of installation. For example restoring of IBM ThinkPad Notebook use Unattended or Scripted installation takes 120–180 minutes.

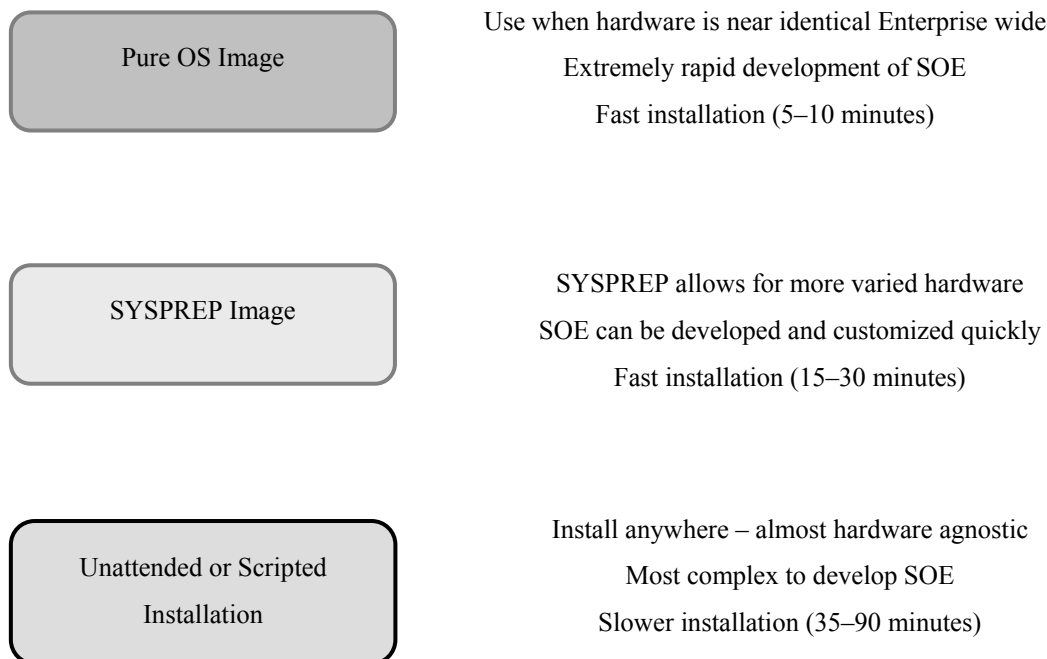


Figure 7. Methods of deploying a base operating system

4. SOE image's distribution

There are 3 main methods for Standard Operating Environment image's distribution.

Locally from CD, DVD, HDD. Through Network to 1 workstation (Network sharing). From Image Server through Network to many workstations at the same time (Multicast Image Server). It is the best approach for fast SOE image deployment in classes, operation centres, call centres, exhibitions, etc.

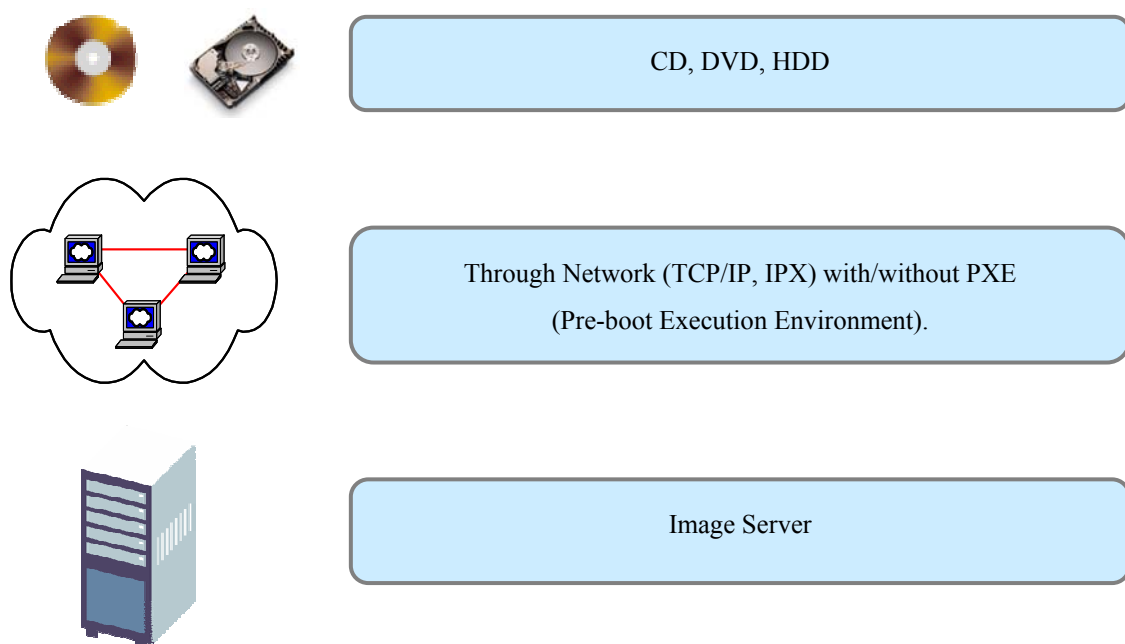


Figure 8. Sources for Users' Computers and Notebooks cloning

4.1. POST SOE DEPLOYMENT

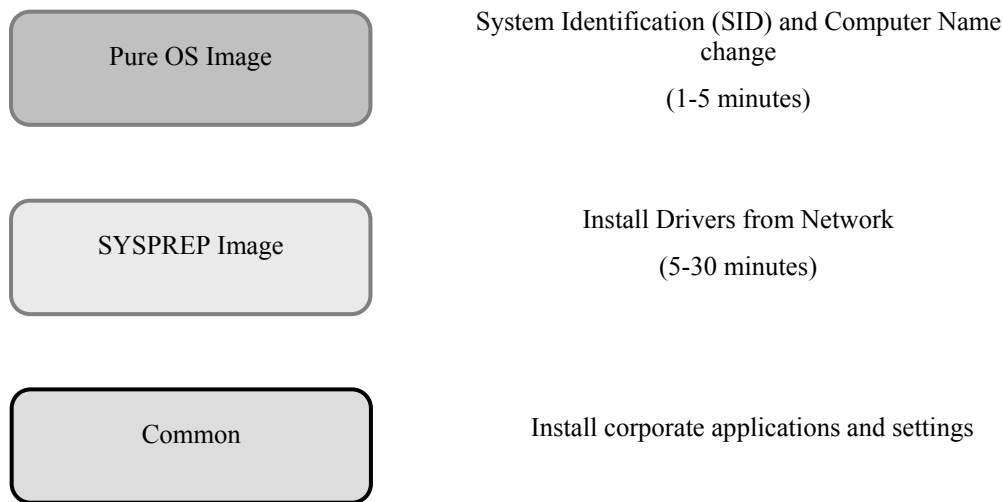


Figure 9. Post SOE Deployment

4.2. PURE OS IMAGE

When you clone a Windows NT/2000/XP installation to many computers, the destination computers have the same SID and computer name as the source Windows installation. Because Windows NT/2000/XP networks use each computer's SID and computer's name to uniquely identify the computer on the network, you must change the SID and computer name on each destination (client) computer after cloning. Computer Security Identifier (SID) and Computer Name should be changed. For example, with Ghost Walker or NewSID programs. Ghost Walker is a Ghost utility included in the corporate Ghost Enterprise versions. Ghost Walker is a DOS program that allows you to change the SID and computer name at each client computer after cloning, that is, before restarting the computer into Windows. NewSID is a program that changes a computer's SID. It is free, comes with full source, and is a Win32 program, meaning that it can easily be run on systems that have been previously cloned. NewSID works on Windows NT 4, Windows 2000, Windows XP and Windows 2003 Server.

4.3. SYSPREP IMAGE

When you clone a Windows NT/2000/XP installation to many computers with different hardware, Drivers from Network servers should be installed. Time for installation depends on Hardware and Network speed, 5-30 minutes.

4.4. COMMON

Finally should be installed corporate applications and settings for current User. Centralized and automated installation of company's applications and patch distribution to SOE workstations is very simple, manageable and scalable solution.

4.5. HARDWARE REQUIREMENTS

Hardware requirements is Pre-Boot Execution Environment (PXE) – compatible Network Card with Ndis2 and Packet Driver. Network Card is needed for SOE imaging and post SOE deployment through network. For using Pure Standard Operation Environment image hardware should be identical.

4.6. CHOICE OF SOFTWARE FOR (SOE)

Our choice of software for Standard Operating Environment (SOE) is the following: If company has NOVELL Network Environment, the best and obvious solution is Novell ZENworks. If company has only classes or operate centres (Educational institutions, Call Centres, etc.) the best solution is Symantec Ghost Solution Suite. If company has only Microsoft Windows Network Environment, the program could be selected from Novell ZENworks and Altiris Client Management Suite.

We chose Symantec Ghost Enterprise Edition for Information Systems Management Institute Windows Standard Operating Environment (SOE).

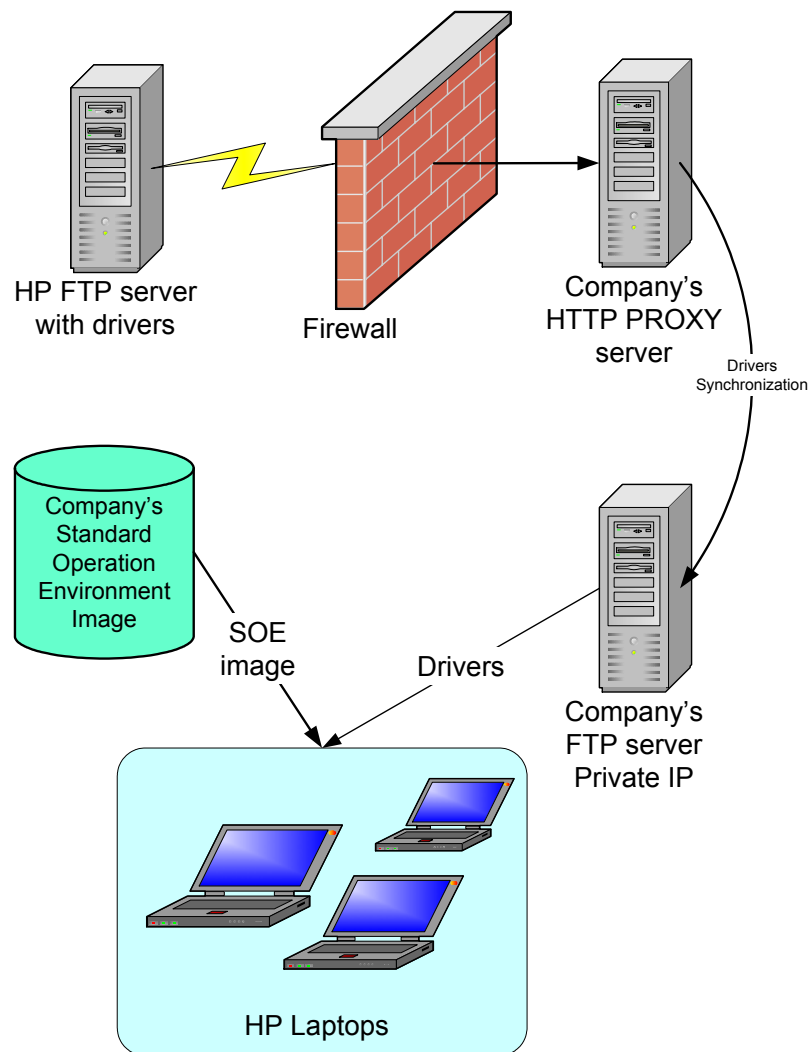


Figure 10. Enterprise solution for deployment Hewlett-Packard workstation in large company with SYSPREP SOE image

4.7. ANALYSES OF STATISTIC INFORMATION OF SOE IMAGE DISTRIBUTION IN INFORMATION SYSTEMS MANAGEMENT INSTITUTE

Microsoft Windows 2000 Professional **Standard Operation Environment** (SOE) image for Information Systems Management Institute has size 6.7 GB with compression (11 CD). Windows SOE has 11 GB size on the HDD. Microsoft Windows 2000 Professional SOE for ISMI includes 85 Applications, Services Pack 4 and all last fixes. There is "Time of classes cloning (ours)" = "SOE image deploying to all classes quantity" * "Classes" * "Time of 1 class cloning", where "Time of 1 class cloning" = 30 minutes from Symantec Ghost Multicast server.

There are “Administrators' ours needed for deployment manually” = “Total images deployment” * “ours needed for manual deployment OS and all applications to 1 workstation”, where “ours needed for manual deployment OS and all applications to 1 workstation” = 40 Administrator's work ours.
There are “Administrators' work days” = “Administrators' ours needed for deployment manually” / “Work ours in day”, where “Work ours in day” = 8 ours.

TABLE 1. SOE image deploying statistics in ISMI classes

SOE image deploying to 54 workstations in ISMI classes					
	2003 -2004		2004 - 2005		
	I semester	II semester	I semester	II semester	Total 1.5 year
SOE image deploying to all classes quantity	6	4	3		13
Student workstations quantity	54	54	54		
Total images deployment	324	216	162		702
Classes	3	3	3		
Time of classes cloning (ours)	9	6	4.5		19.5
Administrators' hours needed for deployment manually	12960	8640	6480		28080.00
Administrators' work days	1620	1080	810		3510.00
Needed Administrators for this deployment manually in semester	18.00	12.00	9.00		13.00
Administrators' costs in semester (Ls)	24 300	16 200	12 150		52 650

There are “Needed Administrators for this deployment manually in semester” = “Administrators' work days” / “Works days in semester”, where “Works days in semester” = 90 days (4.5 months).

There are “Administrators' costs in semester (Ls)” = “Needed Administrators for this deployment manually in semester” * “Administrator's costs in month” * 4.5 (months), where “Administrator's costs in month” = Ls 300.

Finally for SOE clone deployment to 54 student workstation of ISMI in 1.5 years (3 semesters):
Windows **Standard Operation Environment** (SOE) + standardized image deployment software + 1 Computer engineer =

- 702 Windows 2000 SOE images deploying in 1.5 year to 54 students workstations;
- Cut down spending for Ls 52 650 in 1.5 year;
- There are **equivalent for work of 13 administrators**.

Conclusion

For solving the above mentioned in Introduction problems we must standardize operation systems and applications on all desktops and notebooks. The method of standard environment is called Standard Operating Environment (SOE).

The following method – Standard Operating Environment, allows achieving the following results:

- helps to centralize and automate application management, patch management,
- centralizes and automates desktop configuration,
- improves the availability and protection of user's data,
- keeps systems secure,
- keeps up-to-date operation systems by automating the rollout and maintenance of a standard operating environment—including the latest patches and updates—across all desktops as well as the risk of security breaches and virus attacks,
- enables simplified maintenance and reduced help desk calls through standardization,
- facilitates creation and enforcement of a secure computing base for all employees,
- minimizes management variables and costs,
- assures business continuity,
- increases productivity by keeping crucial systems available to users and quickly restores them if a disaster occurs,
- strategically helps to create holistic damage recovery solution.

In my opinion, Standard Operating Environment (SOE) is more than it is needed for Educational institutions, Call Centres, corporations, middle and large company.

References

- [1] Microsoft course 2152, Supporting Microsoft Windows 2000 Professional & Server.
- [2] Microsoft course 2153, Supporting Windows 2000 network infrastructure.
- [3] Microsoft course 2154, Implementing & Administering Windows 2000 directory services.
- [4] Microsoft course 2150, Designing a Secure Windows 2000 network.
- [5] Microsoft course 1561, Designing a MS Windows 2000 Directory Services Infrastructure.
- [6] Symantec Ghost Implementation Guide.
- [7] Novell ZENworks for Desktops Administration Guide.
- [8] <http://support.microsoft.com/default.aspx?scid=kb;en-us;322014#2> (How To Change the Default Location of User Profiles and Program Settings).
- [9] <http://support.microsoft.com/default.aspx?scid=kb;en-us;305709> (How To Create a Custom Default User Profile).
- [10] http://www.windowsecurity.com/articles/Windows_Server_2003_Security_Analysis.html
- [11] <http://support.microsoft.com/default.aspx?scid=kb;en-us;162001> (Do not disk duplicate installed versions of Windows).
- [12] <http://www.sysinternals.com/ntw2k/source/newsid.shtml> (NewSID).
- [13] <http://sea.symantec.com/content/product.cfm?productid=9> (Symantec Ghost Solution Suite).
- [14] <http://support.microsoft.com/default.aspx?scid=kb;en-us;321709> (HOW TO: Use the Group Policy Results Tool in Windows 2000).
- [15] <http://www.microsoft.com/downloads/details.aspx?FamilyID=0a6d4c24-8cbd-4b35-9272-dd3cbfc81887&DisplayLang=en> (Group Policy Management Console with Service Pack 1).
- [16] <http://www.adobe.com/products/acrobat/readstep2.html> (Download Adobe Reader).
- [17] <http://office.microsoft.com/en-us/assistance/HA011363091033.aspx> (Creating an Administrative Installation Point).
- [18] <http://office.microsoft.com/en-us/assistance/HA011363101033.aspx> (Customizing the Office Installation).

Received on the 22nd of April 2006

НЕКОТОРЫЕ МАТЕМАТИЧЕСКИЕ МОДЕЛИ С НЕЛИНЕЙНЫМИ ГРАНИЧНЫМИ УСЛОВИЯМИ ДЛЯ ПРОЦЕССОВ ИНТЕНСИВНОГО ЗАКАЛИВАНИЯ СТАЛИ И ИХ АНАЛИТИЧЕСКИЕ РЕШЕНИЯ

Ш. Э. ГУСЕЙНОВ^{1,2}, Н. И. КОБАСКО³,
А. А. БУЙКИС², А. Г. МАМЕДОВ⁴

¹Институт транспорта и связи
E-mail: sh.e.guseinov@inbox.lv

²Институт Математики и Компьютерных Наук, Латвийский Университет
E-mail: sh.e.guseinov@inbox.lv, buikis@latnet.lv

³IQ Technologies Inc., Akron, USA
E-mail: NIKobasko@aol.com

⁴Институт Математики и Механики Национальной Академии Наук Азербайджана
E-mail: a.g.mamedov@mail.ru

В данной работе показано существование аналитического решения как для нестационарного уравнения теплопроводности, так и для гиперболического уравнения нестационарной теплопроводности с нелинейными граничными условиями, обусловленными нестационарным пузырьковым кипением. Подобные решения необходимы при разработке новых интенсивных и экологически чистых технологий термической обработки материалов. Работа является началом цикла исследований, выполняемых в рамках международного проекта «Database for cooling capacities of various quenchants to be developed with the modern computational and experimental techniques» под эгидой WSEAS: World Scientific and Engineering Academy and Society (www.wseas.org/propose/project/wseas-projects.htm). Кроме того, аналитические решения и их анализ также крайне необходимы при автоматизации и компьютеризации технологических процессов.

Ключевые слова: уравнение теплопроводности, гиперболическое уравнение теплопроводности, нелинейные граничные условия, интенсивные и экологически чистые технологии термической обработки материалов

Введение

Как известно (см., например, [1–3] и список соответствующей литературы в них), охлаждающая способность закалочных сред характеризуется комплексом величин, которые включают критические тепловые потоки, коэффициенты теплоотдачи при пленочном и пузырьковом кипении, а также при однофазной конвекции. Для прогнозирования условий теплообмена на границе необходимо определять начальные тепловые потоки в момент погружения закаливаемого изделия в закалочную среду и сравнивать их с критическими значениями закалочной среды. Для интенсивной закалки основным является отсутствие пленочного кипения, а это означает, что начальный тепловой поток должен быть меньше критического теплового потока для используемой закалочной среды. При вычислении начальных тепловых потоков на основе обычного уравнения теплопроводности результаты вычислений всегда получаются завышенными, значительно превышающими критические значения. Поэтому существует мнение, что при закалке всегда наблюдаются три стадии теплообмена: пленочное кипение, пузырьковое кипение и однофазный конвективный теплообмен. На самом деле пленочное кипение отсутствует, если начальный тепловой поток меньше критического. Правильные начальные тепловые потоки можно получить только на основе решения гиперболического уравнения. Рассмотренная в данной работе математическая модель описывает физический процесс интенсивного закаливания стали (см. [4–6]).

Интенсивная закалка стальных изделий характеризуется отсутствием пленочного кипения и наличием нестационарного пузырькового. В этом случае возникают нелинейные граничные условия, которые усложняют аналитическое решение. В данной статье рассматриваются начально-краевые задачи для двух типов уравнений – для обычного нестационарного уравнения теплопроводности и для гиперболического уравнения нестационарной теплопроводности с нелинейными граничными условиями, отображающими процесс пузырькового кипения. Рассмотрение двух типов уравнений обусловлено тем, что задача с соответствующим нелинейным граничным условием

для обычного нестационарного уравнения теплопроводности исследована различными численными методами и для этой задачи в настоящее время накопилось достаточное количество экспериментальных данных (см., например, [2,3]). А задача с аналогичным нелинейным граничным условием для гиперболического уравнения нестационарной теплопроводности лишь относительно недавно предлагалась как альтернативная математическая модель. В связи с вышесказанным данная работа представляется важной – задача нахождения аналитического решения исходной нелинейной математической модели сводится к задаче решения нелинейного интегрального уравнения Вольтерра, что является более простой задачей по сравнению с исходной. Уместно заметить, что при некоторых предположениях относительно исходных данных, авторами уже доказано существование неподвижной точки полученного нелинейного интегрального уравнения Вольтерра. Следовательно, для нахождения аналитического решения этого интегрального уравнения можно применить метод последовательного приближения. Отметим, что в данной работе доказательство существования неподвижной точки для полученного нелинейного интегрального оператора Вольтерра, а также метод последовательного приближения для решения уравнения не приводятся. Данное обстоятельство связано с тем, что ранее авторы доказали существование неподвижной точки для более широкого класса нелинейных интегральных уравнений Вольтерра, нежели полученное в данной работе нелинейное интегральное уравнение, которое является частным случаем.

Аналогичная постановка задачи и ее приближенное решение на основе параболического уравнения нестационарной теплопроводности и нелинейного граничного условия была представлена в работах [2] и [4]. Необходимость использования гиперболического уравнения нестационарной теплопроводности связана с необходимостью вычисления начальных конечных тепловых потоков в момент погружения стальных изделий в закалочную среду.

1. Постановка исходной прямой начально-краевой задачи для гиперболического уравнения теплопроводности

Рассмотрим следующую прямую задачу: требуется найти функцию $u(x,t)$, которая удовлетворяет гиперболическому уравнению теплопроводности

$$\frac{\partial u(x,t)}{\partial t} + \tau_r \cdot \frac{\partial^2 u(x,t)}{\partial t^2} = a^2 \cdot \frac{\partial^2 u(x,t)}{\partial x^2} + f(x,t), \quad 0 < x < l < \infty, \quad 0 < t \leq T < \infty, \quad (1)$$

$$\text{где } a^2 = \frac{k}{c \cdot \rho}, k, c, \rho, \tau_r \equiv \text{const.} > 0,$$

начальным условиям

$$u(x,t)|_{t=0} = u_0(x), \quad 0 \leq x \leq l, \quad (2)$$

$$\left. \frac{\partial u(x,t)}{\partial t} \right|_{t=0} = u_1(x), \quad 0 \leq x \leq l, \quad (3)$$

граничным условиям

$$\left. \frac{\partial u(x,t)}{\partial x} \right|_{x=l} = 0, \quad 0 \leq t \leq T, \quad (4)$$

$$-k \cdot \left. \frac{\partial u(x,t)}{\partial x} \right|_{x=0} + \beta^m \cdot \left\{ u(x,t) \right\}_{x=0}^m - \theta(t) = 0, \quad 0 \leq t \leq T, \quad (5)$$

$$\text{где } m = \frac{10}{3}, \quad \beta \equiv \text{const} > 0,$$

условиям согласованности

$$\left. \begin{aligned} u'_0(l) &= u'_1(l) = 0, \\ -k \cdot u'_0(0) + \beta^m \cdot \{u_0(0) - \theta(0)\}^m &= 0, \\ m \cdot u'_0(0) \cdot \{u_1(0) - \theta'(0)\} &= u'_1(0) \cdot \{u_0(0) - \theta(0)\}. \end{aligned} \right\} \quad (6)$$

Кроме того, в (1)–(6) предполагается, что исходные функции задачи $f(x, t) \in C\{[0, l] \times [0, T]\}$, $u_i(x) \in C^1[0, l]$ ($i = 0, 1$), $\theta(t) \in C^2[0, T]$ являются заданными функциями, искомая функция $u(x, t) \in C^2\{[0, l] \times [0, T]\}$, исходные константы задачи $\tau_r, l, T, \beta, k, c, \rho, a^2$ также являются заданными.

2. Сведение исходной прямой задачи к эквивалентной ей прямой задаче

Введем новую функцию

$$\mathcal{G}(x, t) \stackrel{\text{def}}{=} e^{\frac{t}{2\tau_r}} \cdot \{u(x, t) - \theta(t)\}, \quad 0 \leq x \leq l, \quad 0 \leq t \leq T. \quad (7)$$

Учтем (7) поочередно в (1)–(6). Тогда из (1) получим гиперболическое уравнение

$$\frac{\partial^2 \mathcal{G}(x, t)}{\partial t^2} = \frac{a^2}{\tau_r} \cdot \frac{\partial^2 \mathcal{G}(x, t)}{\partial x^2} + \frac{1}{4 \cdot \tau_r^2} \cdot \mathcal{G}(x, t) + F(x, t), \quad 0 < x < l, \quad 0 < t \leq T, \quad (8)$$

где

$$F(x, t) \stackrel{\text{def}}{=} e^{\frac{t}{2\tau_r}} \cdot \left\{ \frac{1}{\tau_r} \cdot f(x, t) - \frac{1}{\tau_r} \cdot \theta'(t) - \theta''(t) \right\},$$

из (2) получим, что

$$\mathcal{G}(x, t) \Big|_{t=0} = \mathcal{G}_0(x), \quad 0 \leq x \leq l, \quad (9)$$

где $\mathcal{G}_0(x) \stackrel{\text{def}}{=} u_0(x) - \theta(0)$,

из (3) получим, что

$$\frac{\partial \mathcal{G}(x, t)}{\partial t} \Big|_{t=0} = \mathcal{G}_1(x), \quad 0 \leq x \leq l, \quad (10)$$

где $\mathcal{G}_1(x) \stackrel{\text{def}}{=} \frac{1}{2 \cdot \tau_r} \cdot u_0(x) + u_1(x) - \frac{\theta(0)}{2 \cdot \tau_r} - \theta'(0)$,

из (4) получим, что

$$\frac{\partial \mathcal{G}(x, t)}{\partial x} \Big|_{x=l} = 0, \quad 0 \leq t \leq T, \quad (11)$$

из (5) получим, что

$$-k \cdot \frac{\partial \mathcal{G}(x, t)}{\partial x} \Big|_{x=0} + \beta^m \cdot e^{\frac{m-1}{2\tau_r} t} \cdot \mathcal{G}^m(x, t) \Big|_{x=0} = 0, \quad 0 \leq t \leq T, \quad (12)$$

из (6) получим, что

$$\left. \begin{aligned} \mathcal{G}'_0(l) &= \mathcal{G}'_1(l) - \frac{1}{2 \cdot \tau_r} \cdot \mathcal{G}'_0(l) = 0, \\ -k \cdot \mathcal{G}'_0(0) + \beta^m \cdot \mathcal{G}_0^m(0) &= 0, \\ 2 \cdot m \cdot \tau_r \cdot \mathcal{G}_1(0) \cdot \mathcal{G}'_0(0) + (1-m) \cdot \mathcal{G}'_0(0) \cdot \mathcal{G}_0(0) &= 2 \cdot \tau_r \cdot \mathcal{G}_0(0) \cdot \mathcal{G}'_1(0). \end{aligned} \right\} \quad (13)$$

В задаче (8)–(13) требуется определить функцию $\mathcal{A}(x, t)$.

Так как преобразование (7) является невырожденным, то исходная прямая задача (1)–(6) и полученная прямая задача (8)–(13) являются эквивалентными. Следовательно, если мы нашли решение $\mathcal{A}(x, t)$ задачи (8)–(13), то функция $u(x, t)$, определяемая по формуле

$$u(x, t) = \theta(t) + e^{-\frac{t}{2 \cdot \tau_r}} \cdot \mathcal{A}(x, t), \quad 0 \leq x \leq l, \quad 0 \leq t \leq T,$$

будет решением исходной прямой задачи (1)–(6).

Чтобы решить задачу (8)–(13), сначала мы сформулируем одну граничную обратную задачу, решение которой, как будет показано ниже, есть решение прямой задачи (8)–(13), и тем самым, исходная прямая задача (1)–(6) будет полностью решена.

3. Постановка соответствующей граничной обратной задачи

Рассмотрим уравнение (8) с начальными условиями (9) и (10), граничными условиями второго рода (т.е. краевую задачу Неймана) (11) и

$$\left. \frac{\partial \mathcal{A}(x, t)}{\partial x} \right|_{x=0} = \mathcal{G}_2(t), \quad 0 \leq t \leq T, \quad (14)$$

условиями согласованности

$$\left. \begin{aligned} \mathcal{G}'_0(l) &= 0, \\ \mathcal{G}'_1(l) - \frac{1}{2 \cdot \tau_r} \cdot \mathcal{G}'_0(l) &= 0, \\ \mathcal{G}'_0(0) &= \mathcal{G}_2(0), \\ \mathcal{G}'_1(0) &= \mathcal{G}'_2(0), \\ -k \cdot \mathcal{G}'_0(0) + \beta^m \cdot \mathcal{G}_0^m(0) &= 0, \\ 2 \cdot m \cdot \tau_r \cdot \mathcal{G}_1(0) \cdot \mathcal{G}_2(0) + (1-m) \cdot \mathcal{G}_2(0) \cdot \mathcal{G}_0(0) &= 2 \cdot \tau_r \cdot \mathcal{G}_0(0) \cdot \mathcal{G}'_2(0). \end{aligned} \right\} \quad (15)$$

Теперь сформулируем граничную обратную задачу: требуется определить из (8)–(11), (14), (15) при дополнительном условии (12) неизвестные функции $\mathcal{G}_2(t)$ и $\mathcal{A}(x, t)$.

Прежде чем перейти к решению сформулированной обратной задачи, заметим, что без требования дополнительной информации (12) и при предположении, что известна функция $\mathcal{G}_2(t)$, $0 \leq t \leq T$, задача нахождения функции $\mathcal{A}(x, t)$ ($(x, t) \in C^2 \{[0, l] \times [0, T]\}$) из условий (8)–(11), (14), (15) будет прямой краевой задачей Неймана, в которой все исходные данные являются известными. Данная прямая задача имеет единственное решение (см., например, [9, 10, 12]), которое полностью и однозначно определяется исходными данными. Именно это обстоятельство дает нам «ключ» к решению сформулированной выше обратной задачи: сначала предполагая, что функция $\mathcal{G}_2(t)$ не является неизвестной функцией, а является заданной, мы каким-либо методом, например методом разделения переменных, находим решение $\mathcal{A}(x, t)$ прямой краевой задачи Неймана (8)–(11), (14), (15). Очевидно, что найденное решение $\mathcal{A}(x, t)$ будет зависеть от всех исходных данных, в том числе и от функции $\mathcal{G}_2(t)$. Затем, «вспомнив», что, во-

первых, найденное решение $\mathcal{A}(x, t)$ должно удовлетворять дополнительному условию (12) и, вторых, функция $\mathcal{A}_2(t)$ в самом деле не является заданной функцией, а неизвестна и подлежит определению, мы получим некоторое отношение для определения $\mathcal{A}_2(t)$ (и тем самым, функцию $\mathcal{A}(x, t)$, ибо в выражении для $\mathcal{A}(x, t)$ все входящие константы и функции являются известными, кроме функции $\mathcal{A}_2(t)$). Далее, определив $\mathcal{A}_2(t)$ из упомянутого отношения, мы определяем функцию $\mathcal{A}(x, t)$, удовлетворяющую условиям (8)–(12), (14), (15), т.е. пару функций $\mathcal{A}_2(t)$ и $\mathcal{A}(x, t)$, которые удовлетворяют условиям (8)–(11), (14), (15) и дополнительному условию (12). Другими словами, найденные функции $\mathcal{A}_2(t)$ и $\mathcal{A}(x, t)$ будут решением граничной обратной задачи. Ниже мы математически обоснуем идею, выдвинутую в данной статье.

4. Решение граничной обратной задачи

Будем искать (см. [9,10,12,13],) решение прямой краевой задачи Неймана (8)–(11), (14), (15) в виде

$$\mathcal{A}(x, t) = X(x) \cdot T(t) = \left\{ C_1 \cdot e^{x \cdot \sqrt{\frac{|a| \cdot \lambda}{\tau_r} - \frac{1}{4 \cdot \tau_r^2}}} + C_2 \cdot e^{-x \cdot \sqrt{\frac{|a| \cdot \lambda}{\tau_r} - \frac{1}{4 \cdot \tau_r^2}}} \right\} \cdot \left\{ C_3 \cdot e^{t \cdot \sqrt{\frac{|a| \cdot \lambda}{\tau_r}}} + C_4 \cdot e^{-t \cdot \sqrt{\frac{|a| \cdot \lambda}{\tau_r}}} \right\}.$$

Подставляя это выражение для $\mathcal{A}(x, t)$ в уравнение (8) и учитывая начальные условия (9) и (10), а также граничное условие (11) и условия согласованности (13), после несложных преобразований с

учетом того, что $\left. \frac{\partial \mathcal{A}(x, t)}{\partial x} \right|_{x=0} = \mathcal{A}_2(t)$, мы получим

$$\begin{aligned} \mathcal{A}(x, t) = & \int_0^l \frac{\partial G(x, \xi, t)}{\partial t} \cdot \mathcal{A}_0(\xi) d\xi + \int_0^l G(x, \xi, t) \cdot \mathcal{A}_1(\xi) d\xi + \\ & + \int_0^t d\tau \int_0^l G(x, \xi, t - \tau) \cdot F(\xi, \tau) d\xi - \frac{a^2}{\tau_r} \cdot \int_0^t G(x, \xi, t - \tau) \Big|_{\xi=0} \cdot \mathcal{A}_2(\tau) d\tau, \end{aligned} \quad (16)$$

где через $G(x, \xi, t)$ обозначена функция Грина рассматриваемой задачи, которая имеет вид

$$\begin{aligned} G(x, \xi, t) \stackrel{\text{def}}{=} & 4 \cdot \tau_r \cdot \sum_{n=1}^N \cos\left(\frac{\pi \cdot n \cdot x}{l}\right) \cdot \cos\left(\frac{\pi \cdot n \cdot \xi}{l}\right) \cdot \frac{\sinh\left(\frac{t \cdot \sqrt{\left(2 \cdot a \cdot \pi \cdot n \cdot \sqrt{\tau_r}\right)^2 - l^2}}{2 \cdot l \cdot \tau_r}\right)}{\sqrt{\left(2 \cdot a \cdot \pi \cdot n \cdot \sqrt{\tau_r}\right)^2 - l^2}} + \\ & + 4 \cdot \tau_r \cdot \sum_{n=N+1}^{\infty} \cos\left(\frac{\pi \cdot n \cdot x}{l}\right) \cdot \cos\left(\frac{\pi \cdot n \cdot \xi}{l}\right) \cdot \frac{\sin\left(\frac{t \cdot \sqrt{\left(2 \cdot a \cdot \pi \cdot n \cdot \sqrt{\tau_r}\right)^2 - l^2}}{2 \cdot l \cdot \tau_r}\right)}{\sqrt{\left(2 \cdot a \cdot \pi \cdot n \cdot \sqrt{\tau_r}\right)^2 - l^2}} + \\ & + \frac{2 \cdot \tau_r}{l} \cdot \sinh\left(\frac{t}{2 \cdot \tau_r}\right). \end{aligned} \quad (17)$$

Здесь необходимо сделать некоторое пояснение для функции Грина (17): в формуле (17), не нарушая общности, мы предполагали, что для нескольких первых значений $n = \overline{1, N}$ имеет место неравенство

$$\tau_r \leq \left(\frac{l}{2 \cdot a \cdot \pi \cdot n} \right)^2, \quad (18)$$

а для остальных значений $n = N + 1, N + 2, \dots$ выполняется неравенство

$$\tau_r > \left(\frac{l}{2 \cdot a \cdot \pi \cdot n} \right)^2. \quad (19)$$

Очевидно, что в случае, когда для всех значений $n = 1, 2, 3, \dots$ выполняется неравенство (18), то в формуле (17) сумму и ряд можно объединить надлежащим образом, а именно, функция Грина в этом случае будет иметь вид

$$G(x, \xi, t) \stackrel{\text{def}}{=} 4\tau_r \sum_{n=1}^{\infty} \cos\left(\frac{\pi \cdot n \cdot x}{l}\right) \cos\left(\frac{\pi \cdot n \cdot \xi}{l}\right) \frac{\sinh\left(\frac{t \cdot \sqrt{\left(2 \cdot a \cdot \pi \cdot n \cdot \sqrt{\tau_r}\right)^2 - l^2}}{2 \cdot l \cdot \tau_r}\right)}{\sqrt{\left(2 \cdot a \cdot \pi \cdot n \cdot \sqrt{\tau_r}\right)^2 - l^2}} + \quad (20)$$

$$+ \frac{2 \cdot \tau_r}{l} \cdot \sinh\left(\frac{t}{2 \cdot \tau_r}\right).$$

Аналогично, если для всех значений $n = 1, 2, 3, \dots$ выполняется неравенство (19), то вместо (17) надо пользоваться формулой

$$G(x, \xi, t) \stackrel{\text{def}}{=} 4 \cdot \tau_r \cdot \sum_{n=1}^{\infty} \cos\left(\frac{\pi \cdot n \cdot x}{l}\right) \cdot \cos\left(\frac{\pi \cdot n \cdot \xi}{l}\right) \cdot \frac{\sin\left(\frac{t \cdot \sqrt{\left(2 \cdot a \cdot \pi \cdot n \cdot \sqrt{\tau_r}\right)^2 - l^2}}{2 \cdot l \cdot \tau_r}\right)}{\sqrt{\left(2 \cdot a \cdot \pi \cdot n \cdot \sqrt{\tau_r}\right)^2 - l^2}} + \quad (21)$$

$$+ \frac{2 \cdot \tau_r}{l} \cdot \sinh\left(\frac{t}{2 \cdot \tau_r}\right).$$

Итак, мы нашли решение прямой краевой задачи Неймана (8)–(11), (14), (15), которое выражается формулами (16), (17) (или формулами (16), (20), или формулами (16), (21)). Прежде чем перейти к решению соответствующей обратной задачи (8)–(11), (14), (15) с дополнительной информацией (12), несколько упростим запись формулы (16) в точке $x = 0$. Для этого введем новую функцию

$$V(t) \stackrel{\text{def}}{=} \int_0^l \frac{\partial G(x, \xi, t)}{\partial t} \Big|_{x=0} \cdot \mathcal{G}_0(\xi) d\xi + \int_0^l G(x, \xi, t) \Big|_{x=0} \cdot \mathcal{G}_1(\xi) d\xi +$$

$$+ \int_0^t d\tau \int_0^l G(x, \xi, t - \tau) \Big|_{x=0} \cdot F(\xi, \tau) d\xi,$$

которая, очевидно, является известной функцией, ибо входящие в нее данные являются известными исходными данными рассматриваемой нами задачи. Используя только что введенную функцию, мы можем написать, что

$$\mathcal{G}(x, t)|_{x=0} = V(t) - \frac{a^2}{\tau_r} \cdot \int_0^t G(x, \xi, t - \tau)|_{\xi=0, x=0} \cdot \mathcal{G}_2(\tau) d\tau. \quad (22)$$

Еще раз отметим, что функция Грина, участвующая как в выражении для $V(t)$, так и под знаком интеграла в формуле (22), вычисляется или по формуле (17), или по формуле (20), или по формуле

$$(21) \text{ в зависимости от знака константы } \tau_r - \left(\frac{l}{2 \cdot a \cdot \pi \cdot n} \right)^2.$$

Теперь переходим к решению сформулированной в пункте 3 граничной обратной задачи. Для этого «вспомним», что функция $\mathcal{G}_2(t)$ неизвестна и подлежит определению, а также тот факт, что должно выполняться дополнительное условие (12). Поэтому, мы должны подчинить неизвестную функцию $\mathcal{G}_2(t)$ условию (12). Для этого учтем (14) и (22) в (12):

$$k \cdot \mathcal{G}_2(t) = \beta^m \cdot e^{-\frac{m-1}{2 \cdot \tau_r} t} \cdot \left\{ V(t) - \frac{a^2}{\tau_r} \cdot \int_0^t G(x, \xi, t - \tau)|_{\xi=0, x=0} \cdot \mathcal{G}_2(\tau) d\tau \right\}^m. \quad (23)$$

Уравнение (23) является нелинейным интегральным уравнением типа Вольтерра относительно неизвестной функции $\mathcal{G}_2(t)$. Пусть каким-то способом мы нашли решение $\mathcal{G}_2(t)$ этого интегрального уравнения. Тогда по формулам (16), (17) (или формулами (16), (20), или формулами (16), (21)) мы без труда можем определить искомую функцию $\mathcal{G}(x, t)$, т.е. решение обратной задачи (8)-(11), (14), (15) с дополнительным условием (12). Как уже было сказано выше, определив функцию $\mathcal{G}(x, t)$, мы с помощью преобразования (7) можем найти решение исходной прямой задачи (1)–(6).

Итак, резюмируя вышесказанное, можем утверждать, что проблема решения прямой задачи (1)–(6) сведена к проблеме нахождения решения уравнения (23). Уравнение (23) с помощью описанной ниже процедуры допускает упрощение. Действительно, выносим за скобку функцию $V(t)$ в правой части уравнения (23) и умножаем обе части полученного уравнения на β^{-m} . Тогда получим

$$k \cdot \beta^{-m} \cdot \mathcal{G}_2(t) = \bar{g}(t) \cdot \left\{ 1 - \frac{a^2}{\tau_r} \cdot \frac{\beta^m}{k} \cdot \int_0^t \bar{G}(x, \xi, t - \tau)|_{\xi=0, x=0} \cdot (k \cdot \beta^{-m} \cdot \mathcal{G}_2(\tau)) d\tau \right\}^m, \quad (24)$$

где

$$\bar{G}(x, \xi, t - \tau)|_{\xi=0, x=0} \stackrel{\text{def}}{=} \frac{G(x, \xi, t - \tau)|_{\xi=0, x=0}}{V(t)}, \quad V(t) \neq 0, \quad \bar{g}(t) \stackrel{\text{def}}{=} e^{-\frac{m-1}{2 \cdot \tau_r} t} \cdot V^m(t).$$

Введем новые переменные

$$\begin{cases} t = \frac{k \cdot \tau_r}{\beta^m \cdot a^2} \cdot \varphi, \\ \tau = \frac{k \cdot \tau_r}{\beta^m \cdot a^2} \cdot \psi. \end{cases}$$

Тогда из (24) получим, что

$$\begin{aligned} k \cdot \beta^{-m} \cdot \mathcal{G}_2\left(\frac{k \cdot \tau_r}{\beta^m \cdot a^2} \cdot \varphi\right) &= \bar{g}\left(\frac{k \cdot \tau_r}{\beta^m \cdot a^2} \cdot \varphi\right) \times \\ &\times \left\{ 1 - \int_0^\varphi \bar{G}\left(x, \xi, \frac{k \cdot \tau_r}{\beta^m \cdot a^2} \cdot (\varphi - \psi)\right) \Big|_{\xi=0, x=0} \cdot \left(k \cdot \beta^{-m} \cdot \mathcal{G}_2\left(\frac{k \cdot \tau_r}{\beta^m \cdot a^2} \cdot \psi\right)\right) d\psi \right\}^m. \end{aligned}$$

Отсюда после обозначения

$$\begin{cases} h(\varphi) \stackrel{\text{def}}{=} k \cdot \beta^{-m} \cdot \mathcal{G}_2 \left(\frac{k \cdot \tau_r}{\beta^m \cdot a^2} \cdot \varphi \right), \\ g(\varphi) \stackrel{\text{def}}{=} \bar{g} \left(\frac{k \cdot \tau_r}{\beta^m \cdot a^2} \cdot \varphi \right), \\ G(\varphi, \psi) \stackrel{\text{def}}{=} \bar{G} \left(x, \xi, \frac{k \cdot \tau_r}{\beta^m \cdot a^2} \cdot (\varphi - \psi) \right) \Big|_{\xi=0, x=0}, \end{cases}$$

получим окончательно

$$h(\varphi) = g(\varphi) \cdot \left\{ 1 - \int_0^\varphi G(\varphi, \psi) \cdot h(\psi) d\psi \right\}^m. \quad (25)$$

Таким образом, задача нахождения решения исходной прямой задачи (1)-(6) сведена к задаче определения решения $h(\varphi)$ нелинейного интегрального уравнения (25). Очевидно, что определив функцию $h(\varphi)$ из (25), мы можем по формуле

$$\mathcal{G}_2(t) = \frac{\beta^m}{k} \cdot h \left(\frac{a^2 \cdot \beta^m}{k \cdot \tau_r} \cdot t \right), \quad 0 \leq t \leq T$$

найти функцию $\mathcal{G}_2(t)$ и, следовательно, найти функцию $\mathcal{G}(x, t)$, а затем и искомую функцию $u(x, t)$:

$$\begin{aligned} u(x, t) = & \theta(t) + e^{-\frac{t}{2 \cdot \tau_r}} \cdot \left\{ \int_0^l \frac{\partial G(x, \xi, t)}{\partial t} \cdot [u_0(\xi) - \theta(0)] d\xi + \right. \\ & + \int_0^l G(x, \xi, t) \cdot \left[\frac{1}{2 \cdot \tau_r} \cdot u_0(\xi) + u_1(\xi) - \frac{\theta(0)}{2 \cdot \tau_r} - \theta'(0) \right] d\xi + \\ & + \int_0^t e^{\frac{\tau}{2 \cdot \tau_r}} d\tau \int_0^l G(x, \xi, t - \tau) \cdot \left[\frac{1}{\tau_r} \cdot f(\xi, \tau) - \frac{1}{\tau_r} \cdot \theta'(\tau) - \theta''(\tau) \right] d\xi - \\ & \left. - \frac{a^2 \cdot \beta^m}{\tau_r \cdot k} \cdot \int_0^t G(x, \xi, t - \tau) \Big|_{\xi=0} \cdot h \left(\frac{a^2 \cdot \beta^m}{\tau_r \cdot k} \cdot \tau \right) d\tau \right\}, \end{aligned}$$

где

$$\begin{aligned} G(x, \xi, t) \stackrel{\text{def}}{=} & 4 \cdot \tau_r \cdot \sum_{n=1}^{\infty} \cos \left(\frac{\pi \cdot n \cdot x}{l} \right) \cdot \cos \left(\frac{\pi \cdot n \cdot \xi}{l} \right) \cdot \frac{\sinh \left(\frac{t \cdot \sqrt{\left((2 \cdot a \cdot \pi \cdot n \cdot \sqrt{\tau_r})^2 - l^2 \right)}}{2 \cdot l \cdot \tau_r} \right)}{\sqrt{\left((2 \cdot a \cdot \pi \cdot n \cdot \sqrt{\tau_r})^2 - l^2 \right)}} + \\ & + \frac{2 \cdot \tau_r}{l} \cdot \sinh \left(\frac{t}{2 \cdot \tau_r} \right) \end{aligned}$$

$$\text{при } \forall n \in \mathbb{N} \quad \tau_r \leq \left(\frac{l}{2 \cdot a \cdot \pi \cdot n} \right)^2;$$

$$G(x, \xi, t) \stackrel{\text{def}}{=} 4 \cdot \tau_r \cdot \sum_{n=1}^{\infty} \cos\left(\frac{\pi \cdot n \cdot x}{l}\right) \cdot \cos\left(\frac{\pi \cdot n \cdot \xi}{l}\right) \cdot \frac{\sin\left(\frac{t \cdot \sqrt{(2 \cdot a \cdot \pi \cdot n \cdot \sqrt{\tau_r})^2 - l^2}}{2 \cdot l \cdot \tau_r}\right)}{\sqrt{(2 \cdot a \cdot \pi \cdot n \cdot \sqrt{\tau_r})^2 - l^2}} +$$

$$+ \frac{2 \tau_r}{l} \sinh\left(\frac{t}{2 \cdot \tau_r}\right)$$

$$\text{при } \forall n \in \mathbb{N} \quad \tau_r > \left(\frac{l}{2 \cdot a \cdot \pi \cdot n} \right)^2;$$

$$G(x, \xi, t) \stackrel{\text{def}}{=} 4 \cdot \tau_r \cdot \sum_{n=1}^N \cos\left(\frac{\pi \cdot n \cdot x}{l}\right) \cdot \cos\left(\frac{\pi \cdot n \cdot \xi}{l}\right) \cdot \frac{\sinh\left(\frac{t \cdot \sqrt{(2 \cdot a \cdot \pi \cdot n \cdot \sqrt{\tau_r})^2 - l^2}}{2 \cdot l \cdot \tau_r}\right)}{\sqrt{|(2 \cdot a \cdot \pi \cdot n \cdot \sqrt{\tau_r})^2 - l^2|}} +$$

$$+ 4 \cdot \tau_r \cdot \sum_{n=N+1}^{\infty} \cos\left(\frac{\pi \cdot n \cdot x}{l}\right) \cdot \cos\left(\frac{\pi \cdot n \cdot \xi}{l}\right) \cdot \frac{\sin\left(\frac{t \cdot \sqrt{(2 \cdot a \cdot \pi \cdot n \cdot \sqrt{\tau_r})^2 - l^2}}{2 \cdot l \cdot \tau_r}\right)}{\sqrt{(2 \cdot a \cdot \pi \cdot n \cdot \sqrt{\tau_r})^2 - l^2}} +$$

$$+ \frac{2 \cdot \tau_r}{l} \cdot \sinh\left(\frac{t}{2 \cdot \tau_r}\right)$$

$$\text{при } \exists N \in \mathbb{N} \quad \left[\forall n = \overline{1, N} \quad \tau_r \leq \left(\frac{l}{2a\pi n} \right)^2 \right] \& \left[\forall n = N+1, N+2, \dots \quad \tau_r > \left(\frac{l}{2a\pi n} \right)^2 \right].$$

5. Постановка исходной прямой начально-краевой задачи для обычного нестационарного уравнения теплопроводности

Теперь сформулируем следующую задачу: требуется найти функцию $u(x, t) \in C\{[0, L] \times [0, T]\}$, которая удовлетворяет уравнению теплопроводности

$$\frac{\partial u(x, t)}{\partial t} = a^2 \cdot \frac{\partial^2 u(x, t)}{\partial x^2} + f(x, t), \quad 0 < x < L < \infty, \quad 0 < t \leq T < \infty, \quad (26)$$

где $a^2 = \frac{k}{c \cdot \rho}$, k, c, ρ – положительные постоянные,

начальному условию

$$u(x, t)|_{t=0} = u_0(x), \quad 0 \leq x \leq L, \quad (27)$$

граничным условиям

$$\left. \frac{\partial u(x, t)}{\partial x} \right|_{x=L} = 0, \quad 0 \leq t \leq T, \quad (28)$$

$$-k \cdot \left. \frac{\partial u(x, t)}{\partial x} \right|_{x=0} + \beta^m \cdot \{u(x, t)|_{x=0} - \theta(t)\}^m = 0, \quad 0 \leq t \leq T, \quad m = \frac{10}{3}, \quad \beta \equiv \text{const} > 0, \quad (29)$$

и условиям согласованности

$$\left. \begin{aligned} u'_0(L) &= 0, \\ -k \cdot u'_0(0) + \beta^m \cdot \{u'_0(0) - \theta(0)\}^m &= 0. \end{aligned} \right\} \quad (30)$$

В задаче (26)-(30) предполагается, что являются заданными все константы L, T, k, c, ρ, β и все исходные функции $f(x, t), u_0(x), \theta(t)$, причем

$$f(x, t) \in C\{[0, L] \times [0, T]\}, u_0(x) \in C[0, L], \theta(t) \in C^1[0, T].$$

6. Решение поставленной задачи

Введем новую функцию

$$\mathcal{G}(x, t) \stackrel{\text{def}}{=} u(x, t) - \theta(t) \quad (31)$$

и учтем ее в (26)–(30) поочередно. Тогда будем иметь:

$$\frac{\partial \mathcal{G}(x, t)}{\partial t} = a^2 \cdot \frac{\partial^2 \mathcal{G}(x, t)}{\partial x^2} + F(x, t), \quad 0 < x < L, \quad 0 < t \leq T, \quad (32)$$

$$\text{где } F(x, t) \stackrel{\text{def}}{=} f(x, t) - \theta'(t);$$

$$\mathcal{G}(x, t)|_{t=0} = \mathcal{G}_0(x), \quad (33)$$

$$\text{где } \mathcal{G}_0(x) \stackrel{\text{def}}{=} u_0(x) - \theta(0);$$

$$\left. \frac{\partial \mathcal{G}(x, y)}{\partial x} \right|_{x=L} = 0; \quad (34)$$

$$-k \cdot \left. \frac{\partial \mathcal{G}(x, y)}{\partial x} \right|_{x=0} + \beta^m \cdot \mathcal{G}^m(x, t)|_{x=0} = 0; \quad (35)$$

$$\left. \begin{aligned} \mathcal{G}'_0(L) &= 0, \\ -k \cdot \mathcal{G}'_0(0) + \beta^m \cdot \mathcal{G}_0^m(0) &= 0. \end{aligned} \right\} \quad (36)$$

Итак, мы получили эквивалентную задачу (32)–(36). Чтобы решить эту задачу, сначала предположим, что нам известно граничное условие

$$\left. \frac{\partial (x, t)}{\partial x} \right|_{x=0} = \mathcal{G}_1(t), \quad 0 \leq t \leq T. \quad (37)$$

Рассмотрим вспомогательную задачу (32)–(34), (37), требуя, чтобы выполнялись следующие условия согласованности:

$$\left. \begin{aligned} \mathcal{G}'_0(0) &= \mathcal{G}_1(0), \\ \mathcal{G}'_0(L) &= 0. \end{aligned} \right\} \quad (38)$$

Решение задачи (32)–(34), (37), (38) легко находится стандартным методом разделения переменных:

$$\begin{aligned} \mathcal{G}(x, t) &= \int_0^L G(x, \xi, t) \cdot \mathcal{G}_0(\xi) d\xi + \int_0^L d\xi \int_0^t G(x, \xi, t - \tau) \cdot F(\xi, \tau) d\tau - \\ &- a^2 \cdot \int_0^t G(x, \xi, t - \tau) \Big|_{\xi=0} \cdot \mathcal{G}_1(\tau) d\tau, \end{aligned} \quad (39)$$

где через функции $G(x, \xi, t)$ обозначена функция Грина задачи (32)–(34), (37), (38), которая имеет вид

$$G(x, \xi, t) \stackrel{\text{def}}{=} \frac{1}{L} + \frac{2}{L} \cdot \sum_{n=1}^{\infty} e^{-\left(\frac{a \cdot \pi \cdot n \cdot \sqrt{t}}{L}\right)^2} \cdot \cos\left(\frac{\pi \cdot n \cdot x}{L}\right) \cdot \cos\left(\frac{\pi \cdot n \cdot \xi}{L}\right). \quad (40)$$

Теперь вернемся к задаче (32)–(37) и дополним эту задачу еще одним условием согласованности $\mathcal{G}'_0(0) = \mathcal{G}_1(0)$, т.е. вместо (36) имеем

$$\left. \begin{aligned} \mathcal{G}'_0(0) &= \mathcal{G}_1(0), \\ \mathcal{G}'_0(L) &= 0, \\ -k \cdot \mathcal{G}'_0(0) + \beta^m \cdot \mathcal{G}_0^m(0) &= 0. \end{aligned} \right\} \quad (41)$$

Другими словами, мы рассматриваем задачу (32)–(35), (37), (41). Так как в этой задаче функция $\mathcal{G}_1(t)$ в самом деле неизвестна и подлежит определению, то данную задачу можно интерпретировать как граничную обратную задачу, в которой требуется определить граничную функцию $\mathcal{G}_1(t)$ и функцию $\mathcal{G}(x, t)$, которая удовлетворяет условиям (32)–(34), (37), (41), а также дополнительному условию (35).

Так как решение соответствующей прямой задачи (32)–(34), (37), (38) есть функция $\mathcal{G}(x, t)$, определяемая по формулам (39)–(40), то, чтобы определить искомую граничную функцию $\mathcal{G}_1(t)$, необходимо подставить (39) в (35):

$$-k \cdot \mathcal{G}_1(t) + \beta^m \cdot \left\{ V(t) - a^2 \cdot \int_0^t G(x, \xi, t - \tau) \Big|_{x, \xi=0} \cdot \mathcal{G}_1(\tau) d\tau \right\}^m = 0, \quad (42)$$

где

$$V(t) \stackrel{\text{def}}{=} \int_0^L G(x, \xi, t) \Big|_{x=0} \cdot \mathcal{G}_0(\xi) d\xi + \int_0^L d\xi \int_0^t G(x, \xi, t - \tau) \Big|_{x=0} \cdot F(\xi, \tau) d\tau.$$

Итак, мы имеем уравнение (42) для определения искомой граничной функцию $\mathcal{G}_1(t)$. Как и выше в пункте 4, нелинейное интегральное уравнение типа Вольтерра (42) можно упростить. Для этого введем новые переменные

$$\begin{cases} t = \frac{k}{\beta^m \cdot a^2} \cdot \varphi, \\ \tau = \frac{k}{\beta^m \cdot a^2} \cdot \psi. \end{cases}$$

Тогда, учитывая эти переменные в (42), а затем проводя некоторые несложные преобразования, получим окончательно

$$h(\varphi) = g(\varphi) \cdot \left\{ 1 - \int_0^\varphi G(\varphi, \psi) \cdot h(\psi) d\psi \right\}^m, \quad (43)$$

где

$$\begin{cases} h(\varphi) \stackrel{\text{def}}{=} k \cdot \beta^{-m} \cdot \mathcal{G}_2\left(\frac{k}{\beta^m \cdot a^2} \cdot \varphi\right), \\ g(\varphi) \stackrel{\text{def}}{=} V^m\left(\frac{k}{\beta^m \cdot a^2} \cdot \varphi\right), \\ G(\varphi, \psi) \stackrel{\text{def}}{=} \frac{G\left(x, \xi, \frac{k}{\beta^m \cdot a^2} \cdot (\varphi - \psi)\right)}{V\left(\frac{k}{\beta^m \cdot a^2} \cdot \varphi\right)} \Big|_{\xi=0, x=0}. \end{cases}$$

Таким образом, задача нахождения решения исходной прямой задачи (26)–(30) снова сведена к задаче определения решения $h(\varphi)$ нелинейного интегрального уравнения (43). Очевидно, что если функция $h(\varphi)$ есть решение интегрального уравнения (43), то следующая замкнутая формула будет решением исходной прямой задачи (26)–(30):

$$\begin{aligned} u(x, t) = & \theta(t) + \int_0^l \frac{\partial G(x, \xi, t)}{\partial t} \cdot [u_0(\xi) - \theta(0)] d\xi + \int_0^t d\tau \int_0^l G(x, \xi, t - \tau) \cdot [f(\xi, \tau) - \theta'(\tau)] d\xi - \\ & - \frac{a^2 \cdot \beta^m}{k} \cdot \int_0^t G(x, \xi, t - \tau) \Big|_{\xi=0} \cdot h\left(\frac{a^2 \cdot \beta^m}{k} \cdot \tau\right) d\tau \Big\}, \end{aligned}$$

где функция Грина $G(x, \xi, t)$ вычисляется по формуле (40).

Заключение

В работах авторов впервые предлагается аналитический метод определения начальных тепловых потоков на основе решения гиперболического уравнения теплопроводности, учитывающего конечную скорость распространения тепла. Указанный начальный тепловой поток необходим для его сравнения с критическими тепловыми потоками различных закалочных сред с целью прогнозирования тепловых процессов, которые в зависимости от величины начальных тепловых потоков могут быть: развитым пленочным кипением, переходным процессом или преобладающим пузырьковым кипением.

Работа представляет большой практический интерес, в частности, при разработке интенсивных методов закалки, где важным является определение продолжительности нестационарного пузырькового кипения в условиях отсутствия пленочного кипения. Управляемый процесс нестационарного пузырькового кипения является основой двухступенчатого интенсивного способа закалки, который применяется широко на практике.

Вследствие чрезвычайной практической важности интенсивных технологий была организована команда известных ученых (математиков, теплофизиков, материаловедов) для решения сформулированных задач в рамках WSEAS и IARAS. Данная работа является началом исследований, выполняемых по теме “Database for cooling capacities of various quenchants to be developed with the modern computational and experimental techniques” (www.wseas.org/propose/project/wseas-projects.htm). На этом этапе получен ряд значимых результатов. В частности,

- в статье доказано, что задачи нахождения решения как обычного нестационарного уравнения теплопроводности, так и гиперболического уравнения нестационарной теплопроводности с нелинейными граничными условиями, обусловленными нестационарным пузырьковым кипением, сводятся к решению нелинейного интегрального уравнения одного и того же класса.
- полученные решения могут быть использованы для определения начальных тепловых потоков и продолжительности нестационарного пузырькового кипения, которые являются базовыми факторами интенсивной технологии упрочнения материалов. Указанные технологии являются экологически чистыми, поскольку вместо масел и полимеров используется обычная вода.

Литература

- [1] Kobasko N. I. (1980) *Steel Quenching in Liquid Media under Pressure*. Naukova Dumka, Kyiv. 206 pp.
- [2] Kobasko N. I. (2005) Self-regulated thermal processes during quenching of steels in liquid media. *Int. Journal of Microstructure and Materials Properties* 1, No. 1, 110–125.
- [3] Kobasko N. I. (2005) Steel Superstrengthening Phenomenon, Part I. *Int. Journal of Materials and Product Technology* 24, No. 1 (4), 361–374.
- [4] Kobasko N. I., Moskalenko A. A., Totten G. E., Webster G. M. (1997) Experimental Determination of the First and Second Critical Heat Flux Densities and Quench Process Characterization. *Journal of Materials Engineering and Performance* 6(1), 93–101.
- [5] Guseynov Sh. E., Buikis A., Kobasko N. I. (2006) Mathematical statement of a problem with the hyperbolic heat transfer equation for the intensive steel quenching processes and its analytical solution. *Proc. of the 7th Int. Conf. “Equipment and Technologies for Heat Treatment of Metals and Alloys”* 2, April 24–28, OTTOM-7, Kharkov, Ukraine, 22–27.
- [6] Guseynov Sh. E. (2003) Methods of the solution of some linear and nonlinear mathematical physics inverse problems. *Doctoral Thesis*, University of Latvia, Riga, Latvia, 146 pp.
- [7] Guthrie R.T.L. (1989) *Engineering in Process Metallurgy*. Clarendon Press, Oxford, 1989. 423 pp.
- [8] Tikhonov A. N., Arsenin V. Ya. (1986) *Solution methods for ill-posed problems*. Nauka, Press, Moscow. 288 pp. (in Russian)
- [9] Tikhonov A. N., Samarski A. A. (1999) *Equations of Mathematical Physics*. Moscow State University Press, Moscow. 799 pp. (in Russian)
- [10] Carslow H. S., Jaeger J. C. (1971) *Conduction of Heat in Solids*. Oxford University Press, London. 203 pp.
- [11] McDowell E.R.H. (1964) *Transient Heat Transfer in Solids*. Doctoral Thesis, California Institute of Technology, Pasadena, California. 560 pp.
- [12] Vladimirov V. S. (1984) *Equations of Mathematical Physics*. Mir Press, Moscow. 464 pp.
- [13] Vladimirov V. S. (1986) *A Collection of Problems on the Equations of Mathematical Physics*. Springer Press. 288 pp.

Received on the 12th of September 2006

A SURVEY OF DISTANCE ENGLISH TEACHING

T. LOBANOVA

*Information Systems Management Institute, Riga, Latvia
E-mail: lobanova@isma.lv*

Mankind has just graced the threshold of a new millennium. What will unite people in the future? Probably, a common language – the English language most presumably. Distance teaching-learning, which guarantees the highest degree of democracy and human rights to everyone, might be a means of facilitating the process of language learning and acquisition.

Distance education is an active process, in which people actively construct knowledge from their experiences in the world. People do not get ideas; they make them. Teaching styles are changing. Students are demanding it. Technology is enabling it. Distance education demands that we reshape the content, process and delivery of our educational offerings. It is the essence of our educational concept not to give the right answers, but to ask the right questions.

As world practice shows, well-thought out distance education offers students far greater involvement in the process of learning the language and gives the results as good as traditional classes and sometimes even better.

Keywords: *distance education, English, module education*

1. Foundations of distance education

Each of us in one way or some other has learned at a distance, since most education has always taken place at a distance. When we choose a book for reading or listen to music, observe art or watch a film or TV program, we do not realize that we are learning from an author, a composer, an artist, who are afar. We do not consider this kind of learning experience as a traditional learning with an instructor who offers solutions and students in the classroom, who are under pressure for change. And we are usually motivated to choose a particular kind of information to fill in a sort of emptiness inside ourselves – be it emotional, experiential, educational or whichever. In other words, we are engaged in constructing personally-meaningful products, important for ourselves and others around us. Distance education has very similar foundations, when a student chooses a particular course from a huge range of qualifications offered by institutions all over the world.

Distance education is described in a bewildering variety of terms and parlance. In North America and Europe, for example, it is known as 'Home study' and 'open learning or education'. 'External' or 'off – campus study' are terms used in Australia. In some countries it is termed 'independent' or 'flexible learning'; in New-Zealand 'extramural' education. Whatever term is given, the main characteristic feature is separation of the learner from the teacher or instructor.

As the name itself suggests, distance education takes place when a teacher and students are physically separated by a distance and online teaching-learning materials serve as a bridge to fill in the educational gap and to get access to the world educational treasures.

Distance learning has won its popularity over the last few years, as the Internet has become a reliable transmitter of educational information. The English language holds the same ground in its vitality and urgency, since it has become a global language – the language of progressive science and technology, global trade, commerce and business, cultural relations, diplomacy and tourism. In an era of rapid technological change and international economic integration, an educated, adaptable work force, well conversant with languages, enables countries to prosper. It is generally recognized nowadays that in any job a good rapport with a computer and good language skills are beneficial to all.

There is no need to look for specific groups of learners opting for distance education as a preferred alternative to conventional study (disabled students, full-time employed, living afar or having family commitments, regular army service, etc.). There is always something to be learned and there is always somebody to learn from or update the knowledge base.

Our body of knowledge seems to get limited with every passing day due to an explosion of technology in all spheres of our life. The language is also constantly developing. Thousands of new words and meanings enter the English language every year, including technical terms. The rapid turnover of knowledge mandates that we help learners acquire the skills in language use and language acquisition to continue learning outside the walls of a formal educational institution.

Distance education in language learning is catching up in almost all countries in the world because of its usefulness and potential not only to provide great access to language acquisition, but also its ability to make available an innovative and flexible system of education.

2. How distance learning is different from traditional education?

Many hundreds of thousands of comparative investigations have been made worldwide in the past whether students are getting the same education in the technologically delivered classes as in the traditional classroom. The usual result after the studies of student performance and achievement in language acquisition proves that there is no significant difference. The main differences lie in the material presentation and the role of the teacher and students.

In our old traditional classroom presentation, the responsibility is totally on the teacher to be fully prepared, to be expert, the interpreter of educational information, who adapts it to a particular auditorium and controls the speed, sequence, progression. Communication is often one-way and static. Not all the students might be actively involved into the process.

In distance learning the traditional 'sage on the stage' role of the teacher is changing. The student himself controls the speed, sequence and progression. Communication is dynamic and collaborative. The teacher is the guide whose responsibility is to help the learner learn how to think differently, how to process multiple bits of information and make it usable and applicable to a variety of situations. He gives consultations and recommendations and makes adjustments to the course (taking into consideration the needs of learners, different learning styles, etc.), thus, implementing a continuous, on-going interaction with students.

Nowadays technology enhanced learning environments have become common for both traditional and distance students. Still, practice proves that students learn better when they are engaged in constructing personally-meaningful product and are in charge of their own learning.

3. Technology and pedagogy

How technologies coordinate with pedagogy? Lots of us feel perplexed at the task of distance education. But there is the main and the most essential principle that we have to realize: nothing can replace the live instructor. Students do not learn from the technology. They learn from a competent mentor who teaches through the technology.

TECHNOLOGY enhanced distance learning involves Authoring, Delivery, Assessment and Management (ADAM) of course content via video, audio, CD-ROM/DVD, WWW, LMS (Learning Management System) and virtual classroom using the Internet. Teams of media specialists, content experts, editors, writers, instructional designers and software engineers are working to develop distance courses at different educational establishments. Such learning environment is often superior to the classroom experience.

Learning styles are different. Some students are more visual, while others perceive and learn primarily through auditory channels. Using only one teaching modality will not meet the needs of all the learners.

Educational information is presented through the various mediators of learning including direct lectures, books, journals, audio-visual media, computer-aided instruction and computer conferencing. Cooperative learning, workshops, buzz groups, games, simulations, role playing and drama, panel discussions and symposia are used where appropriate to enhance learning. In short, distance education can use all forms of media and information transfer methods.

PEDAGOGY – is a means to literacy using all this arsenal of computer networks and multimedia to speed the flow of educational information and feedback from the teacher to learner and vice versa – anytime anyplace (ATP) in a highly personality-oriented, on-demand mode in order to accelerate the outcome performance and enable the learner to become a creator.

The teacher can choose from a wide range of technological options, which are commonly divided into four categories:

Print – is a foundational element of distance education. Various print formats are available including textbooks, periodicals, study guides, workbooks, lecture notes, course syllabi, and case studies. Magazines, encyclopaedias, reference books are also available on CD and the Internet. Print is also delivered via e-mail, fax.

Voice – is an instructional audio tool, which includes such interactive technologies as telephone, audio conferencing, computer audio conferencing, tapes, CD, Internet audio.

Video – is an instructional video tool, which includes slides, pre-produced films, videotapes and real-time audio conferencing. Multimedia presentations combine slides with video and voice and can be delivered on CD, DVD or the Internet.

Data – is the term used to describe a broad category of instructional tools when computers send and receive information electronically.

Information teaching technologies

Effective distance education is focused on the needs of the learners, the requirements of the content and qualitative outcomes, but not on the technology or delivery. The systematic approach will result in a mix of media, each serving a specific purpose. The challenge in distance education is to use the good pedagogical techniques from the classroom and apply them across time and distance.

4. Interactive communication – synchronous and asynchronous

Distance education is a two-way interactive communication, which might be synchronous and asynchronous.

Synchronous or simultaneous – it means that everyone is participating at the same time, such as virtual classes, video/audio conferencing, telephone, and computer.

Asynchronous or self-paced – it is an on-line approach, which provides participation at different times such as exchange of information by print correspondence, e-mail, video/audio materials and on-going Web forums. It gives plenty of time and opportunity for the review of difficult material.

Before starting a term, each learner is supplied with 30–100% pre-packed course materials, combined with on-line mentors. The materials include the following:

- individual plan;
- study materials and supplies;
- list of recommended literature;
- online schedule;
- questions for the tests or exam;
- Web sites of libraries.

Distance education demands attention to the tasks (goal-directed and outcome-focused). The instructor has to

- carefully set and communicate the learning objectives;
- ensure the objectives are clear and understood;
- work out and implement the instructional strategies to meet the objectives;
- collect the data on progress towards meeting the learning objectives and
- modify, make adjustments or improvements to the course.

The student in such approach is viewed as not a passive recipient, but as an active learner, participant and contributor, self-constructing his own education.

5. Identifying the language needs of learners

Before planning an English course for distance learning, the instructor has to identify the needs of the learners to meet the goals of a course. There are a number of different reasons for language study.

Some learners want to study English because they think it offers a chance for advancement in their professional lives. They will get a better job with two languages than if they only know their mother tongue.

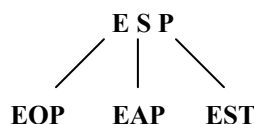
Some language students for some reason or other go to live in a target language community (either temporarily or permanently). For students of English an English-speaking country would be a TLC (target language community) and they would need to learn English to survive in that community.

There are situations where students have some special or specific reasons for wanting to learn the language – English for Special or Specific Purposes. For example, students majoring in Business, need English for international trade. Students of Tourism learn the language because they want to know more about the culture of the TLC, the people and places where the language is spoken. Waiters may need English to serve the customers. Hotel administrators need the language to receive guests and supply them with accommodation. These needs have often been referred to as EOP (English for Occupational Purposes).

Students who are going to study at Universities in the USA, Great Britain, Australia or Canada, may need English so that they can write reports or essays and function in seminars – EAP (English for Academic Purposes).

Students of some scientific disciplines need to be able to read articles and textbooks about those subjects in English. This is often referred to as EST (English for Science and Technology).

We can summarize these differences in the following way:



Information teaching technologies

Most students, who make the decision to study in their own time, do so for a mixture of reasons mentioned above. That is why the instructor has finally to come to some conclusion about a student's needs:

- what contexts and situations the student will probably use English in at some future date;
- what is order of priority for the different language skills (including sub-skills) that the student will need when using English;
- what level the student need to reach and what kind of language they need to be able to use or understand (e.g. formal/informal, spoken/written, scientific/business, etc.).

Overall, some good pedagogical principles that contribute to meeting the goals include:

- courses should focus on learning rather than teaching (student-centred vs. teacher centred);
- interaction with the material should be student-controlled rather than teacher-controlled;
- courses should be structured so that students interact with material in a pedagogically sound way;
- content delivery should be based on student knowledge guided by continuous feedback and on-going assessment.

6. Levels and time limits in distance English teaching

In the process of teaching English, the most significant thing is to work out psychologically and pedagogically sound provision of the course, where the main methodical principle – ‘from simple things towards complicated’ is implemented. For that reason we would offer three levels of the English language acquisition. Each level is based on a step-by-step approach that will guide the learner through the development and implementation process, regardless of his/her previous quality experience.

The First Level:

Pre-Intermediate Profile English (majoring in specialty). It may take between two or four years.

The Second Level:

Intermediate Business English (majoring in Business and Management) with two or three years of study.

The Third Level:

MBA Course – Upper Intermediate Business English - with one or two years of study.

A higher education course typically takes 5–7 hours a week for about ten months a year. However, time limits are not very restricted, allowing each learner to move throughout a course at his/her own pace.

7. Distance English teaching – module education

Although distance education occurs as Module education in its layout, it remains subject-focused in form. Under the term ‘module’ we understand a packet of educational information joined by a common topic and serving the purpose of attaining clearly identified and defined goals.

Each course comprises between 10–12 Modules with 5–7 assignments by a lesson and 2–3 practices. We can present the components of a Module in the following way (Figure 1):

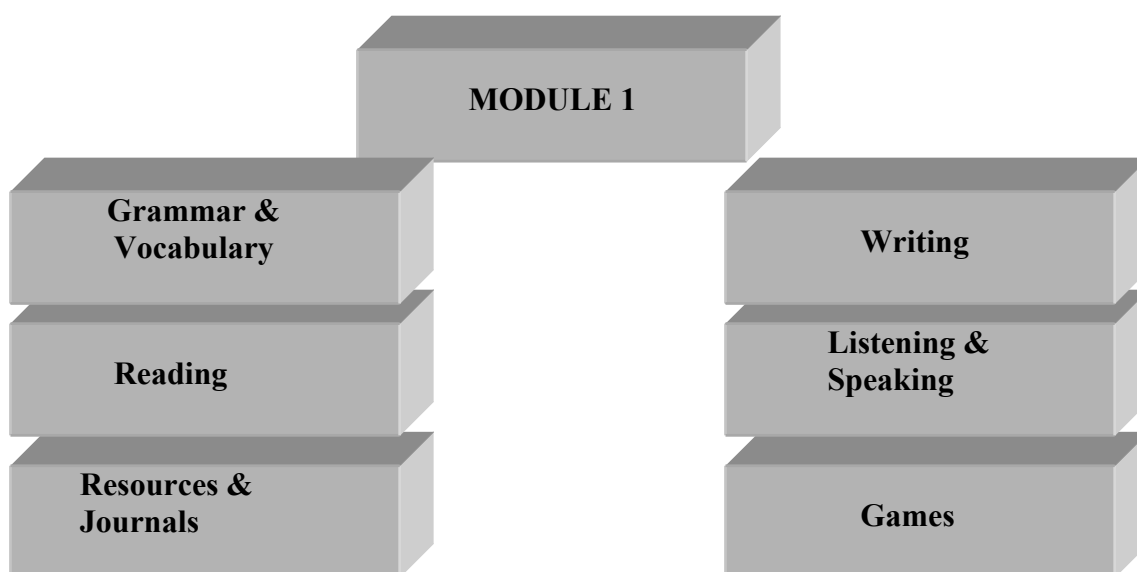


Figure 1. Module Education

Each Module includes all the aspects of developing language skills:

- Reading
- Writing
- Listening
- Speaking
- Grammar and Vocabulary

It may be enhanced by Games, serving different purposes of mastering language skills. The section on Resources and Journals is also supplied to facilitate the process.

8. Student performance evaluation and achievement assessments

The new paradigms of online instruction call for new paradigm of evaluation. The evaluation of online learning is multifaceted and subtle, and learning competence is only part of the evaluation need. Sometimes students' learning cannot be tested on discreet skill tests and quantified.

The introduction of new educational technologies, including computer networking, benefits from educational evaluation and assessment. Assessment includes both top-down accountability approaches (reporting of results for accountability purposes) and bottom-up instructional improvement (helping individual students gain most from instruction). Both perspectives share a common goal of improving education and are important at all stages of adopting technological innovations.

To be successful at evaluating student learning outcomes (SLOs) we have to have a clear understanding of the following:

- what we want students to know by the time they finish a course or the major;
- what we want students to be able to do with what they know by the time they finish a course or the major.

We can summarize the components of instructional inputs, processes applied, outputs, outcomes, and systematic and systemic interventions and evaluations at all stages in the following way (Figure 2):

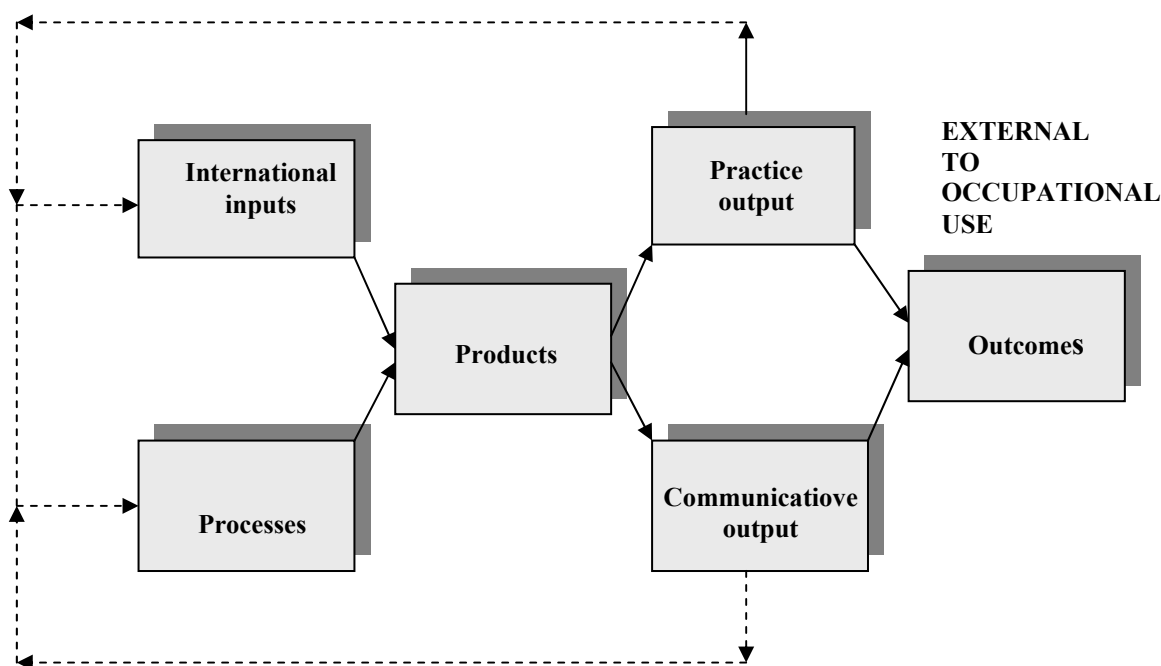


Figure 2. Components of instructional inputs, processes applied, outputs, outcomes, and systematic and systemic interventions and evaluations at all stages

The dotted lines show how outputs – and the learner's (and the teacher's) reaction to these (evaluation) – may feed back into instructional inputs until the degree of success is achieved.

Information teaching technologies

To sustain motivation and get positive results in learner's progress, the ARCS approach in feedback evaluation is instrumental as a reaction of learner/teacher to the materials in use and the processes implemented, where

- A – attention levels during the instruction;
- R – relevancy of the instruction and material to the interest;
- C – confidence levels in learning;
- S – satisfaction levels toward instruction as well as the instructor.

Thus, summing up the aforementioned, we can conclude that student performance evaluation and achievement assessment – is a process focused on student learning. It has to be:

- systematic and systemic;
- ongoing at all stages;
- information rich;
- improvement-oriented;
- resulting in positive change.

9. Alternative assessments

Over the last 10 years a number of fundamental innovations and changes in the area of student performance evaluation and achievement assessment have occurred. Today a large array of assessment approaches is available to the educator. Two major categories of alternative subjective approaches for the formal assessment of student performance and achievement have emerged:

Authentic/performance assessment – the major goal of it is to assess the ability applying knowledge in order to solve the real-life problems. It can be described in six main characteristics:

- uses open-ended tasks;
- focuses on higher order skills;
- employs context sensitive strategies;
- often uses complex problems requiring several types of performance and significant student time;
- consists of either individual or group performance;
- may involve a significant degree of student choice.

This type of assessment makes learners more actively involved in careful planning and applying knowledge in presumably new and different ways. They reach more complex cognitive skills as well.

Portfolio assessment – is a purposeful collection of student work that exhibits his/her efforts, progress or achievement in a particular area. This collection must include:

- student participation in selection of portfolio content;
- the criteria for selection;
- the criteria for judging merit;
- evidence of student self-reflection.

Portfolio, even more than other forms of performance assessment, call on the learner to be highly involved in planning the entries, choosing what to include and providing the rational reasons behind those decisions – why to include. Portfolios, thus, allow not only to assess the end product, but to some extent, the process of its creation.

Alongside with the innovative processes in alternative assessments, some developments in objective testing have been brought about due to advances in computer technology.

Computerized adaptive testing (or tailored testing) – is a conventional objective testing when after each response to each item, a program estimates the examinee's ability based on his/her responses to all previous items. The program then selects for the next item, one with the difficulty which best matches the examinee's estimated ability. The process then repeated iteratively until some criterion, such as a preset level of score precision is met.

Computer assisted testing – is the item banking approach. In this approach, objective test items are stored in a central computer server. As needed, various equivalent versions of the same test can be generated through such procedures as random selection of items or selection of items based on a specified mix of difficulty level and discrimination power. This approach to assessment is not very different from the conventional paper-and-pencil objective test. Items are presented on screen instead of on a piece of paper and students respond by making selections on screen.

Conclusion

Good instructional design is paramount to the success of education offered at distance. Careful planning, based on sound knowledge of who is going to learn what, by what means, in what kind circumstances, to what effect and with what purpose in mind, needs to be combined with effective ways to ensure, through formative evaluation based on feedback from the learner that intended purposes are met.

References

- [1] Naidu S. (2005) *Distance Education*. Carfax Publishing, University of Melbourne, Australia.
- [2] Baker E. L., O'Neil H. F. Jr. (2001) *Technology Assessment in Education and Training*. Corwin Press. University of Southern California/CRESST.
- [3] Warschauer M., Slietzer H., Meloni Ch. (2000) *Internet for English Teaching*. U.S. State Department Office of English Language Publications.

Received on the 6th March 2006

MULTIFACTOR DYNAMIC LONELINESS MODEL

I. ISHMUHAMETOV

Transport and Telecommunication Institute, Riga, Latvia
Lomonosova 1, Riga, LV-1019, Latvia
E-mail: ishgali@tsi.lv

Loneliness is a complicated emotion capturing the whole personality with her (his) thoughts, actions and behaviour. This is a depressed feeling linked with the real or imaginary absence of the satisfactory social relations. This work investigates the contemporary comprehension of the loneliness phenomenon through the social psychological prism, develops the dynamic model of its contents and analyses its approbation under the youth age conditions. In a multi-factor dynamic model of loneliness exists the following: "loneliness", "solitude" and "self-isolation", "isolation caused by circumstances". Understanding of the nature of loneliness will allow developing the optimal strategies of its overcoming under the conditions of the unstable and indefinite situation.

Keywords: *Dynamic Loneliness Model, Loneliness Type, loneliness, solitude, self-isolation, isolation conditioned by circumstances, youth age*

1. Introduction

The interest to loneliness in the XXI century is considered to be quite natural. The intensive changes, especially in the human self-consciousness, cause the feeling of instability and engender the thoughts of lost and senseless existence for a considerable group of people. The most unpleasant thing is that they have lost a constant image of the world and of the usual surroundings. All the abovementioned factors give rise to the negative sufferings of loneliness for different age groups of people, but they are especially typical for youth. The importance of the theme of this investigation is proved by the fact that the "Google" Internet searching system finds the English word "loneliness" 21 200 000 times, the Russian word «оди́ночество» 7 880 000 times and the Latvian word "vientulība" 24 200 times (2006.04.07.).

Loneliness is more often determined as a hard emotional comprehensive experience capturing feelings, thoughts, and personal activity. It runs through the whole personal structure and spreads on cognitive, emotionally – regulative and active – volitional sphere. On the whole the negative components of lonely persons are the following: emotional component (depressed emotional tone, negative emotional background, tension, emotional instability); cognitive, component (low self-esteem, presence of stereotype complexes, wrong attitude to themselves and surrounding world, lack of clear notion (conception) about themselves, disbalance of "I – real" and "I – ideal"; behaviour component (reduction of physical, mental and social activity, development of negative nature inclinations, lack of personal and socially important abilities and skills).

Causes of loneliness are shown most often in a complex, i.e. in a certain interconnection and interconditionality. There is a great number of objective socio – psychological reasons, which being interpreted through the personal ones acquire subjective character. For example, inadequate identity for young people, search for meaning of life, age crisis may cause a state of loneliness. Sometimes unfavourable social conditions may give rise to psychological prerequisites of future personal qualities closely connected with the loneliness. These prerequisites may acquire their own stimulating force and its logics of development even in the absence of conditions once caused them.

The survey of the scientific literature points out the works of A. Rokach [12], A. Rokach and H. Brock [10, 11], R. Andre [1], in which the factors causing loneliness as well as coping – strategies for the lonely people were considerably reflected. Scientists connect loneliness with anxiety, depression, inter – personal hostility [3, 6], drug and alcohol addiction [8, 9], and even with suicides [14]. A number of authors emphasize the interconnection between the feeling of loneliness and Internet system, the depressive influence of some mass media and modern technologies on youth [4, 5, 2, 13].

2. Constructing the theoretical dynamic model of the Loneliness Content

The analyses of the contents and interrelations of the "loneliness", "solitude" and "isolation" notions with distinguishing their difference, similarity and interconnection affirm the opportunity of their use in the dynamic loneliness model.

The main difference between the notion of “loneliness” and “solitude” lies in the fact that the latter is not connected with the negative emotional evaluation of a state; solitude means the voluntary going away from contacts with surrounding people. It is a necessary condition of the normal personality development and existence, it is understood as self – isolation in the name of some meaningful aim and acquires quite a different personal sense. In this case the individuality is always given an opportunity of going away from the situation.

Creating the dynamic model of loneliness we have decided to follow the point that loneliness and solitude are phenomena having their own contents and factors explaining their expressiveness.

A group of factors having the direct attitude to loneliness was named “the factors of loneliness”.

Factors of loneliness:

- people (absence);
- relatives and friends (absence);
- interpersonal relations, their quality (dissatisfaction);
- climate in the micro group (conflicts, lack of cohesion);
- conditions limiting peoples’ communication choice;
- unity, social identification (lack);
- communication, skills (not enough).

The intensity of sufferings can be increased with the growth of the amount of their low level or lack factor and depends on the degree of importance of these factors for people. Their low level or lack is a source of the “non – loneliness” state. Under ordinary conditions the presence of “non – loneliness” is perceived as natural and not high stimulating solitude.

The second group of factors influences directly the human solitude. These factors got the name of “solitude factors”. They are connected with the human aspiration to their abilities, goals and tasks realization, with the aspiration to creativity and development of personality.

Factors of solitude:

- self – perfection;
- abilities of creative and professional growth;
- work, studies, requiring independence and responsibilities;
- success, spare time acknowledgement;
- ideas;
- individualized forms of spending leisure time.

Only these factors stimulate the voluntary escape from the surrounding people to stay in solitude. The lack or not enough amounts of factors of solitude do not cause the human loneliness. Human can be satisfied with the situation when he (she) has an opportunity to be sole or has such an opportunity sometimes, even if it frustrates him (her). Maximum of solitude is achieved in case of solitude factors presence and in case of low level of completeness or lack of "solitude factors" (Figure 1).

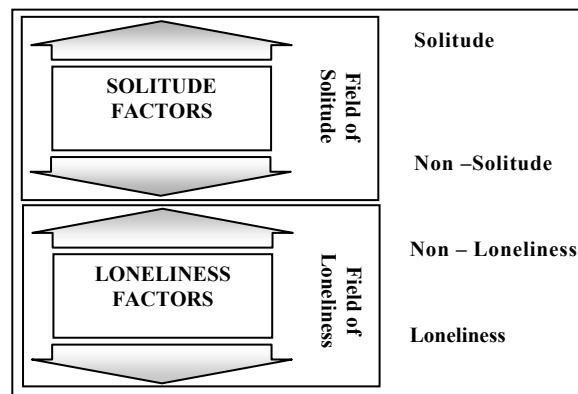


Figure 1. Two – factor Dynamic Loneliness Model

Factors of solitude can partially compensate the factors of loneliness. Under actual frustration of solitude factors (for example, losing job, re-evaluation of values etc.) an acute increase of loneliness experience may occur. Hence the factors of solitude are becoming the basis helping to reduce significance of loneliness factors, facilitating learning of new relationships and strategies of behaviour in a social environment.

Under the manifestation of personality connected with loneliness and solitude one can regard the disposition defined by G. Allport [21] as cardinal, central and secondary. Under cardinal disposition all

the human deeds can be generalized into influence of loneliness or solitude, under central disposition into the visible qualities of a lonely or sole person and under secondary – all the characteristics being dependent on the situation.

Such approach shows that if we want to achieve a marked improvement of life quality without loneliness we have to concentrate on 'solitude factors' and to enrich the contents of relations with social surroundings as well as interpersonal contacts, to diversify the monotony of spare time, labour, interaction with the others. If you are really touched with the problem of loneliness you should pay attention to the question – how factors of loneliness are actualized and, if possible, try to eliminate this problem independently or with the help of others, simultaneously developing 'factors of solitude'.

Multi-factor dynamic model of loneliness based on the "loneliness", "solitude", "isolation". The loneliness can't be matched to physical isolation, because isolation is the state, which is subjected to observation; it is regulated and controlled by a person. More often this notion is examined in the context of a group and understood as "social isolation". It is determined as the absence of other people nearby, existence without support, understanding, and feed-back from the side of surrounding people. The use of this term in psychological research is an exception where it is understood as protective mechanism [18]. The notion of "loneliness is connected with the notion of "isolation" on a level of cause and effect relations.

Depending on the used criteria such types of isolation can be picked out as individual and group with the following division of each type into voluntary isolation where a person comes to a decision himself (herself) whether to be in the condition of loneliness and into forced (accidental) isolation when a person is isolated from the society because of the situation or of other peoples' will. The forced individual isolation, other things being equal, is taken much harder than voluntary. One more criterion for picking out different types of isolation is a presence or absence of the opportunity of its interruption.

Isolation may become the prerequisite of the personal loneliness. The situation of isolation often leads to sensor and social deprivation and in the first place it has an effect on emotional and regulative spheres [17, 231; 19, 31]. Analysis of the papers contents [22, 15] where the situation of voluntary isolation is described shows that the greatest part of reactions that are of man's nature, refers to emotional and regulative spheres. The absence of violation in cognitive sphere may be explained by the man's readiness to the situations of isolation and their own activity. In this case isolation acquires quite a different personal sense and its subjective meaning is closer to the solitude.

In a multi-factor dynamic model of loneliness "loneliness", "solitude" and "self-isolation", "isolation caused by circumstances" exists.

Such approach allows singling out the following types of loneliness: solitude – self-isolation stipulated by a personal choice; solitude – isolation stipulated by circumstances, forced loneliness – self-isolation; loneliness – isolation stipulated by circumstances (Figure 2).

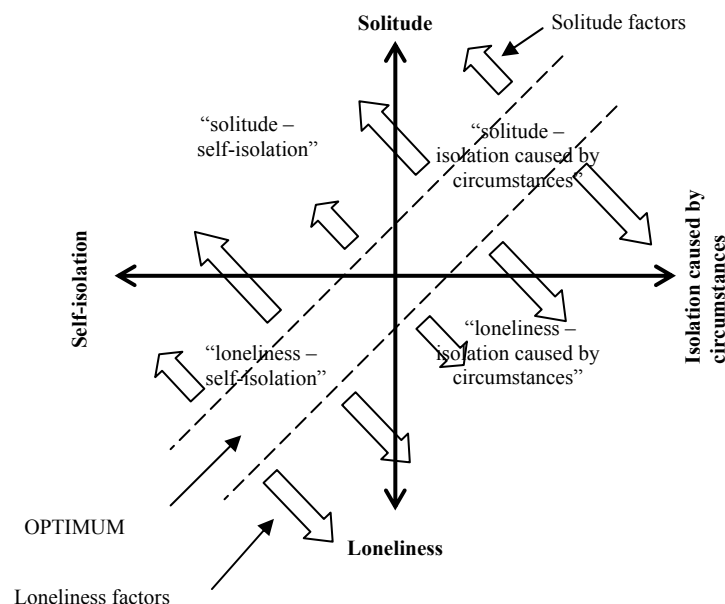


Figure 2. Multifactor Dynamic Loneliness Model

Solitude – self-isolation assumes the reception and interpretation of the situation as the necessary condition of existence and self – perfection. This is a motivated loneliness. Contacts with others are settled only necessarily, for solving tasks.

Isolation is seen in behaviour. A person feels his (her) loneliness subjectively positively. He (she) may identify himself (herself) with a part of a group, be the bearer of certain goals, feel spiritual unity with God, etc.

Solitude – isolation, stipulated by circumstances. Circumstances force a person to be outside the society of important people. This may work in other town or abroad, business trips, etc. A person is regarded with attention to this situation because it is temporary, and he (she) can interrupt these conditions at any time by his (her) will.

He (she) devotes much more attention of his (her) activity to his (her) filled position, self-development, lives in the name of his (her) goal, future, and the situation acquires personal sense.

Loneliness – self- isolation bears serious negative consequences. A person himself (herself) forms his (her) loneliness conditions. It may be explained by the loss of close friends and disability to form new relations, fear of new acquaintances. Here we see a person's suffering of loneliness, longing for people and communication. A person understands that he (she) is lonely. The world is apprehended more often through mentioning of his (her) loneliness. Nevertheless he (she) still lives in loneliness, in the best case using solitude factors as compensatory protective mechanism. He (she) thinks that it'll be better for him (her) if he (she) lives in isolation. It may be also connected with self-estrangement on emotional, cognitive and behaviour level.

Loneliness – isolation stipulated by circumstances is understood as negative loneliness, not forced by a person's will to stay lonely. He (she) doesn't have any choice. He (she) is forced to stay under such conditions where there is no important communication. He (she) sometimes doesn't know when his (her) loneliness is over. It may be stipulated by the external estrangement from the side of the society, lack of social-psychological protection, and lack of professional realization guarantees and chances of future job placement. Acculturation stress and anomie depression may serve as an example of estrangement, as O. Dolginova says [16].

Dialectical comprehension of connection between loneliness and solitude allows us saying that under certain conditions a negative display of loneliness may acquire a positive character. In this case the "loneliness – self-isolation" and "loneliness – isolation stipulated by circumstances" type may show the characteristics of "solitude – isolation stipulated by circumstances". These changes are connected with the features of the attitude to loneliness goal components, loneliness perception, explaining loneliness for him (her) (negatively or positively).

Technology of switching over to the positive way of thinking is very significant as the re-estimation of personal situations, of understanding loneliness as the necessity, opportunity and resource of self-development (as solitude), defining its urgency and working out personal active positions towards this feeling. This can be connected with the "I" – form of sufferings and with finding the sense of personal life under the definite living situations and self-attitude [20].

The given approach is based on the ratio of indices of cognitive, emotional and behavioural components of loneliness, considering them in close interdependence and inter-stipulation. Coming across the situation of loneliness a person makes its cognitive evaluation: summarizes the current information and its possible consequences (primary evaluation), determines the ways of influencing on the situation and its realization and finds the mechanisms and resources of overcoming loneliness; he (she) decides what is necessary to do in the given situation (secondary evaluation). Then the situation is considered by the so-called "fresh look". The cognitive evaluation of the situation takes place. After having evaluated the situation the person starts developing the mechanisms of loneliness overcoming (coping-process) and actualizes his (her) resources and chooses the behaviour strategies [according to 7].

The zone of "optimum" is connected with the activity, autonomy of Ego, with the attitude to loneliness experienced under the conditions of loneliness and isolation and stipulated by circumstances, dispositions being optimum on the level of "secondary" [21]. That is why this zone passes through the type "loneliness – self-isolation", and "solitude – isolation".

The intensity of loneliness feeling increases in "loneliness-isolation caused by circumstances" and drastically decreases in "solitude-self isolation". The last one in the situation of evident factors of solitude (e.g., in case of loss of social contacts, avoiding other people because they disturb, distract and annoy you) may bring potential loneliness, which can engulf person in case of solitude factors frustration.

Non-lone person is in the "optimum" zone because regulation processes providing his (her) equilibrium in the environment, progresses evenly and systematically. This regulation is caused by long-run adaptation to environmental conditions of a person who, using his (her) previous life experience, has worked out some set of algorithms of reacting on the relatively often repeating situations. The adopted

behaviour doesn't demand definite regulation mechanisms for supporting both organism important constructs and psycho processes, providing adequate reflection of reality in definite borders. The loneliness representation a person has and familiar behaviour strategies under loneliness conditions help these processes.

But the face, defining the person's equilibrium, isn't a line but some range of fluctuations and individual differences.

"The breach" of this face happens under the influence of loneliness factors. It is absolutely individual for every functional-dynamic system, taking in all the peculiarities of psycho mentality and human capability for reacting.

It can be a loss of a close person, a break of familiar system of relations, a loss of important values, incapability of reaching goals etc. Loneliness is followed by negative feelings, non-adoption, incapability to assess situation and to find an exit of it.

Intensive loneliness feeling can gradually decrease at any level if provocative loneliness factors lose their actuality or solution is found, or the solitude factors balance the influence of loneliness factors and gradually reduce their importance, and a reassessment of human motivation and evaluation sphere takes place, and new coping-strategies in new circumstances are worked out.

3. Loneliness Theoretical Model Approbation under the Youth Age Group Conditions

3.1. METHOD AND PROCEDURE

The research is connected with the approbation of loneliness models on the basis of how young people understand loneliness, compiling the questionnaire "Loneliness Types" in accordance with multi-factorial dynamic model, conducting research and results analysis.

1. Compiling the questionnaire "Loneliness Types" consisted of several sub-stages:

a) Making up the first variant of the questionnaire "Loneliness Types" (seven experts took part in the discussion, pre-test (pilot study) included 30 people), conducting research in order to get empirical data (203 people) and statistical analysis, to define structures, measuring scales and to confirmation of the basic questionnaire.

b) Compiling the main questionnaire, conducting research, statistical analysis and its final correction.

2. 417 people (213 young man and 204 young girls, aged 18 to 24, random choice) took part in the research with a help of questionnaire "Loneliness Types" and UCLA Loneliness Scale (Version 3)¹.

Statistical Development Methods – Computing Programme SPSS (v.11.5.0) (Statistical Package for the Social Science).

3.2. RESULTS

In order to define the content of such components as "loneliness", "solitude", "self isolation" and "isolation caused by circumstances" that are a part of the dynamic models of loneliness we have considered representation of affirmations reflecting emotional experience related to loneliness, attitude of a person to loneliness, solitude, surrounding people, spare time, work, choice of a situation, circumstances and their understanding, as well as behavioural stereotypes and reactions (40 affirmations).

After factor analysis of the first variant of the "Loneliness Types" questionnaire statements data were grouped as "loneliness", "solitude", self-isolation" and "isolation caused by circumstances". The final questionnaire has 32 statements – 8 for every component. Four negatively formulated ("lonely") and four positively formulated ("not lonely") statements were used in the component "Loneliness".

The questionnaire check up concerning reliability was conducted by checking inner coordination. Chronbach's Coefficient is equal to .88, which confirms high level of statements coordination and questionnaire reliability.

Correlation analysis (Pearson) of the statistical characteristics of the questionnaire statements with the UCLA Loneliness Scale (Version 3) shows that all statements have correlation at level $p < 0,01$.

Indices of components – *loneliness*, *solitude*, *self-isolation*, *isolation conditioned by circumstances* – have high correlation with each other. The results of research with the questionnaire „Loneliness Types" show that „loneliness" has mean value 14,7; „solitude" – 13,2; „self-solitude" and „solitude conditioned by circumstances" – 15,4 and 15,0 correspondingly. Dispersion of indices is in the range 8,39 to 17,78. Kurtosis values confirm the distribution form as that close to normal (Table 1).

¹ Ph. D. Daniel W. Russel permitted 1p use the UCLA Loneliness Scale (Version 3) in our scientific work

TABLE 1. Statistical Characteristics of the „Loneliness Types” Components

	Range	Minimum	Maximum	Mean	Std.	Variance	Skewness	Kurtosis
LONELINESS	19,00	8,00	27,00	14,6619	2,89699	8,393	.652	1,278
SOLITUDE	15,00	8,00	23,00	13,1799	3,39878	11,552	.856	.330
SELF-ISOLATION	19,00	8,00	27,00	15,3645	4,21667	17,780	.465	-.459
ISOLATION CONDITIONED BY CIRCUMSTANCES	19,00	8,00	27,00	15,0216	3,60715	13,012	.580	.144

Indicators of “loneliness” up to 12 points – low factor expression, 16 plus – high expression, “solitude”: up to 11 points – low expression, 15 plus – high expression, „self-isolations” – 12 and 18 and „isolations conditioned by circumstances”: – 12 and 17 correspondingly.

The analysis of sex differences that is of the „Loneliness Types” indicators of girls’ and boys’ was verified with the help of t-criterion for independent selections. There are significant differences in the components „loneliness”, „solitude”, and “isolation conditioned by circumstances” at level $p < 0,01$.

Conclusions

1. Conceiving loneliness as a complicated, dynamic phenomenon determined by many factors made it possible to work out a model of the loneliness, which includes the following structural components – loneliness, solitude, self-isolation and isolation conditioned by the circumstances in dynamic interconnection. There was taken into account the correlation of the cognitive, emotional, and behaviour levels of loneliness. They were considered in close interdependence (realising a state of loneliness; emotional assessment of a lonely state, personal interpretation of inter-psychological connections in a state of loneliness).

2. There are defined the types of loneliness: *solitude – self-isolation; solitude – isolation, conditioned by circumstances; loneliness – self-isolation; loneliness – forced isolation conditioned by circumstances.*

3. Defining the two-factor model of the loneliness shows the dynamics of the factors’ interaction connected by loneliness and solitude. The person’s balance between „loneliness” and „solitude” is not a straight line but rather some range of fluctuations and individual differences. If we wish to increase notably the quality of life without experiencing loneliness, we should concentrate on the factors of „solitude” and to enrich the content of relations with the surrounding people, of inter-personal contacts, to diversify the content of leisure, labour, and interactions with other people.

4. In the multifactor dynamic model the component of „loneliness” has the mean value 14,7; „solitude” – 13,2; „self-isolation” and „isolation conditioned by circumstances” – 15,4 and 15,0 correspondingly. Kurtosis values confirm the form of distribution as that of close to normal.

5. In the dynamic model of loneliness, the most optimal state (non-loneliness) is connected with the activity, the autonomy of „I” in relation to loneliness, the certainty of the person’s relations with the surrounding medium, which help to minimize the intensity of loneliness when such state occurs. Intensive experience of loneliness may be lowered when the factors, which brought up loneliness, have lost their actuality and some decision has been found or when the factors of loneliness have balanced the loneliness factors and gradually lowered their actuality.

References

- [1] Andre R. (1991) *Positive solitude*. A practical program for mastering loneliness and achieving self-fulfilment. New York: HarperCollins.
- [2] Franzen A. (2000) Does the Internet Make Us Lonely? *European Sociological Review* **16**, 427–438.
- [3] Jones W. H., Rose J., & Russell D. (1990) Loneliness and social anxiety. In: *Handbook of social and evaluation anxiety*, H. Leitenberg (Ed.). New York: Plenum, 247–266.
- [4] Korgaonkar Pradeep K., and Lori D. Wolin (1999) A Multivariate Analysis of Web Usage. *Journal of Advertising Research* **39** (2), 53–68.
- [5] Kraut R., Lundmark V., Patterson M., Kiesler S., Mukopadhyay T. and Scherlis W. (1998) Internet Paradox: A Social Technology that Reduces Social Involvement and Psychological Well-Being? *American Psychologist* **53**, 1017–1031.
- [6] Lau S., & Kong C.K. (1999) The acceptance of lonely others: Effects of loneliness and gender of the target person and loneliness of the perceiver. *Journal of Social Psychology* **139**, 229–241.

- [7] Lazarus R. S. Folkman S. (1984). *Stress, appraisal, and coping*. New York: Springer.
- [8] McWhirter B. T. & Horan J. J. (1996) Construct validity of cognitive-behavioral treatments for intimate and social loneliness. *Current Psychology* **15**(1), 42–53.
- [9] Orzeck T., Rokach A. (2004) Men Who Abuse Drugs and Their Experience of Loneliness. *European Psychologist* **9**, No. 3, September 2004, 163–169.
- [10] Rokach A. & Brock, H. (1997) Loneliness: A multidimensional experience. *Psychology: A Journal of Human Behavior* **34**, 1–9.
- [11] Rokach A. (1996) The Subjectivity of Loneliness and Coping with It. *Psychological Reports* **79**, 475–481.
- [12] Rokach A. and Brock H. (1998) Coping with Loneliness'. *Journal of Psychology* **132**, 107–127.
- [13] Russell D. W., Flom E. K., Gardner K. A., Cutrona C. E., & Hessling R. M. (2003) Who makes friends over the internet? Loneliness and the “virtual” community. *International Scope Review* **5**(10), 1–19.
- [14] Tundo L., & Baldessarini R.J. (2001) „Suicide: Causes and Clinical Management.” *Medscape Internet Publications*. <http://www.medscape.com/Medscape/psychiatry/ClinicalMgmt/CM.v03/public/index-CM.v03.html> (2005.06.07)
- [15] Бомбар А., Блайт Ч. (1997) *За бортом по своей воле. Немыслимое путешествие*. М.:Терра - Книжный клуб.
- [16] Долгинова О. (1996) *Одиночество и отчужденность в подростковом и юношеском возрасте*. СПб.
- [17] Лапланш Ж. Понталис Ж.-Б. (1996) *Словарь по психоанализу*. (пер.с фр.) М.: Высшая школа.
- [18] Леонтьев Д. А. (1997) *Очерк психологии личности*. М.: Смысл.
- [19] Оллпорт Г. В. (2002) *Становление личности*. Избранные труды. М.: Смысл.
- [20] Слокам Д. (2001) *Один под парусами вокруг света*. М.: Дрофа.

ПСИХОМЕТРИЧЕСКИЕ ХАРАКТЕРИСТИКИ ШКАЛЫ ОДИНОЧЕСТВА UCLA (ВЕРСИЯ 3): ИЗУЧЕНИЕ СТУДЕНТОВ ВУЗА

И. Н. ИШМУХАМЕТОВ

*Институт транспорта и связи
 ул. Ломоносова, 1, Рига, LV-1019, Латвия
 E-mail: ishgali@tsi.lv*

В данной статье рассматриваются психометрические параметры Шкалы одиночества UCLA (*University California Los-Angeles*) (версия 3). В ней представлены результаты применения Шкалы одиночества UCLA (версия 3) в условиях Латвии и эмпирические данные, характеризующие особенности проявления одиночества в юношеском возрасте. Подтверждается надежность Шкалы одиночества UCLA (версия 3). Коэффициенты Кронбаха (α) показателей утверждений первого исследования 0,86, повторного (через 1 месяц) – 0,89, которые указывают на высокую внутреннюю согласованность Шкалы одиночества UCLA (версия 3). Показатель корреляции (Pearson) данных первого и повторного исследований равен 0,81, при $p < 0,01$. Исследуется с помощью факторного анализа возможность использования данной Шкалы для определения причин одиночества, обусловленных социально-психологическими факторами.

Выбор темы исследования обусловлен желанием помочь специалистам, работающим в социальной сфере, осмыслить и диагностировать одиночество, учитывая достижения современной психологической науки, а также стремлением привлечь их внимание к негативным психологическим состояниям, связанным с одиночеством.

Ключевые слова: одиночество, измерение одиночества, Шкала одиночества UCLA (версия 3), юношеский возраст

1. Введение

Известно, что одиночество определяется как крайне неблагоприятное, порождающее тяжелые переживания явление. Как состояние оно способно пронизывать всю структуру личности и распространяться на когнитивную, эмоционально-регулятивную и действенно-волевую сферы. Даже человек, способный справляться с переживаниями, в регулировании остроты одиночества может испытывать пассивность и беспомощность. Одиночество – это сложный, многогранный, динамичный феномен, детерминированный многими факторами.

Неоднозначность содержания одиночества предполагает различные подходы к его изучению, к причинам его появления, к возможностям преодоления и способам противостояния. Это обуславливает многогранность его научного и индивидуального осмысления. Например, Я. Купершмидт, К. Сигда, М. Веглер и К. Седикидес [6] указывали на связь между одиночеством и эмоциональными (низкое чувство собственного достоинства, депрессия и социальное беспокойство), социальными (преследование, отсутствие дружеских и доверительных отношений) и поведенческими проблемами (застенчивость, обособленность, уменьшение контактов с окружающими, участия в общих мероприятиях). Л. Андерсон [1], Д. Перлман и Д. Рассел [11], П. Тиккайнен и др. [16] отмечали связь между одиночеством и такими психологическими проблемами, как плохое физическое самочувствие, самоубийство или попытка самоубийства, зависимость от алкоголя и др. Связь одиночества с низким уровнем образованности и низким уровнем дохода, ограниченными социальными связями находится в центре внимания Н. Савикко и др. [15]. Много работ посвящено одиночеству пожилых людей [5, 17].

Переживание одиночества наиболее ярко проявляется в юношеском возрасте. В это время, с одной стороны, вследствие индивидуализации досуга, работы, учебы, перехода от личностных отношений к формализованным социальным ролям и многочисленным поверхностным социальным контактам с окружающими появляется все большее и большее стремление к уединению и дистанцированию, к самоизоляции, с другой – возникает острая потребность в доверительных, близких отношениях с кем-либо. Не последнюю роль в этом играет и неустойчивое социальное положение юношей и девушек. Например, результаты исследований одиночества населения (15 лет и старше) в рамках программы «*Quality of Life in New Zealand's Largest Cities Survey 2004*» [7] показывают, что в 2004 году 18% новозеландцев чувствовали себя одиноко в течение 12 месяцев, из них 15% сказали «иногда», 2% – «часто», 1% – «всегда». Одиночество оказалось наиболее распространенным явлением среди молодежи. Среди 15–24-летних чувствует себя одиноко «иногда», «часто» и «постоянно» 21%, среди 65-летних и старше – 19%, среди 24–49-летних – 17%, среди 50–64-летних – 15 % (см. рис. 1).

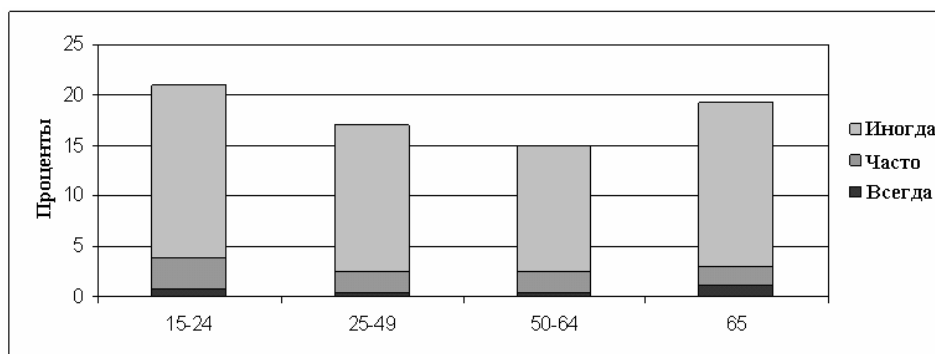


Рис. 1. Переживание одиночества в разных возрастных группах [7]

Следует отметить, что похожие результаты были получены в исследованиях К. Рубинштейн и Ф. Шейвер [20], проведенных в Нью-Йорке и Уорчестере (США). Они убедительно доказали, что «... одиночество – проблема главным образом молодых» [20, 329], и отметили, что похожие результаты были получены в исследованиях Шанаса (E. Shanas) и ее коллег, Лауэнтала (M. Lowenthal), Тэрнера (M. Thurner), Чирибогой (D. Chirboga) [20, 329], тем самым опровергая распространенное мнение о том, что одиночество характерно для пожилых людей. Респонденты старшего возраста в большей степени удовлетворены своими дружескими связями, они относятся к различным социальным группам, обнаруживают различные установки в отношении самих себя, чувствуют более «независимо», у них более высокая самооценка, чем у молодых людей.

Несмотря на общее мнение исследователей о том, что одиночество – достаточно распространенное явление, идентификация его затруднена тем, что личность, испытывающая одиночество, не всегда заявляет об этом открыто. По этой причине для диагностики используются различные методы – наблюдение, анкеты, тесты, беседы, анализ биографических данных, письма-откровения и др.

При измерении одиночества, с точки зрения Д. Рассела [19], существует два различных концептуальных подхода: многомерный и одномерный. Первый изучает одиночество как многогранное явление и пытается выделить гипотетические типы или проявления одиночества. Это дает большие возможности для идентификации самых разнообразных случаев одиночества, что может быть особенно полезным в организации помощи одиноким людям. Одномерный концептуальный подход рассматривает одиночество как целостное явление, которое отличается, прежде всего, интенсивностью испытываемого переживания. Этот подход допускает, что в переживании одиночества имеется нечто общее, что лежит в основе одиночества, испытываемого всеми индивидами, и не принимает во внимание, чем для индивида является каждый отдельный случай одиночества.

Шкала одиночества UCLA (*University California Los-Angeles*) была задумана как глобальный, или одномерный, подход к измерению одиночества и основана на общем опыте переживаний, испытываемых широким кругом людей. Работа над ней была начата Д. Расселом и его коллегами еще в 1976 году [14, 13, 19]. Они попытались создать адекватную в психометрическом отношении и удобную в употреблении Шкалу.

Она получила наибольшее распространение в качестве надежного инструмента исследования одиночества разных возрастных и социальных групп – молодых и пожилых людей, студентов, преподавателей, работников больницы, мужчин и женщин и т.д. Имеется множество психометрических данных, доказательств о надежности и валидности Шкалы UCLA [14, 13, 19, 12, 4, 8, 18, 2]. Вопрос о том, является ли Шкала одиночества одномерным или многомерным конструктом, обсуждался в работах Д. Рассела [12] и других исследователей [9, 4, 10, 18].

Шкала одиночества UCLA (версия 3), как и предыдущие версии, основана на общем опыте переживаний, испытываемых широким кругом людей. Д. Рассел [12] отмечает чрезвычайную надежность Шкалы как в плане внутренней согласованности (коэффициент альфа расположился от 0,89 к 0,94), так и при повторном тестировании через 12 месяцев ($r = 0,73$). В Шкале одиночества UCLA (версия 3) используется 11 отрицательно сформулированных («одинок») и 9 положительно сформулированных («не одинок») утверждений.

2. Метод и результаты

Для исследования нами взята Шкала одиночества UCLA (версия 3) (Russell, 1996), любезно предоставленная доктором психологии Дениэлом Расселом (Ph.D. Daniel W. Russell). В исследовании участвовали 526 студентов г. Риги (Латвия). Из них – 252 юноши и 274 девушки. Возраст: от 18 до 24 лет. Для статистического анализа данных была использована программа SPSS версии 11.5.0.

При адаптации опросника Шкалы одиночества UCLA (версия 3) к условиям Латвии мы учитывали особенности родного языка респондентов, обсуждали «прямые» и «обратные» переводы, а также использовали анализ данных пилотажного исследования (pretest). В результате нам удалось максимально приблизить концепцию Шкалы одиночества UCLA (версия 3) к культурно-языковым традициям и особенностям исследуемой группы, а также построить опросник Шкалы одиночества UCLA (версия 3), который представлен ниже (табл. 1).

ТАБЛИЦА 1. Вопросы Шкалы одиночества UCLA (версия 3)

№	Вопросы
1.	Как часто Вы чувствуете себя "на одной волне" с окружающими людьми?
2.	Как часто Вы чувствуете недостаток в дружеском общении?
3.	Как часто Вы чувствуете, что нет никого, к кому можно обратиться?
4.	Как часто Вы чувствуете себя одиноким?
5.	Как часто Вы чувствуете себя частью группы друзей?
6.	Как часто Вы чувствуете, что у Вас есть много общего с окружающими людьми?
7.	Как часто Вы чувствуете, что Вы больше не испытываете близости к кому-либо?
8.	Как часто Вы чувствуете, что окружающие Вас люди не разделяют Ваших интересов и идей?
9.	Как часто Вы чувствуете себя открытым для общения и дружелюбным?
10.	Как часто Вы чувствуете близость, единение с другими людьми?
11.	Как часто Вы чувствуете себя покинутым?
12.	Как часто Вы чувствуете, что Ваши отношения с другими поверхностны?
13.	Как часто Вы чувствуете, что Вас никто не знает по-настоящему?
14.	Как часто Вы чувствуете себя изолированным от других?
15.	Как часто Вы чувствуете, что можете найти себе компанию, если Вы этого захотите?
16.	Как часто Вы чувствуете, что есть люди, которые Вас действительно понимают?
17.	Как часто Вы чувствуете стеснительность?
18.	Как часто Вы чувствуете, что есть люди вокруг Вас, но не с Вами?
19.	Как часто Вы чувствуете, что есть люди, с которыми Вы можете поговорить?
20.	Как часто Вы чувствуете, что есть люди, к которым Вы можете обратиться?

Надежность Шкалы исследовалась проверкой на внутреннюю согласованность путем разделения Шкалы на две половины (split-half) и повторным тестированием (test – retest) через 1 месяц. Получены высокие коэффициенты эквивалентных форм Спирмена-Брауна (на основе результатов первого исследования 0,83; повторного – 0,87) и такой же высокий уровень критерия надежности половинного расщепления Гутмана (Guttman Split-half), полученного путем вычисления нижних пределов (первого – 0,82; повторного – 0,87). Коэффициенты Кронбаха (α) показателей утверждений первого исследования 0,86, повторного – 0,89, которые указывают на высокую внутреннюю согласованность Шкалы одиночества UCLA (версия 3). Показатель корреляции (Pearson) данных первого и повторного исследований равен 0,81 при $p < 0,01$. Он считается высоким, чтобы определить Шкалу одиночества UCLA (версия 3) устойчивым во времени (табл. 2). В исследованиях Д. Рассела [12] получен (интервал – 12 месяцев) коэффициент корреляции 0,73 (Pearson; $p < 0,01$).

ТАБЛИЦА 2. Показатели корреляции Шкалы одиночества UCLA (версия 3) первого и повторного исследований (временной интервал - 1 месяц)

		Первое исследование	Повторное исследование
ПЕРВОЕ ИССЛЕДОВАНИЕ	Коэффициент корреляции Пирсона	1	0,814(**)
	Уровень значимости (2-стор.)	-	0,000
	N	526	526
ПОВТОРНОЕ ИССЛЕДОВАНИЕ	Коэффициент корреляции Пирсона	0,814(**)	1
	Уровень значимости (2-стор.)	0,000	–
	N	526	526

** корреляция на уровне значимости 0,01 (2-стор.).

Диаграмма рассеивания показателей Шкалы одиночества UCLA (версия 3) первого и повторного исследований достаточно ровная. Она напоминает форму овала и четко показывает выраженность и сгруппированность (рис. 2).

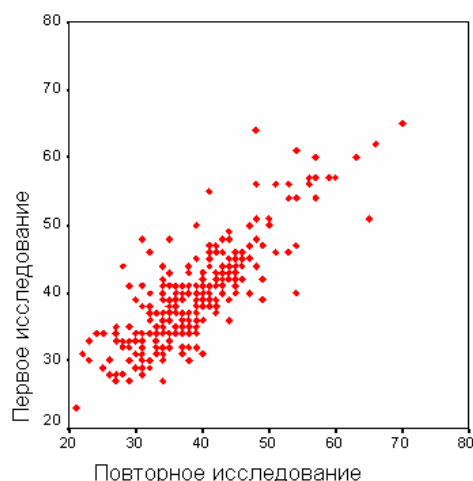


Рис. 2. Диаграмма рассеивания показателей Шкалы одиночества UCLA (версия 3) первого и повторного исследований (N = 526)

Таким образом, полученные результаты подтверждают надежность измерения Шкалы одиночества UCLA (версия 3). Следовательно, в своих исследованиях мы можем ее использовать как серьезную методику для измерения одиночества и надеяться на получение адекватной картины одиночества юношеского возраста. Это подтверждают и корреляции Пирсона (на уровне $p < 0,01$) между данными Шкалы одиночества UCLA и вопросами Шкалы (табл. 3).

ТАБЛИЦА 3. Показатели корреляции Шкалы одиночества UCLA (версия 3) с вопросами Шкалы (Pearson Correlation, N = 526)

Вопросы	Шкала одиночества UCLA (версия 3)	Вопросы	Шкала одиночества UCLA (версия 3)
1.	0,540(**)	11.	0,634(**)
2.	0,545(**)	12.	0,517(**)
3.	0,650(**)	13.	0,630(**)
4.	0,650(**)	14.	0,627(**)
5.	0,601(**)	15.	0,518(**)
6.	0,577(**)	16.	0,597(**)
7.	0,339(**)	17.	0,456(**)
8.	0,515(**)	18.	0,580(**)
9.	0,555(**)	19.	0,594(**)
10.	0,635(**)	20.	0,662(**)

**корреляция на уровне значимости 0,01 (2-стор.).

* корреляция на уровне значимости 0,05 (2-стор.).

Результаты статистического анализа характеристик Шкалы одиночества UCLA (версия 3) показывают, что при опросе студентов нами получены показатели, близкие результатам исследования Д. Рассела [12] (табл. 4).

ТАБЛИЦА 4. Показатели статистических характеристик Шкалы одиночества UCLA (версия 3)

Статистические характеристики	Исследование автора	Студенты [12]
N	526	487
СРЕДН. ЗНАЧЕНИЕ	39,53	40,08
МЕДИАНА	39,00	40,00
СТАНД.ОТКЛОНЕНИЕ	7,411	9,50
МОДА	41	41
РАЗМАХ	42	54
МИНИМУМ	23	20
МАКСИМУМ	65	74

Для определения различий одиночества у юношей и девушек применен однофакторный дисперсионный анализ (ANOVA). Из результатов следует, что $F = 7,05$ при $p < 0,01$, это означает, что различия статистически достоверны на высоком уровне значимости. Показатели Шкалы одиночества UCLA (версия 3) юношей и девушек распределились следующим образом: среднее значение у юношей ($N = 252$) – 38,6; у девушек ($N = 274$) – 40,4. Есть расхождения по размаху (у юношей – 37; девушек – 42); моде (34 и 37); дисперсии (57,9 и 51).

Полученные эмпирические данные Шкалы одиночества UCLA (версия 3) были подвергнуты также факторному анализу (Factor Analysis). Критерий адекватности выборки Кайзера-Мейера-Олкина (Kaizer-Meyer-Olkin) оказался равным 0,897. Это свидетельствует о том, что наша выборка предполагает высокую адекватность применимости данного вида анализа. После выделения факторов для их вращения был использован метод Varimax.

После проведенных процедур анализа выделены четыре фактора Шкалы одиночества UCLA (версия 3) (табл. 5).

ТАБЛИЦА 5. Преобразованная матрица факторных нагрузок Шкалы одиночества UCLA (версия 3) ($N = 526$), метод вращения -Varimax

№ вопроса	Факторы			
	1-ый фактор	2-ой фактор	3-й фактор	4-ый фактор
1	0,767	0,166	0,055	0,059
6	0,752	0,078	0,189	0,121
9	0,644	0,037	0,132	0,283
5	0,643	0,193	0,056	0,288
10	0,548	0,073	0,355	0,334
15	0,490	0,343	-0,162	0,287
11	0,138	0,719	0,299	0,095
2	-0,020	0,687	0,098	0,295
17	0,154	0,662	0,109	-0,085
3	0,100	0,614	0,092	0,513
4	0,241	0,489	0,309	0,281
14	0,312	0,472	0,393	0,063
12	0,108	0,071	0,743	0,154
7	-0,100	0,041	0,681	0,051
13	0,220	0,267	0,574	0,209
18	0,242	0,359	0,545	-0,001
8	0,140	0,325	0,493	0,057
19	0,255	0,145	0,060	0,775
20	0,275	0,224	0,114	0,753
16	0,295	-0,005	0,285	0,657

Группировка вопросов Шкалы одиночества UCLA (версия 3) по факторам позволила обозначить их следующим образом: 1-й фактор – *отсутствие общности, единения с окружающими*; 2-й фактор – *отсутствие межличностных контактов, взаимодействия*; 3-й фактор – *обособленность, отчужденность, изолированность*; 4-й фактор – *неудовлетворенность качеством отношений с окружающими*.

Выявленное в нашем исследовании наличие четырех факторов предполагает, что Шкала одиночества UCLA (версия 3) является не только одномерным, но и многомерным конструктом. Конечно, в пользу одномерности конструкта говорит достаточно высокая согласованность, корреляция вопросов Шкалы и выделенных факторов между собой. Результаты другого исследования, проведенного автором, в котором участвовали 417 человек, также подтвердили наличие выделенных нами четырех факторов. Мы должны обратить внимание на то, что позитивно сформулированные пункты («не одинок») составили 1-й и 4-й факторы, а негативно сформулированные («одинок») – 2-й и 3-й факторы. Четкое разделение на две группы, возможно, обусловлено некоторым влиянием самих формулировок вопроса, некоторой податливостью респондентов на позитивно и негативно сформулированные вопросы.

Выделенные факторы подтверждают наше понимание одиночества как переживания, возникающего в результате осознания неудовлетворительности качеством межличностных отношений

со значимыми людьми, референтной группой, а также появляющегося в связи с недостаточностью социальных связей, отсутствием единения с другими, постоянного восприятия себя как непохожего на окружающих [3].

На вопрос, как часто юноши и девушки чувствуют себя одинокими, получены ответы «иногда» – 22,8%, «всегда» – 1,9% (4-й вопрос Шкалы). Они близки данным, полученным в ходе исследования жителей Новой Зеландии (см. выше).

3. Выводы

1. Шкала одиночества UCLA (версия 3) может использоваться как надежный инструмент глобального измерения одиночества. Полученные результаты доказывают возможность его использования для проверки опросников на критериальную валидность.

2. По Шкале одиночества UCLA (версия 3) среднее значение равно 39,5; максимальный балл – 65, минимальный – 23. Дисперсия равна 54,92. Эксцесс (0,963) подтверждает нормальный вид распределения. Различия групп юношей и девушек статистически достоверны на высоком уровне значимости (ANOVA; $F = 7,05$ при $p < 0,01$). Среднее значение у юношей – 38,64; девушек – 40,35.

3. Шкалу одиночества UCLA (версия 3) при необходимости можно рассматривать как многомерный конструкт со следующими факторами:

- отсутствие единения с окружающими;
- отсутствие межличностных контактов, близкого человека;
- обособленность, отчужденность, изолированность;
- неудовлетворенность качеством отношений с окружающими.

Это позволяет обратить внимание на те аспекты, с которыми связано одиночество человека.

Литература

- [1] Andersson L. (1998) Loneliness research and interventions: a review of the literature. *Aging & Mental Health*, 2(4), 264–274.
- [2] Hawkey L. C., Burleson, M. H., Berntson, G. G., & Cacioppo, J. T. (2003) Loneliness in everyday life: Cardiovascular activity, psychosocial context, and health behaviors. *Journal of Personality and Social Psychology* 85, 105–120.
- [3] Išmuhametovs I. (2002) Vientulības izpratne pusaudžu un jauniešu vecumā. *ATEE Spring University*, R., lpp. 114–121.
- [4] Knight R. G., Chisholm B. J., Marsh N. V., & Godfrey H. P. D. (1988) Some normative, reliability, and factor analytic data for the revised UCLA Loneliness Scale. *Journal of Clinical Psychology* 44, 203–206.
- [5] Koropecykj-Cox T. (1998) Loneliness and depression in middle and old age: Are the childless more vulnerable? *Journal of Gerontology: Social Sciences* 53, 302–312.
- [6] Kupersmidt J. B., Sigda K. B., Voegler M. E. & Sedikides C. (1999) Social self-discrepancy theory and loneliness during childhood and adolescence. In: Rotenberg, K. & Hymel, S., ed. *Loneliness in childhood and adolescence*. New York: Cambridge University Press., pp. 263–279.
- [7] Loneliness. Social Connectedness. *Social Report 2006*, <http://www.socialreport.msd.govt.nz/social-connectedness/loneliness.html> (2006.05.10)
- [8] Mahon N. E., St. Yarcheski A. (1990). The dimensionality of the UCLA Loneliness Scale in early adolescents. *Research in Nursing and Health* 13, 45–52.
- [9] Marangoni C. & Ickes W. (1989) Loneliness: A theoretical review with implications for measurement. *Journal of Social and Personal Relationships* 6, 93–128.
- [10] Miller T. R., & Cleary T. A. (1993) Direction of wording effects in balanced scales. *Education and Psychological Measurement* 53, 51–60.
- [11] Perlman D, Russell D. (2004) Loneliness and health. In: Ed. Andeson, N.B. *Encyclopedia of health & behavior*. Volume 2, pp. 585–589.
- [12] Russell D. W. (1996) The UCLA Loneliness Scale (Version 3): Reliability, validity, and factor structure. *Journal of Personality Assessment* 66, 20–40.
- [13] Russell D. W., Peplau L. A., & Cutrona, C.E. (1980) The revised UCLA Loneliness Scale: Concurrent and discriminant validity evidence. *Journal of Personality and Social Psychology* 39, 472–480.
- [14] Russell D., Peplau L.A., & Ferguson M. (1978) Developing a measure of loneliness. *Journal of Personality Assessment* 42, 290–294.

- [15] Savikko N., Routasalo P., Tilvis R. S., Strandberg T. E. and Pitkala K. H. (2005) Predictors and subjective causes of loneliness in an aged population. *Archives of Gerontology and Geriatrics* **41**, 223–233.
- [16] Tiikkainen P., Heikkinen R-L. & Leskinen E. (2004) The structure and stability of perceived togetherness in elderly people during a 5-year followup. *The Journal of Applied Gerontology*, **23**(3), 279–294.
- [17] Victor C.R., Scambler S., Bond J. and Bowling A. (2002) Loneliness in Later Life: Preliminary findings from the Growing Older project. *Quality in Ageing – Policy, Practice and Research*, Vol. **3** (1).
- [18] Wilson D., Cutts J., Lees I., Mapungwana S., & Maunganidze L. (1992) Psychometric properties of the revised UCLA loneliness scale and two short-form measures of loneliness in Zimbabwe. *Journal of Personality Assessment*, **59**(1), 72–81.
- [19] Рассел Д. (1989) Измерение одиночества. *Лабиринты одиночества*. Пер. с англ. М.: Прогресс, с. 192–226.
- [20] Рубинштейн К. Шейвер Ф. (1989) Одиночество в двух городах Северо-Востока. *Лабиринты одиночества*. Пер. с англ. М.: Прогресс, с. 320–342.

Authors ' index

Ben-Yair A.	7
Borisov A.	41
Buikis A.A.	62
Chernishev V.	41
Chizhov Yu.	41
EVARESTOV R.A.	14
Greenberg D.	7
Golenko-Ginzburg D.	7
Gopeyenko V.	53
Gryaznov D.V.	29
Guseinov Sh.E.	62
Ishmuhametov I.	82,89
Kobasko N.I.	62
Kotomin E.A.	14,29
Kuleshova G.	41
Lobanova T.	75
Mamedov A.G.	62
Mastrikov Yu.A.	14,29
Nemenman A.	7
PISKUNOV S.N.	14
Shunin Yu.N.	14, 29
Zenin V.	53
ZHUKOVSKII YU.F.	14



Yuri N. Shunin (born in Riga, March 6, 1951)

- Vice-rector on academic issues (Information Systems Management Institute), professor, Dr.sc.habil., Member of International Academy of Refrigeration
- *Director of Professional Study Programme* Information Systems (Information Systems Management Institute)
- *Director of Master Study Programme* Computer systems (Information Systems Management Institute)
- **University study:** Moscow physical and technical institute (1968-1974)
- Ph.D. (physics & mathematics) on solid state physics (1982, Physics Institute of Latvian Academy of Sciences), Dr.sc.habil. (physics & mathematics) on solid state physics (1992, Ioffe Physical Institute of Russian Academy of Sciences)
- **Publications:** 300 publications, 1 patent
- **Scientific activities:** solid state physics, physics of disordered condensed media, amorphous semiconductors and glassy metals, semiconductor technologies, heavy ion induced excitations in solids, mathematical and computer modelling, system analysis



Igor V. Kabashkin (born in Riga, August 6, 1954)

- Vice-rector for Research and Development Affairs of Transport and Telecommunication Institute, Professor, Director of Telematics and Logistics Institute
- PhD in Aviation (1981, Moscow Institute of Civil Aviation Engineering), Dr.sc.habil. in Aviation (1992, Riga Aviation University), Member of the International Telecommunication Academy, Member of IEEE, Corresponding Member of Latvian Academy of Sciences (1998)
- **Publications:** 330 scientific papers and 67 patents
- **Research activities:** information technology applications, operations research, electronics and telecommunication, analysis and modelling of complex systems, transport telematics and logistics



Tamara Lobanova (born in Rezekne, Latvia)

Mg.paed, Information Systems Management Institute, Head of Foreign Languages Department

University study: Latvian University (1980), Foreign Languages Faculty, Doctoral student at Latvian University – PPF (Pedagogy-Psychology)

Scientific interests:

- Linguistics
- Pedagogical-psychological aspects of teaching languages

Professional activities: TOEIC test administrator in Latvia

Publications: 22



Victor Gopeyenko (born in 1958, Siktivkar, Russia)

Dr.sc.eng, Associate Professor of Natural Sciences and Computer Technologies Department, Information Systems Management Institute, vice-rector on innovation issues

University study: Riga Civil Aviation Engineer Institute (1967)

Professional interests: signal processing, computer network administration, computer modelling

Publications: about 100



Eugene Kotomin (born September 20, 1949, Vilnius, Lithuania)

Professor, Dr.sc.habil., Head of Theoretical Laboratory of Institute Solid State Physics, University of Latvia

University study: University of Latvia (Faculty of Physics), 1971

Dr.habil.phys. (in Solid State Physics) (Doctor of Science in former USSR). Title of Thesis: "Theory of Defect Accumulation and Recombination in Ionic Crystals Controlled by Electron Tunnelling", Institute of Physics, Latvian Academy of Sciences, 1988

Publications: 3 books and more than 300 papers

Interests:

Theoretical and Statistical Physics; Solid State Physics; Chemical Physics of Condensed Matter; Theory of Defects in Non-metallic Solids

Head of Project. Physics of Metal/Oxide Interfaces. *Joint project with University College London, UK, 1998-1999*

Head of Project. Large Scale Computer Modelling of Materials. *Joint project with Royal Academy of Sciences, Sweden, 1999-2000*



Yuri F. Zhukovskii (born February 2, 1949, Riga, Latvia) ,

Theoretical Laboratory of Institute Solid State Physics , University of Latvia

Education: 1966-75. **B.S. + M.S. degrees:** Department of Physics and Mathematics, the University of Latvia, Riga, Latvia. 1986-92. **Ph.D. degree (Dr. chem.):** Institute of Inorganic Chemistry, Latvian Academy of Sciences, Latvia, and Institute of Physics, St. Petersburg State University, Russia.

Advisors: Dr. chem. A.K. Lokenbach (Riga) and Dr. phys. E.P. Smirnov (St. Petersburg).

Title of the Thesis: "Quantum-chemical investigations of water chemisorptions on aluminium surface"

Publications: 80 papers and conference abstracts dealing with the quantum chemistry.

CONFERENCES : 32 presentations dealing with the quantum chemistry were prepared for 27 international conferences, meetings, seminars and symposiums organized in 12 countries (with 28 published abstracts)

01-03.2000. Visiting scientist, Centre for Materials Research, University College London, Great Britain; 04-05. and 10-11.2000. Visiting scientist, the Ångström Laboratory, Inorganic Chemistry, Uppsala University, Sweden



Andris Buikis (born March 15, 1939, Valka, Latvia)

Professor, University of Latvia, Faculty of Physics and Mathematics, Department of Mathematics

Director, Science and Dialogue centre of Latvia

Director, Head of Laboratory of Mathematical Physics, Institute of Mathematics Latvian Academy of Sciences, University of Latvia

Education:

University of Latvia (Faculty of Physics and Mathematics), 1963

Dr.math. (Candidate of Science in former USSR), University of Latvia, 1970

Dr.habil.math. (Doctor of Science in former USSR), University of Kasan, Russia, 1988

Professor, University of Latvia, 1991

Interests:

Mathematical Modelling, Filtration Theory, Mathematical Problems /Especially for Layered Media/ Numerical Methods for Partial Differential Equations, Innovative Energetics, Philosophy of Science



Sharif Guseinov

Doctor of Science in Mathematics, Associate Professor of Transport and Telecommunication Institute, The Leading Researcher of Institute of Mathematics, Latvian Academy of Sciences and University of Latvia

University study: Azerbaijan State University and Moscow State University, including post-graduation (1983-1991)

Scientific activities:

Mathematical Physics, Mathematical Modelling, Inverse and Ill-posed Problems, Partial Differential Equations, Integral Equations, Operator Equations, Functional Analysis and Applications, Computational Methods, Optimal Control and Optimization Methods, Game Theory and Operations Research, Actuarial Mathematics, Discrete Mathematics, Probability Theory and Mathematical Statistics, Logistics (logistic systems, models and methods)

Publications: 96 scientific papers



A. Ben-Yair

University of Ben-Gurion of Negev, Israel

Professional interests: Economical aspects of reliability, planning net-project management



Ishgaley Ishmuhametov

Mg.paed.psyh., Senior Lecturer

Education:

1983-1988 Ural State University, Faculty of Philosophy, Diploma

1988-1989 Leningrad State University, Special Faculty of Practical Psychology for High School

1993-1996 Latvian Aviation University, Retraining Faculty, Master's Degree

2000-2006 Daugavpils University, Doctoral Studies

Interests:

Trainings in Social Psychology Unemployment and Personality

Loneliness Problem in Teenage and Youth

CUMULATIVE INDEX

COMPUTER MODELLING and NEW TECHNOLOGIES, volume 10, No. 3, 2006

(Abstracts)

A. Ben-Yair, D. Golenko-Ginzburg, D. Greenberg, A. Nemenman. Upon Multi-Parametrical Optimization in Risk Management, *Computer Modelling and New Technologies*, vol. 10, No 3, 2006, pp. 7–13.

In order to demonstrate the role and the place of the harmonization modelling theory [12-14], we have to show its utilization in certain management areas. It can be well-recognized that harmonization models are applicable mostly to organization systems under random disturbances. This, in turn, enables analyzing various sources of uncertainty, e.g. reliability values including hazardous failures, various environmental parameters, etc. We will examine henceforth two important cases of project management: large-scale complicated projects and medium-level public service projects.

Keywords: project risk analysis; risk assessment models; public service projects; on-line control models; trade-off project optimization models

Yu. F. Zhukovskii, R. A. Evarestov, E. A. Kotomin, Yu. A. Mastrikov, S. N. Piskunov, Yu. N. Shunin. The Simplest Defect in SrTiO_3 Perovskite Crystals: Atomic and Electronic Structure of a Single F Centre, *Computer Modelling and New Technologies*, vol. 10, No 3, 2006, pp. 14–28.

Various properties of a cubic phase of SrTiO_3 perovskite containing single F centres (O vacancies), including energies of their formation and migration, were simulated using different formalisms of Density Functional Theory (DFT) as implemented into *CRYSTAL-2003* and *VASP* computer codes. The lattice relaxation around the F centre was found to be sensitive to both shape and size of used supercells. The larger is supercell, the closer *defect energy level* in the band gap lies to the conduction band bottom. It approaches the optical ionization energy of 0.49 eV for 270- and 320-atomic supercells, where the distance between neighbouring defects is as large as four lattice constants. The defect bandwidth decreases for these supercells down to 0.02 eV, *i.e.* the defect-defect interaction becomes negligible. Thus, different first principles periodic approaches being combined provide results, which are converged with respect to the supercell size.

Keywords: DFT calculations, *CRYSTAL-2003* and *VASP* computer codes, cubic phase of SrTiO_3 perovskite, supercell shape and size, the F centre, formation and migration, electronic properties

E. A. Kotomin, Yu. A. Mastrikov, D. V. Gryaznov, Yu. N. Shunin. First Principles Calculations of the Atomic and Electronic Structure of LaMnO_3 (001) Surface, *Computer Modelling and New Technologies*, vol. 10, No 3, 2006, pp. 29–40.

The results of *ab initio* DFT plane-wave periodic structure calculations of the surface of LaMnO_3 (001) are presented and discussed. The effects related to three different kinds of pseudopotentials, the slab thickness, magnetic ordering, and surface relaxation are analysed. The antiferromagnetic surface lowest in energy (that is, spins on Mn ions are parallel in basal plane and anti-parallel from plane to plane) has a considerable atomic relaxation up to forth plane from the surface. The calculated (Bader) effective charges and the electronic density maps demonstrate a considerable reduction of the Mn atom ionicity on the surface accompanied by a covalent contribution to the Mn-O bonding. These results are compared with hybrid LCAO-B3PW calculations.

Keywords: *ab initio* DFT plane-wave periodic structure calculations, LaMnO_3 (001) surface

V. Chernishev, Ju. Chizhov, G. Kuleshova, A. Borisov. Investigation of Algorithms for Goal-Based Agent Control Using Evolutionary Computation, *Computer Modelling and New Technologies*, vol. 10, No 3, 2006, pp. 41–52.

The aim of this paper is to study properties of genetic programming algorithm and perform a comparative analysis with Elman neural network using agent control task in a cellular world. In order to solve this task, two programmes have been created: the first implements genetic programming algorithm and the second implements Elman neural network. These programmes are developed in Borland Delphi environment using Object-Pascal programming language. In the paper each method is analysed separately and their comparative analysis is performed.

Keywords: genetic algorithm, genetic programming, Elman's neuron network, cell world, agent's navigation

V. Gopeyenko, V. Zenin. Development of Standard Operating Environment (SOE) Expanding On the Basement of Automated and Standardized System Imaging, *Computer Modelling and New Technologies*, vol. 10, No 3, 2006, pp. 53–61.

It would perhaps be no exaggeration to say that using computers in business increases the productivity and the effectiveness of management. However, with the increasing of the quantity of workstations in the long run, grows the heterogeneity of computer systems on workstations. Non-homogeneous systems make the installation of additional applications and users' support more difficult, increase help desk calls and time for new application compatibility testing, as well as time of system restoring on desktops; create the unstable platform for business applications and decrease uptime. It should be noted as well that increasing the time of updating operation systems and patch distribution decreases the security on the whole. As a result, the costs for supporting workstations extend.

The method of deployment of computer workplaces in educational institutes, middle and large corporations, the principals of the creation of different types of clones of Standard Operating Environment, the design, creation and deployment of the real system of Standard Operating Environment based on Microsoft Windows 2000 Professional and Microsoft Windows 2000 Server for the classrooms of Information Systems Management Institute are discussed.

Keywords: Operating system imaging, Standard Operating Environment

Sh. E. Guseinov, N. I. Kobasko, A. A. Buikis, A. G. Mamedov. Some Mathematical Models with Non-Linear Boundary Conditions for Intensive Cooling of Steel and Analytical Solutions, *Computer Modelling and New Technologies*, vol. 10, No 3, 2006, pp. 62–74.

It has been shown that there exists the analytical solution of both non-stationary heat transfer equation and hyperbolic equation of non-stationary heat transfer with nonlinear boundary conditions for the account of non-stationary nuclear boiling. Such solutions are necessary for the development of new intensive and ecologically clean heat treatment technologies. This paper is the beginning of the cycle of joint research fulfilled within the framework of the international project "Database for cooling capacities of various quenchants to be developed with the modern computational and experimental techniques" under the aegis of WSEAS (www.wseas.org/propose/project/wseas-projects.htm). Analytical solutions and their analysis are also very important for the automation and computerization of the production processes. The work can be used in the development of ecologically clean technologies.

Keywords: heat transfer equation, hyperbolic equation of non-stationary heat transfer, nonlinear boundary conditions, intensive and ecologically clean heat treatment technologies

T. Lobanova. A Survey of Distance English Teaching, *Computer Modelling and New Technologies*, vol. 10, No 3, 2006, pp. 75–81.

Mankind has just graced the threshold of a new millennium. What will unite people in the future? Probably, a common language – the English language most presumably. Distance teaching-

learning, which guarantees the highest degree of democracy and human rights to everyone, might be a means of facilitating the process of language learning and acquisition.

Distance education is an active process, in which people actively construct knowledge from their experiences in the world. People do not get ideas; they make them. Teaching styles are changing. Students are demanding it. Technology is enabling it. Distance education demands that we reshape the content, process and delivery of our educational offerings. It is the essence of our educational concept not to give the right answers, but to ask the right questions.

As world practice shows, well-thought out distance education offers students far greater involvement in the process of learning the language and gives the results as good as traditional classes and sometimes even better.

Keywords: distance education, English, module education

I. Ishmuhametov. Multifactor Dynamic Loneliness Model, *Computer Modelling and New Technologies*, vol. 10, No 3, 2006, pp. 82–88.

Loneliness is a complicated emotion capturing the whole personality with her (his) thoughts, actions and behaviour. This is a depressed feeling linked with the real or imaginary absence of the satisfactory social relations. This work investigates the contemporary comprehension of the loneliness phenomenon through the social psychological prism, develops the dynamic model of its contents and analyses its approbation under the youth age conditions. In a multi-factor dynamic model of loneliness exists the following: “loneliness”, “solitude” and “self-isolation”, “isolation caused by circumstances”. Understanding of the nature of loneliness will allow developing the optimal strategies of its overcoming under the conditions of the unstable and indefinite situation.

Keywords: Dynamic Loneliness Model, Loneliness Type, loneliness, solitude, self-isolation, isolation conditioned by circumstances, youth age

I. Ishmuhametov. Psychometric Characteristics of the UCLA Loneliness Scale (Version 3): A research of Loneliness of the Higher School Students, *Computer Modelling and New Technologies*, vol. 10, No 3, 2006, pp. 89–95.

In this article Psychometric Properties of the UCLA Loneliness Scale (Version 3) are presented. UCLA Loneliness Scale (Version 3) statistical characteristics under the conditions of Latvia and empirical data characterizing loneliness representation peculiarities at the youth age (students) have been obtained. The results received confirm the reliability of UCLA Loneliness Scale (Version 3) measurement. Chronbach’s coefficient of data received after the first study is equal to .86, the second (in a month time) -.89. The data correlation (Pearson) index of the first and the repeated investigation is equal to .81 when $p < 0,01$. The factor analysis shows the opportunity of using the mentioned scale for the determination of reasons of loneliness.

The choice of the scientific theme can be explained by the desire to attract professionals’ attention to the negative psychological states of contemporary people and by the urgent need to change the diagnostics of loneliness in accordance with the tendencies of modern science development.

Keywords: measurement of loneliness, loneliness, UCLA Loneliness Scale (Version 3), youth age

A. Ben-Yair, D. Golenko-Ginzburg, D. Greenberg, A. Nemenman. Par multi-parametrisko optimizāciju riska vadībā, *Computer Modelling and New Technologies*, 10.sēj., Nr.3, 2006, 7.–13. lpp.

Lai parādītu harmonizācijas modelēšanas teorijas lomu un vietu, mums ir jāparāda tās izmantošanu noteiktās vadības jomās. Tas ir labi zināms, ka harmonizācijas modeļus var pielietot lielākoties organizācijas sistēmās ar nejaušām nekārtībām. Tas, savukārt, dod iespēju analizēt nejaušību dažādos avotos, e.g. drošuma vērtības, ieskaitot bīstamas neveiksmes, dažādus ekoloģiskos parametrus, etc. Autori turpmāk rakstā izpēta divus svarīgus gadījumus projekta vadībā: sarežģītus plaša mēroga projektus un vidēja līmeņa sabiedrisko pakalpojumu projektus.

Atslēgvārdi: projekta riska analīze, riska novērtējuma modelis, on-line kontroles modelis

Yu. F. Zhukovskii, R. A. Evarestov, E. A. Kotomin, Yu. A. Mastrikov, S. N. Piskunov, Yu. N. Shunin. Visvienkāršākais defekts SrTiO_3 peroksīda kristālos: vienkārša F centra atomu un elektroniskā struktūra, *Computer Modelling and New Technologies*, 10.sēj., Nr.3, 2006, 14.–28. lpp.

Dažādas SrTiO_3 peroksīds, kas satur vienkāršus F centrus (O vakances), ieskaitot to formēšanās un migrācijas enerģijas, kubiskās fāzes īpašības, tika modelētas, pielietojot dažādus *Density Functional Theory (DFT)* formālus, kā ieviestus *CRYSTAL-2003* un *VASP* datora kodos. Režģa atslābināšana F centra apkārtnē, tika konstatēta kā jutīga gan pielietoto superšūnu formai, gan izmēram. Jo lielāka ir superšūna, jo tuvāks enerģijas defekta līmenis stieples spraugā vadītspējai izvietojas stieples apakšējā daļā.

Tādējādi, dažādas pirmo principu periodiskās pieejas, kas tiek apvienotas, lai nodrošinātu rezultātus, kuri tiek konverģēti, ņemot vērā supešūnas izmērus.

Atslēgvārdi: *DFT* aprēķini, *CRYSTAL-2003* un *VASP* datora kodi, SrTiO_3 peroksīds kubiskās fāzes, superšūnas forma un izmērs, elektroniskās īpašības, F centrs, veidošanās un migrācija

E. A. Kotomin, Yu. A. Mastrikov, D. V. Gryaznov, Yu. N. Shunin. LaMnO_3 (001) virsmas atomu un elektroniskās struktūras pirmo principu aprēķini, *Computer Modelling and New Technologies*, 10.sēj., Nr.3, 2006, 29.–40. lpp.

Rakstā tiek piedāvāti un diskutēti *ab initio* DFT plaknes viļņa periodiskie LaMnO_3 (001) virsmas struktūras aprēķini. Efekti, kas attiecas uz pseidopotenciālu trīs dažādajiem veidiem: plātnes biežums, magnētiskais kārtojums un virsmas atslābums, tiek analizēti tekstā. Antiferromagnētiskajai virsmai, kas ir viszemākā pēc enerģijas (tas ir, Mn jonu griešanās ir paralēla bazālajā plaknē un anti-paralēla no plaknes uz plakni), piemīt ievērojama atomiskā relaksācija (atomiskais atslābums) līdz pat turpmākajai plaknei no virsmas. Izskaitļotie (*Bader*) efektīvie lādiņi un elektroniskās blīvuma kartes demonstrē ievērojamu Mn atoma jonizācijas redukciju uz virsmas, kas tiek pavadīts ar kovalento devumu Mn-O savienojumā. Šie rezultāti tiek salīdzināti ar hibrīda LCAO-B3PW aprēķiniem.

Atslēgvārdi: *ab initio* DFT plaknes viļņa periodiskie LaMnO_3 (001) virsmas struktūras aprēķini, LaMnO_3 (001) virsma

V. Chernishev, Ju. Chizhov, G. Kuleshova, A. Borisov. Aģenta vadīšanas algoritmu izpēte, kas pamatots ar mērķi, pielietojot evolūcijas skaitļojumus, *Computer Modelling and New Technologies*, 10.sēj., Nr.3, 2006, 41.–52. lpp.

Pētījuma mērķis ir izziņāt algoritma ģenētiskās programmēšanas īpašības un veikt salīdzinošo analīzi ar Elmana neironu tīklu, lietojot aģenta kontroles uzdevumu celulārajā jeb šūnu pasaulē. Lai veiktu minēto uzdevumu, tika izstrādātas divas programmas: pirmā ietver ģenētiskās programmēšanas

algoritmu un otrā ietver Elmana neironu tīklu. Šīs programmas ir izstrādātas Borland Delfi vidē, lietojot Object-Pascal programmēšanas valodu. Rakstā katra metode tiek analizēta atsevišķi, kā arī tiek veikta to salīdzinošā analīze.

Atslēgvārdi: ģenētiskais algoritms, ģenētiskā programmēšana, Elmana neironu tīkls, šūnu pasaule, aģenta navigācija

V. Gopeyenko, V. Zenin. Standarta operacionālās apkārtējās vides attīstība, izplešoties uz automatizētās un standartizētās sistēmas attīstīšanas pamata, *Computer Modelling and New Technologies*, 10.sēj., Nr.3, 2006, 53.–61. lpp.

Tas nebūtu pārspīlējums, ja teiktu, ka datoru lietošana uzlabo biznesa produktivitāti un pārvaldes efektivitāti. Tomēr, palielinoties darbstaciju skaitam ilgtermiņā, palielinās datorsistēmu heterogenitāte uz darbstacijām. Ne-homogēnās sistēmas padara papildu lietošanas un lietotāju atbalsta instalāciju grūtāku, palielina palīglogu signālus un jaunu savietojamības testēšanas lietošanas laiku, kā arī sistēmas atjaunošanu uz darbvirsmām, rada nestabilu platformu biznesa lietojumiem un samazina darbības laiku. Ir jāatzīmē, ka palielinot laiku operāciju sistēmu darbībai un saikņu sadale samazina drošību kopumā. Rezultātā izmaksas darbstaciju atbalstam palielinās.

Atslēgvārdi: Darbības sistēmas attīstīšana, Standarta darbības vide

Sh. E. Guseinov, N. I. Kobasko, A. A. Buikis, A. G. Mamedov. Daži matemātiskie modeļi ar nelineāriem robežapstākļiem tērauda intensīvās rūdīšanas procesiem un to analītiskiem risinājumiem, *Computer Modelling and New Technologies*, 10.sēj., Nr.3, 2006, 62.–74. lpp.

Darbā tiek parādīts, ka pastāv analītiskais risinājums, kā nestacionāram siltuma vadāmības vienādojumam, tā arī hiperboliskajam nestacionārā siltuma vadāmības vienādojumam ar nelineāriem robežapstākļiem, ņemot vērā nestacionāro nukleāro vārīšanos. Šādi risinājumi ir nepieciešami jaunu intensīvu un ekoloģiski tīru siltuma režīma tehnoloģiju attīstībai. Šis raksts ir tikai sākums kopīgam starptautiskajam pētījumam par minēto tēmu „Datu bāze atvēršanas kapacitātēm, kas tiek izstrādātas ar mūsdienu skaitļošanas un eksperimentālām tehnoloģijām”, kas tiek veikts WSEAS – World Scientific and Engineering Academy and Society (www.wseas.org/propose/project/wseas-projects.htm) aizgādībā. Analītiskie risinājumi un to analīze arī ir ļoti svarīgi faktori šo ražošanas procesu automatizācijā un kompjuārizācijā. Darbu var lietot tikai ekoloģiski tīru tehnoloģiju izstrādei.

Atslēgvārdi: siltuma vadāmības vienādojums, nestacionārā siltuma vadāmības hiperboliskais vienādojums, nelineārie robežapstākļi, intensīvās un ekoloģiski tīrās siltuma režīma tehnoloģijas

T. Lobanova. Angļu valodas tālmācības pārskats, *Computer Modelling and New Technologies*, 10.sēj., Nr.3, 2006, 75.–81. lpp.

Pavisam nesen kā cilvēce izdaiļoja jaunā gadu tūkstoša sliksni. Kas gan vienos cilvēkus nākotnē? Ļoti iespējams, ka kopīga valoda – visticamāk, tā varētu būt angļu valoda. Mācīšanās ar tālmācības iespēju, kas garantē vislielāko demokrātijas līmeni un cilvēktiesības ikvienam, tas varētu būt veicinošs līdzeklis valodas apguves procesā.

Tālmācība – tas ir aktīvs process, kurā cilvēki aktīvi veido savu zināšanu bagāžu, par pamatu ņemot viņu pašu pieredzi. Cilvēki nedabū idejas no kaut kurienes, viņi paši tās veido. Mācību stils mainās nepārtraukti: to pieprasa studenti. Kā to pierāda pasaules prakse, labi organizēta tālmācība studentiem var dot daudz vairāk nekā ierastās nodarbības un bieži vien arī vēl pat vairāk.

Atslēgvārdi: tālmācība, angļu valoda, moduļa izglītība

I. Ishmuhametov. Daudzfaktoru dinamiskais vientulības modelis, *Computer Modelling and New Technologies*, 10.sēj., Nr.3, 2006, 82.–88. lpp.

Vientulība – ir sarežģīts pārdzīvojums, kas aptver personību kopumā, t.i., jūtas, domas, rīcību. Tā ir nepatīkama un nomācoša izjūta, kas ir saistīta ar reālu vai iedomātu apmierinošu sociālo kontaktu trūkumu. Šajā darbā pētīta vientulības fenomena mūsdienu izpratnē, lai noskaidrotu vientulības

īpatnību sociāli psiholoģisko būtību un izstrādātu vientulības satura sociāli psiholoģisko modeli, kā arī analizētas tā aprobācijas iespējas jauniešu vecuma grupā. Vientulības modelis balstās uz „vientulības”, „nošķirtības”, „paizolācijas” un „apstākļu noteiktas izolācijas” jēdzieniem, kas tiek analizēti to dinamiskajā saistībā. Vientulības būtības izpratne nepieciešamības gadījumā ļaus izstrādāt optimālas stratēģijas tās adekvātai pārvarēšanai mūsdienu nestabilajā un nenoteiktajā situācijā.

Atslēgvārdi: vientulības dinamiskais modelis, vientulības tipi, vientulība, nošķirtība, izolācija, jauniešu vecums

I. Ishmuhametov. Vientulības skalas UCLA (3. Versija) psihometriskie raksturojumi: augstskolas studentu vientulības pētījums, *Computer Modelling and New Technologies*, 10.sēj., Nr.3, 2006, 89.–95. lpp.

Šajā rakstā tiek analizētas Vientulības skalas UCLA (University California Los-Angeles) (3. versija) psihometriskās īpašības. Tiek dots šīs skalas statistiskais raksturojums Latvijas apstākļiem un empīriskie dati, kas raksturo vientulības izpausmes īpatnības jauniešu vecumā (studenti). Tādējādi iegūtie rezultāti apstiprina Vientulības skalas UCLA (3. versija) mērījumu ticamību. Esam ieguvuši Kronbaha (α) koeficientus pirmā pētījuma apgalvojumu rādītājiem – ,86 un atkārtotā – ,89. Tie norāda uz vientulības skalas UCLA (3. versija) augstu iekšējo saskaņotību. Pirmā un otrā, kā arī atkārtotā (test-retest; pēc mēneša) pētījuma datu korelācijas Pīrsona rādītājs līdzinās ,814 pie $p < 0,01$. Ar faktoranalīzes palīdzību tika pētīta Vientulības skalas iespējamā izmantošana vientulības cēloņu noteikšanai.

Pētījuma tēmas izvēli nosaka vēlēšanās pievērst sociālajā sfērā strādājošo dažādu jomu speciālistu uzmanību daudzu mūsu līdzcilvēku negatīvajiem psihiskajiem stāvokļiem, nepieciešamībai izmainīt vientulības teorētisko izpratni un diagnostiku saskaņā ar mūsdienu zinātnes atziņām pasaulē, Latvijas iedzīvotāju psiho higiēnas uzlabošanai šajā aspektā.

Atslēgvārdi: vientulības mērīšana, vientulība, vientulības skala UCLA (3. versija), jauniešu vecums

**COMPUTER MODELLING
&
NEW TECHNOLOGIES**

ISSN 1407-5806 & ISSN 1407-5814(on-line)

EDITORIAL BOARD:

Prof. Igor Kabashkin (Chairman of the Board), *Transport & Telecommunication Institute, Latvia*
Prof. Yuri Shunin (Editor-in-Chief), *Information Systems Management Institute, Latvia*
Prof. Adolfas Baublys, *Vilnius Gediminas Technical University, Lithuania*
Dr. Brent Bowen, *University of Nebraska at Omaha, USA*
Prof. Olgierd Dumbrajs, *Helsinki University of Technology, Finland*
Prof. Eugene Kopytov, *Transport & Telecommunication Institute, Latvia*
Prof. Arnold Kiv, *Ben-Gurion University of the Negev, Israel*
Prof. Anatoly Kozlov, *Moscow State University of Civil Aviation, Russia*
Prof. Juris Zakis, *University of Latvia*
Prof. Edmundas Zavadskas, *Vilnius Gediminas Technical University, Lithuania*

Editors:

Literary editor Lucija Paegle, *Transport & Telecommunication Institute, Latvia*
Technical editor Christina Hamroon, *Information Systems Management Institute, Latvia*

Host Organization:

Transport and Telecommunication Institute – Eugene Kopytov, Rector

Co-Sponsor Organization:

PAREX Bank, Latvia – Valery Kargin, President

Supporting Organizations:

Latvian Academy of Sciences – Juris Ekmanis, Vice-President
Latvian Transport Development and Education Association – Andris Gutmanis, President
Latvian Operations Research Society – Igor Kabashkin, President
University of Nebraska at Omaha, USA – Brent Bowen, Director of Aviation Institute
The Khaim Kordonsky Charitable Foundation, USA – Inna Kordonsky-Frankel

**THE JOURNAL IS DESIGNED FOR PUBLISHING PAPERS CONCERNING THE
FOLLOWING FIELDS OF RESEARCH:**

- mathematical and computer modelling
- mathematical methods in natural and engineering sciences
- physical and technical sciences
- computer sciences and technologies
- semiconductor electronics and semiconductor technologies
- aviation and aerospace technologies
- electronics and telecommunication
- navigation and radar systems
- telematics and information technologies
- transport and logistics
- economics and management
- social sciences

Articles can be presented in journal in English (preferably), Russian, German and Latvian (at the option of authors). All articles are reviewed.

Computer Modelling & New Technologies * Preparation of publication

EDITORIAL CORRESPONDENCE

Transporta un sakaru institūts (Transport and Telecommunication Institute)
Lomonosova iela 1, LV-1019, Riga, Latvia. Phone: (+371)-7100593. Fax: (+371)-7100535
E-mail: journal@tsi.lv, [http:// www.tsi.lv](http://www.tsi.lv)

COMPUTER MODELLING AND NEW TECHNOLOGIES, 2006, Vol. 10, No.3

Scientific and research journal of Transport and Telecommunication Institute (Riga, Latvia)
The journal is being published since 1996.

Computer Modelling & New Technologies * Preparation of publication

The Camera-Ready Copies

PREPARATION OF CAMERA-READY TYPESCRIPT: COMPUTER MODELLING AND NEW TECHNOLOGIES

A Guide for Authors

A.N. AUTHOR

Affiliation

Institute address

Abstract reviews the main results and peculiarities of a contribution. Abstract is presented always in English or in English and the second (presentation) language both.

Keywords: main terms, concepts

1. Introduction

These instructions are intended to provide guidance to authors when preparing camera-ready submissions to a volume in the **CM&NT**. Please read these general instructions carefully before beginning the final preparation of your camera-ready typescript.

Two ways of preparing camera-ready copy are possible:

- (a) preparation on a computer using a word processing package;
- (b) printed copy fitted for scanning.

2. Printer Quality, Typing Area and Fonts

IMPORTANT:

If you produce your camera-ready copy using a laser printer, use a 15 x 23 cm typing area (in A4 format: 30 mm – left, 30 mm – right, 30 mm – top, 30 – bottom, line spacing – single), as in these instructions, in combination with the **10 points Times** font. The pages will then be reproduced one to one in printing.

Fonts

The names and sizes of fonts are often not the same on every computer system. In these instructions the Times font in the sizes 10 points for the text and 8 points for tables and figure legends are used. The references section should be in the 10 points font.

3. Format and Style

The text should be in clear, concise English (or other declared language). Please be consistent in punctuation, abbreviations, spelling (**British English**), headings and the style of referencing.

Camera-ready copy will be printed exactly as it has been submitted, so please make sure that the text is proofread with care.

In general, if you prepare your typescript on a computer using a word processing package, use styles for the font(s), margin settings, headings, etc., rather than inserting these layout codes every time they are needed. This way, you will obtain maximum consistency in layout. Changes in the layout can be made by changing relevant style(s).

4. Layout of the Opening Page

A sample for the opening page of a contribution is shown in Figure 1 on page 3.

Requirements for the opening page of a contribution are (see also Figure 1): the titles should always be a centered page and should consist of: the title in capital letters, bold font, flush center, on the fourth text line; followed by the subtitle (if present) in italics, flush center, with one line of white space above. The author's name(s) in capitals and the affiliation in italics should be centered and should have two lines of white space above and three below, followed by the opening text, the first heading or the abstract.

Computer Modelling & New Technologies * Preparation of publication

5. Headings

Please distinguish the following four levels of headings:

1. First-order Heading

This heading is in bold, upper and lowercase letters, numbered in Arabic figures, and has two lines of space above and one line below. The text begins full out at the left margin.

1.1. SECOND-ORDER HEADING IN CAPITALS

This heading is in roman capitals, numbered in Arabic figures and has one line of space above and below. The text begins full out at the left margin.

1.1.1. *Third-order Heading in Italics*

This heading is in italics, upper and lower case letters, numbered in Arabic figures and has one line of space above and no space below. The text begins full out at the left margin.

Fourth-order Heading in Italics. This heading is in italics, upper and lowercase letters, with one line of space above the heading. The heading has a full stop at the end and the text runs on the same line.

↕ 3 blank lines	TITLE OF CONTRIBUTION <i>Subtitle of Contribution</i>
↕ 2 blank lines	A.N. AUTHOR <i>Affiliation</i> <i>Institute address</i>
↕ 3 blank lines	<i>Abstract</i>
↕ 2 blank lines	First text line

Figure 1. Example of an opening part of contribution to a Volume of CM&NT

6. Figures and Photographs

- *Line drawings* must be submitted in original form, on good quality tracing paper, or as a glossy photographic print.

- *Halftone photographs* must be supplied as glossy prints.

- *Colour illustrations.* Colour illustrations are more expensive and the author is expected to cover the extra costs. Please consult with Editors about this.

Mount all illustrations directly into the text at the appropriate places. Alternatively, it is acceptable to leave the appropriate space blank in the text, and submit the illustrations separately. In this case You must put the figure numbers in pencil in the open spaces in the text and on the back of the figures. Also indicate the top of the illustration.

For computer plotting the ORIGIN Software is preferable.

Computer Modelling & New Technologies * Preparation of publication

- Legends for figures/illustrations should not be incorporated in the figure itself and they should be listed in numerical order (headed as "Figure 1.", "Figure 2." etc.). The legends should be set centered, below the figure.

7. Displayed Equations

Displayed equations should be in the left side of the page, with the equation number in parentheses, flush right.

$$E_{int} = \iint \psi^+(\mathbf{x})\psi(\mathbf{x})K(\mathbf{x}-\mathbf{x}')(-div\mathbf{P}(\mathbf{x}'))d^3x d^3x', \quad (1)$$

$$K(\mathbf{x}-\mathbf{x}') = C_0 \frac{\exp(-\lambda|\mathbf{x}-\mathbf{x}'|)}{|\mathbf{x}-\mathbf{x}'|}. \quad (2)$$

Font sizes for equations are: 12pt – full, 7pt – subscripts/superscripts, 5pt – sub-subscripts/superscripts, 18pt – symbols, 12pt – subsymbols.

8. Tables

Please center tables on the page, unless it is necessary to use the full page width. Exceptionally large tables may be placed landscape (90° rotated) on the page, with the top of the table at the left-hand margin. An example of a table is given below:

TABLE 1. National programs of fusion research [1]

Experiment	Type	Laboratory	Task	Begin of operation
JET	tokamak	Joint European Torus, Culham, UK	Plasma physics studies in the region close to ignition	1983
TEXTOR	tokamak	FA, Jülich, Germany	Studies of plasma-wall interaction	1982
TORUS SUPRA	tokamak	CEA, Cadarache, France	Testing of superconducting coils, stationary operation	1988
ASDEX Upgrade	tokamak	IPP, Garching, Germany	Plasma boundary studies in divertor plasmas	1990
WENDELSTEIN 7-AS	stellarator	IPP, Garching, Germany	Testing the principles of "advanced stellarator"	1988
WENDELSTEIN 7-X	stellarator	IPP, Greifswald, Germany	Testing feasibility of "advanced stellarator" for power station	2004

9. References

The References should be typeset in a separate section as a numbered list at the end of your contribution in the following style:

Journal articles should consist of as follows: author's name, initials, year, title of article, journal title, volume number, inclusive page numbers, e.g.:

- [1] Dumbrajs O. (1998) Nuclear Fusion. *RAU Scientific Reports & Computer Modelling & New Technologies* **2**, aa-zz
- [2] Kiv A.E., Polozovskaya I.A., Tavalika L.D. and Holmes S. (1998) Some problems of operator-machine interaction. *RAU Scientific Reports & Computer Modelling & New Technologies* **2**, aa-zz
- [3] Shunin Yu.N. (1996) Elementary excitations and radiation defects in solids induced by swift heavy ions. *RAU Scientific Reports & Solid State Electronics & Technologies* **1**, 15-35
- [4] Schwartz K. (1996) Excitons and radiation damage in alkali halides. *RAU Scientific Reports & Solid State & Electronics & Technologies* **1**, 3-14

Computer Modelling & New Technologies * Preparation of publication

Book references should consist of as follows: author's name, initials, year, title of book, publisher, place of publication, e.g.:

- [5] Schwartz K. (1993) The Physics of Optical Recording. Springer-Verlag, Berlin Heidelberg New York
- [6] Shunin Yu.N. and Schwartz K.K. (1997) Correlation between electronic structure and atomic configurations in disordered solids. In: R.C. Tennyson and A.E. Kiv (eds.). Computer Modelling of Electronic and Atomic Processes in Solids. Kluwer Academic Publishers, Dordrecht, pp. 241-257 .

Unpublished papers should consist of as follows: author's name, initials, year (or: in press), title of paper, report, thesis, etc., other relevant details, e.g.:

- [7] Shunin Yu.N. (1995) Elementary Excitations in amorphous solids accompanying the swift heavy ions passages. Private communication. GSI Seminar. Darmstadt

The references above should be cross-referenced by numbers within square brackets: ...as cited in [1], or Kiv *et al.* [2]... The use of author's initials for cross-references is not encouraged.

10. Authors Index

Editors form the author's index of a whole Volume. Thus, all contributors are expected to present personal colour photos with the short information on the education, scientific titles and activities.

11. Submission

Check your typescript very carefully before it is submitted. Submit two copies of the typescript to the Editors of the Volume. Always retain a copy of all material submitted as backup.

11.1. DISK FORMATS AND WORD PROCESSING PACKAGES

If you want to present contributions electronically please before submitting accord with the Editors the details on your computer system, your word processing package and version (MS Word 6 and above versions are preferable) and the way of transfer on the information (disk or Internet).

Acknowledgements

Acknowledgements (if present) mention some specialists, grants and foundations connected with the presented paper. The first page of the contribution should start on page 1 (right-hand, upper, without computer page numbering). Please paginate the contributions, in the order in which they are to be published. Use simple pencil only.



The K. Kordonsky
Charitable Foundation

The 7th International Conference
RELIABILITY and STATISTICS
in TRANSPORTATION and COMMUNICATION (RelStat'07)
24-27 October 2007. Riga, Latvia

PURPOSE

The purpose of the conference is to bring together academics and professionals from all over the world to discuss the themes of the conference:

- Theory and Applications of Reliability and Statistics
- Reliability and Safety of Transport Systems
- Rare Events and Risk Management
- Modelling and Simulation
- Intelligent Transport Systems
- Transport Logistics
- Education Programmes and Academic Research in Reliability and Statistics

DEDICATION

The Conference is devoted to the memory of Prof. Kh.Kordonsky.

OFFICIAL LANGUAGES

English and Russian will be the official languages of the Conference.

SUPPORTED BY:

Transport and Telecommunication Institute (Latvia) and
The K. Kordonsky Charitable Foundation (USA) in co-operation
with:
Latvian Transport Development and Education Association
(Latvia)
Telecommunication Association of Latvia (Latvia)
Latvian Academy of Science (Latvia)
Baltic Operations Research Society

SPONSORED BY

Transport and Telecommunication Institute (Latvia)
The K. Kordonsky Charitable Foundation (USA)
Latvian Operations Research Society
PAREX bank (Latvia)

HOSTED BY

Transport and Telecommunication Institute (Latvia)

SECRETARIAT

Prof. Igor Kabashkin, Latvia – Chairman
Ms. Inna Kordonsky-Frankel, USA – Co-Chairman
Prof. Irina Yatskiv, Latvia – Co-Chairman
Ms. Elena Rutkovska, Latvia – Secretary

DEADLINES AND REQUIREMENTS

Submission of abstracts:	15 May	2007
Acceptance of abstracts:	29 May	2007
Submission of final papers:	3 July	2007
Acceptance of final papers:	4 September	2007

Abstracts (about 600 words in length) and papers submitted for review should be in English and, should present a clear and concise view of the motivation of the subject, give an outline, and include information on all authors (the full name, affiliation, address, telephone number, fax number, and e-mail address of the corresponding author).

Submitted abstracts and papers will be reviewed. Accepted and invited papers will be published in the proceedings of the conference and in the journal "Transport and Telecommunication" (ISSN 1407-6160).

Instruction for papers preparing can be found on the conference WWW page: <http://RelStat.tsi.lv>.

INVITED SESSIONS (workshops)

Proposals for invited sessions (workshops) within the technical scope of the conference are accepted. Each proposal should describe the theme and scope of the proposed session. The proposal must contain the title and theme of the session and a list of paper titles, names and email addresses of the corresponding authors. Session proposals and paper must be submitted by **21 May 2007**.

REGISTRATION FEE

The registration fees will be **Euro 100** before 10 September 2006, and **Euro 150** after this date. This fee will cover the participation in the sessions, coffee breaks, daily launch, hard copy of the conference proceedings.

VENUE

Riga is the capital of the Republic of Latvia. Thanks to its geographical location, Riga has wonderful trade, cultural and tourist facilities. Whilst able to offer all the benefits of a modern city, Riga has preserved its historical charm. It's especially famous for its medieval part – Old Riga.

Old Riga still preserves many mute witnesses of bygone times. Its old narrow streets, historical monuments, organ music at one of the oldest organ halls in Europe attract guests of our city. In 1998 Old Riga was included into the UNESCO list of world cultural heritage.

ACCOMMODATION

A wide range of hotels will be at the disposal of participants of the conference and accompanying persons (http://eng.meeting.lv/hotels/latvia_hotels.php).

FURTHER INFORMATION

Contact:

Elena Rutkovska, Secretary, RelStat'07
Transport and Telecommunication Institute
Lomonosova 1, Riga, LV-1019, Latvia
Telephone: +(371)-7100665
Fax: +(371)-7100535
E-mail: RelStat@tsi.lv
<http://RelStat.tsi.lv>